UNIVERSITY OF OKLAHOMA

GRADUATE COLLEGE

SUBSIDY INTERMEDIARIES: THE ROLE OF AQUATIC PLANTS IN STORING AND TRANSFERRING RESOURCES FROM AQUATIC BIOGEOCHMICAL HOTSPOTS TO TERRESTRIAL ECOSYSTEMS

A DISSERTATION

SUBMITTED TO THE GRADAUTE FACULTY

in partial fulfillment of the requirements for the

Degree of

DOCTOR OF PHILOSOPHY

By

JONATHAN WILLIAMS LOPEZ

Norman, Oklahoma

2022

SUBSIDY INTERMEDIARIES: THE ROLE OF AQUATIC PLANTS IN STORING AND TRANSFERRING RESOURCES FROM AQUATIC BIOGEOCHMICAL HOTSPOTS TO TERRESTRIAL ECOSYSTEMS

A DISSERTATION APPROVED FOR THE

DEPARTMENT OF BIOLOGY

BY THE COMMITTEE CONSISTING OF

Dr. Caryn Vaughn, Chair

Dr. Daniel Allen

Dr. Michael Kaspari

Dr. Lara Souza

Dr. Robert Nairn

ACKNOWLEDGEMENTS

I would like to thank the Department of Biology and the University of Oklahoma for the opportunity to pursue my Ph.D. here in Norman. The faculty, staff, and students here have been tremendously supportive, and I have learned from, collaborated with, and developed relationships with far too many people to thank them each individually here, but for those who I cannot mention here, I am still sincerely grateful.

First and foremost, I would like to thank my advisor, Dr. Caryn Vaughn. Caryn took a chance on me for which I will be forever indebted to her. She has infinite patience and tact and has empowered me to develop my own skills as a scientist and as a leader. She made me feel like I mattered and like I can accomplish goals I might never have dreamed possible five long years ago. Caryn never hesitated to support me in my research: verbally, physically, or financially. Thank you. I am also grateful to my advisory committee, each of whom provided unique and integral support during my Ph.D. Dr. Dan Allen for running my samples and co-authoring two chapters; Dr. Lara Souza for her kind words and helpful feedback; Dr. Mike Kaspari for always challenging me to think broadly and deeply; and Dr. Robert Nairn for his perspective and willingness to serve as the Graduate College representative to my committee.

I also owe a tremendous thank you to Dr. Thomas Parr. Thomas was a postdoc in the Vaughn Lab when I started graduate school. He co-authored two of my chapters and continues to be a mentor, a role model, but most importantly, a valued friend to me. The other members of the Vaughn Lab were also tremendously supportive while I conducted lab and field work. Traci Dubose for her relentless positivity and willing support, Noé Ferreira-Rodríguez for his infectious joy and boundless work ethic, Alex Franzen for tolerating my hijinks for many hours in the field and helping me collect samples, and Janell Hartwell for helping me with all sorts of

odd jobs. Ed Higgins and I started our Ph.D. programs the same semester and went through so many things together, and he deserves special thanks. Ed is another valued friend, and I will miss him dearly as we move on from OU.

Kyle Baker, Ranell Madding, George Martin (and his crew), Trina Steil, Liz Cooley, Jessie Tate, and the rest of the Biology and Oklahoma Biological Survey staff all supported me with logistical and financial questions and needs. Their support made everything so much smoother and more efficient, and I truly enjoyed getting to know them. I would also like to thank Dr. J.P. Masly, the Biology graduate student liaison for much of my time here. J.P. is honest and pragmatic and has been truly dedicated to helping the graduate students in this department have successful and healthy careers at OU and beyond, so I have been grateful for his insights.

I would also like to thank fellow (former) graduate student (Dr.) Trai Spikes. Trai and I shared a lot of laughs, thoughts, arguments, and drinks. I do not know how I would have made it through the COVID pandemic without Trai's friendship, and that of his partner and my friend Elyse Ellsworth. I am also grateful for the friendships I have developed with Sam Eliades, Chloe Bryen, John Muller, Alex Cooper, Will Oakley, Heather LePage, and many others.

Finally, this dissertation is dedicated to my mother, Julie King Lopez, and my father, Mike Lopez, Sr. None of this would have been possible without the love and support of my family. My mom is the kindest woman I have ever known, and my dad has supported me no matter what I do. Thanks to my brother, Michael, Jr., and my favorite sister-in-law, Chanel, for your support. And finally, to Yogi, who came with me from Raleigh to Nashville to Norman and kept me company when no one else could. I miss you, buddy. No one accomplishes anything alone. So, to all the people mentioned here, and whoever might be reading this, thank you.

TABLE OF CONTENTS

LIST OF TABLES

Chapter Two

LIST OF FIGURES

Chapter One

Chapter Two

ABSTRACT

The roles mobile animals and abiotic processes play as vectors for resource transfers between ecosystems (subsidies) are well-studied. Trophic interactions between mobile animals and their food sources often convey subsidies across ecosystem boundaries. However, the quality and quantity of such ecological subsidies may be altered by indirect interactions between seemingly unconnected taxa. For example, resources from animals with limited mobility may be transported across ecosystem boundaries through intermediate taxa. In freshwater ecosystems in North America, freshwater mussels (Bivalvia: Unionoida) can have major biogeochemical impacts, including the creation of nutrient cycling hotspots of biologically necessary elements (bioelements) such as nitrogen (N) and phosphorus (P). Such hotspots are also inhabited by dense beds of aquatic macrophytes, which may mediate transfers of aquatic-derived nutrients from immobile mussel aggregations to terrestrial ecosystems when macrophytes are consumed by terrestrial herbivores. For my dissertation research I studied the nutrient and mineral dynamics that drive multi-step aquatic-to-terrestrial resource subsidies from mussel-generated biogeochemical hotspots, to emergent aquatic macrophytes, and to terrestrial herbivores.

In Chapter One, I conducted a mesocosm experiment to test whether mussel-generated biogeochemical hotspots increase growth or N and P content in the macrophyte *Justicia americana*. *J. americana* biomass production increased and belowground biomass allocation changed with increasing mussel density. At high mussel density, water column phosphorus increased and carbon (C):P ratios in *J. americana* tissues decreased. I also deployed motion-sensing cameras to explore herbivory on *J. americana* growing along the margins of the Kiamichi River, Oklahoma, USA, and documented feeding by large mammals (*Odocoileus virginianus, Sus scrofa, and Bos taurus*).

In Chapter Two, I used an ionomic approach to simultaneously explore whether freshwater mussel density covaries with the cycling of 10 major bioelements (Ca, Cu, Fe, K, Mn, Na, Mg, P, S and Zn) across a naturally occurring mussel density gradient in the US Interior Highlands. I sampled this suite of bioelements in three different locations within the stream ecosystem: the water column, riverine gravel bar subsurface, and *J. americana*. In streams, higher mussel density was associated with elevated levels of calcium in gravel bars and *J. americana*. There were also contrasting associations of mussels with lower levels of trace elements in the gravel bar subsurface (Fe, Mn) and higher levels in *J. americana* (Fe, Cu, Zn). This effect was mediated by sediment size and may indicate these macrophytes preferentially adsorb certain bioelements when they are scarce.

In Chapter Three, I built on the findings of Chapter One by conducting field studies testing (1) whether the density and the N and P content of *J. americana* increase in response to mussel density under natural conditions, and (2) whether terrestrial herbivores preferentially consume macrophytes from mussel-generated hotspots, promoting aquatic-to-terrestrial subsidies. Mussel density did not have strong effects on N and P concentrations in sediment porewater or on macrophyte density, but N isotopes in *J. americana* leaves indicated assimilation of mussel-derived nutrients. Further analysis of the data from the motion-sensing camera surveys conducted in Chapter One indicated that terrestrial herbivores fed more frequently at mussel-generated hotspots. C and N concentrations and isotopes in white-tailed deer (*Odocoileus virginianus*) feces suggested that deer receive nutritional benefits from macrophyte consumption and convey nutrients from *J. americana* into terrestrial ecosystems.

Thus, biogeochemical hotspots generated by aquatic animal aggregations can promote macrophyte production that subsequently is transferred by herbivores to nearby terrestrial

habitats that are relatively nutrient limited. Macrophytes adsorb mussel-derived nutrients, and mussel beds are associated with elevated calcium and trace element concentrations in macrophyte tissues. Because mussel-generated hotspots appeared to have stronger effects on calcium and mineral bioelements than N and P, my findings indicate that elevated mineral content in macrophytes may drive increases in terrestrial mammal herbivory. Calcium and other minerals and trace elements such as iron have been proposed as key drivers of ecological processes. Such mineral elements may be important determinants of animal-driven ecological subsidies because they are relatively scarce in the environment and in plants, but essential to animal physiology. More broadly, my research suggests that reductions in aquatic animal biomass may have bottom-up impacts that indirectly affect terrestrial ecosystems via plant-animal interactions bridging ecosystem boundaries.

CHAPTER ONE

Animal aggregations promote emergent aquatic plant production at the aquatic-terrestrial interface

Keywords:

aquatic plant; aquatic–terrestrial linkage; biogeochemical hotspots; emergent macrophyte; freshwater mussel; macrophyte herbivory; nutrient subsidy; resource subsidy

Published in *Ecology*

Lopez, J.L., T.B. Parr, D.C. Allen, C.C. Vaughn. 2020. Animal aggregations promote emergent aquatic plant production at the aquatic-terrestrial interface. *Ecology*. 10:e03126

Abstract

The roles mobile animals and abiotic processes play as vectors for resource transfers between ecosystems ("subsidies") are well-studied, but the idea that resources from animals with limited mobility may be transported across boundaries through intermediate taxa remains unexplored. Aquatic plants ("macrophytes") are globally distributed and may mediate transfers of aquatic-derived nutrients from aggregations of aquatic animals to terrestrial ecosystems when consumed by terrestrial herbivores. We used mesocosms (94×44 cm) to test whether aquatic animal-generated biogeochemical hotspots increase growth and nutrient content in macrophytes using the macrophyte *Justicia americana* and freshwater mussels. *J. americana* biomass production increased and belowground biomass allocation changed with increasing mussel density. At high mussel density, water column phosphorus increased and carbon:phosphorus ratios in *J. americana* tissues decreased. We deployed motion-sensing cameras to explore herbivory on *J. americana* growing along the margins of the Kiamichi River, Oklahoma, and documented feeding by large mammals (*Odocoileus virginianus, Sus scrofa, and Bos taurus*). Thus, biogeochemical hotspots generated by aquatic animal aggregations can promote macrophyte production that subsequently is transferred to terrestrial animals. More broadly, this suggests that reductions in aquatic animal biomass may have bottom-up impacts that indirectly affect terrestrial ecosystems via plant-animal interactions bridging ecosystem boundaries.

Introduction

Resource flows between ecosystems ("subsidies") influence ecosystem structure and function reciprocally. Processes that drive variation in terrestrial-to-aquatic resource subsidies are well studied, but recent research highlights the importance of subsidies from aquatic to terrestrial ecosystems (Schindler and Smits 2017). Aquatic-to-terrestrial subsidies may be achieved by mobile animals crossing the aquatic-terrestrial interface such as aquatic insects emerging as flying adults (Baxter et al. 2005), by hydrologic factors like floods (Junk et al. 1989), or by both as in salmon runs (Ben-David et al. 1998). However, the roles that plant-animal interactions play in facilitating cross-ecosystem resource subsidies are not well understood.

The importance of ecological subsidies depends on their quantity, quality, timing, and duration (Subalusky and Post 2019). Aquatic plants (macrophytes) and animals may interact to subsidize terrestrial ecosystems during the growing season. Macrophytes are dominant primary producers in the aquatic habitats embedded within terrestrial ecosystems globally (Chambers et al. 2008) and represent a large and understudied nutrient pool and flux. Nitrogen (N) and phosphorus (P) pools in plant tissues are metrics of food quality, and often correlate with ambient N and P concentrations (Sterner and Elser 2002). Further, macrophytes are thought to be a higher quality food than terrestrial plants because they have fewer low quality, carbon (C)-rich structural compounds (Sterner and Elser 2002). In terrestrial, marine and freshwater ecosystems, nutrient recycling by animal aggregations can create biogeochemical hotspots of N and P (McNaughton et al. 1988, Allgeier et al. 2017, Atkinson et al. 2017). Macrophytes growing near these hotpots should be nutrient-rich, which may increase the amount of macrophyte production consumed by herbivores (Cebrian and Lartigue 2004). Shoots of emergent macrophytes extend

above the water and are available to terrestrial herbivores, providing an intermediate storage pool between ecosystems for aquatic-derived nutrients. Terrestrial herbivores browsing on macrophytes can translocate nutrients through subsequent egestion, excretion, or mortality on land (Ceacero et al. 2014, Bump 2018), which should have cascading implications for terrestrial ecosystems.

In streams, dense multi-species aggregations of freshwater mussels (Bivalvia: Unionoida) filter suspended material and excrete and biodeposit nutrients near the river bottom, creating biogeochemical hotspots of nutrient cycling (Atkinson and Vaughn 2015). Mussel aggregations are often next to dense stands of the widely distributed macrophyte, American water willow (*Justicia americana*), which has thick root networks that form gravel bars at river margins (Fritz et al. 2004a). Terrestrial herbivores forage at gravel bars, and where *J. americana* and terrestrial herbivores co-occur, its shoots often show evidence of browsing (e.g. Dick et al. 2004, see Appendix S2), although peer-reviewed evidence is scant. Substrate stability is key to mussel habitat suitability (Allen and Vaughn 2010) and is facilitated by *J. americana* roots (Fritz et al. 2004a). In return, *J. americana* derives nutrients from mussel excreta (Atkinson et al. 2014).

It is unknown if mussel-derived nutrients influence *J. americana* productivity, biomass allocation, or nutrient composition. Uptake of mussel-derived N and P may increase nutrient content in plant tissues because autotrophs can store excess nutrients (Sterner and Elser 2002). Although *J. americana* aboveground biomass senesces in the fall, the underground biomass survives in the sediment, providing overwinter storage of resources. Elevated nutrient availability tends to increase total plant biomass and decrease the proportion allocated to belowground structures in herbaceous plants (Müller et al. 2000), and *J. americana* adjusts its biomass allocation based on environmental factors (Fritz et al. 2004b). In turn, biomass

allocation may influence the availability and palatability of *J. americana* to herbivores.

Here, we asked how mussel-generated biogeochemical hotspots affect *J. americana* biomass production and allocation, nutrient stoichiometry, and consumption by terrestrial herbivores. We simulated *J. americana* gravel bars in a mesocosm experiment with varying mussel densities and tested three hypotheses: (**H1**) mussels increase ambient availability of N and P by recycling and excreting these nutrients in inorganic forms, (**H2a**) increased mussel density promotes *J. americana* biomass production and (**H2b**) shifts biomass allocation away from belowground structures towards aboveground structures due to increased nutrient availability, (**H3a**) C:P and C:N ratios in *J. americana* decrease as mussel density increases because plant tissues incorporate more P and N associated with mussel nutrient recycling and (**H3b**) *J. americana* tissues will exhibit elevated $\delta^{15}N$ signatures as mussel density increases because animal-derived nitrogen is enriched in ^{15}N relative to inorganic sources. We documented field herbivory of *J. americana* by terrestrial vertebrates with motion-sensing cameras and used these observations to supplement our experimental findings and make inferences on the potential role of *J. americana* as a mediator of aquatic-to-terrestrial resource subsidies.

Methods

Experimental design and sampling – Recirculating mesocosms (94×44 cm) consisted of molded plastic liners suspended in fiberglass basins (Appendix S1: Fig S1) that have been used successfully in other experiments examining mussel ecosystem effects (Appendix S1). We sampled water column nutrients at the beginning (wk 1), mid-point (wk 5), and end (wk 9) of the experiment, prior to water changes. We quantified ammonium (μg NH_4^+-N L^{-1}) by the phenol-hypochlorite method, and orthophosphate, SRP (μg P L^{-1}) by the molybdate blue method (U.S.

EPA 1983). Mats of filamentous algae formed over the course of the experiment. To account for this, we quantified algal cover at wk 9 by photographing each mesocosm with a fixed objective lens placed 1 m above the water surface. Photos were randomized and scored from 0-10 based on the surface coverage of algae by 5 independent observers following Parr et al. (2019).

We quantified total *J. americana* wet biomass in each mesocosm at wk 0 and wk 9, after manually removing periphyton and dead biomass, and gently spinning plants to remove excess water (Bickel and Perrett 2016). At wk 9, we dried plant tissue at 70°C for 72 h and separated aboveground (leaves and stems) and belowground (roots and runners) dry biomass. We were not able to determine initial aboveground versus belowground biomass allocation because sampling was destructive, but we attempted to plant consistent root biomass proportions in establishing the experiment. Flowering was negligible; thus, its contributions were not assessed. Thus, biomass allocation is a static measure at the end of the experiment, while biomass production represents estimated change in biomass over time. We pooled final *J. americana* biomass measurements (n = 38) to create a wet mass-dry mass regression (dry mass = 0.20×wet mass + 0.14, R^2 = 0.88) to determine initial dry biomass and thus biomass gained during the experiment.

We assessed C:N:P stoichiometry using molar ratios and the ^{15}N isotopic signature of each biomass compartment. We quantified C and N content and ^{15}N at the University of Oklahoma Environmental Stable Isotope Lab using a Thermo Isolink CN Elemental Analyzer integrated with a Thermo Delta V Advantage IRMS through a Conflo IV (Thermo Fischer Scientific, West Palm Beach, FL, USA). $\delta^{15}N$ values of samples were calibrated using externally certified standards (USGS 40 and 41a for $\delta^{15}N$ relative to air, and C and N content of samples were calibrated using an Algae (*Spirulina*) standard (Elemental Microanalysis Limited, Devon, UK) for C and N content. Total P content was estimated by combustion at 500° C and acid-

digestion at 105° C followed by SRP analysis as described above (U.S. EPA 1983).

Camera trap surveys – We placed a motion-sensing game camera (Model# TR10i35A-7, Wildgame Innovations, Grand Prairie, TX) at 10 locations along a 72 km stretch of the Kiamichi River, OK, from 5 August – 10 October 2019 (Appendix S2: Figure S1). We affixed cameras to tree trunks overlooking *J. americana* stands and set them to record 30-second time-stamped videos upon triggering at a range up to ~18 m. To quantify the number of herbivory events caught on camera, we recorded the species-level identity and behavior of terrestrial vertebrate herbivores that visited *J. americana* stands. If herbivores were observed directly consuming *J. americana,* that visit received a binary score of 1, and if not, it received a 0. To prevent double counting, videos showing the same species of the same sex and approximate size within a one-hour period were assumed to be the same individual and counted as a single herbivory event.

Statistical analyses – We conducted all analyses in R v3.5.1 (R Core Team 2018). To evaluate mussel density effects on water column nutrient concentrations (**H1**), we evaluated changes in NH_4^+-N by backwards stepwise GLMM comparison (package *Rcmdr*) with mussel biomass, *J. americana* biomass production, and final algae cover as fixed effects and with week and water temperature as random effects. SRP showed a nonlinear threshold effect in response to mussel density, so we analyzed this relationship with a piecewise regression (package *segmented*) on $\log_e$+1 transformed SRP values. We used linear regression to relate mussel biomass to plant biomass production (**H2a**) and pair-wise Spearman correlations to evaluate tradeoffs in biomass allocation between tissue compartments, followed by linear regression to determine if significant tradeoffs were related to mussel density (**H2b**). We used linear regression to evaluate relationships between mussel density and *J. americana* C:N, C:P, and N:P ratios (**H3a**) and $\delta^{15}N$ (**H3b**). We compared $\delta^{15}N$ from an initial subsample of *J. americana* from

a reference tank to post-experimental samples and between mussel treatments and controls using Wilcoxon tests. We further analyzed a subset of the data above the threshold breakpoint (*BP*) determined by our piecewise regression (i.e. when mussel density affected SRP). We used median-based robust regression, which limits influence by outliers in small datasets (package *mblm*), to determine if the increase in SRP influenced *J. americana* C:P and N:P (**H3a**).

Results

Mats of filamentous algae formed in all mesocosms containing mussels, likely seeded from remnant algae on mussel shells despite vigorous cleaning. With one exception, algal mats did not develop in the non-mussel controls. Filamentous algae influence nutrient dynamics in mesocosms (Parr et al. 2019) and thus indirectly compete with *J. americana* for nutrients, so we removed control treatments from our analyses but present their means in Appendix S3: Table S1.

High mussel density increases water column phosphorus– Ambient NH_4^+-N concentration (± SE) was 82.56 ± 5.41 µg NH_4^+-N L^{-1}. The best GLMM contained only week as a significant random effect ($P = 0.01$) and thus no response to mussel density (Appendix S3: Fig. S1). Mean SRP (± SE) was 7.55 ± 1.23 µg P L^{-1} and showed a nonlinear threshold effect; there was no relationship between mussel density and SRP at low mussel densities, switching to a log-linear positive relationship at higher mussel densities (Fig. 1a). Piecewise regression analysis estimated the breakpoint (*BP*) and the magnitude of the change in slope ($U = \text{slope}_{\text{above}BP} - \text{slope}_{\text{below}BP}$) of the nonlinear SRP response to mussel density ($df = 82$, *BP* [± SE] = 301.54 ± 114.54 g m^{-2}, *U* [± SE] = 0.0033 ± 0.0021, $R^2 = 0.11$; Fig. 1a).

Mussel density increases algal and plant biomass – Algal cover strongly increased with mussel density ($F_{1,30} = 61.15$, $P < 0.001$, $R^2 = 0.66$; Fig. 1b). Mean *J. americana* biomass

production was 13.99 ± 0.52 g (4.91 ± 0.27 %) and increased linearly with mussel density ($F_{1,30}$ = 5.18, P = 0.03, R^2 = 0.12; Fig. 1c). Pooled aboveground biomass increased marginally ($F_{1,30}$ = 3.39, P = 0.076, R^2 = 0.08; Appendix S3: Fig. S2a) and belowground biomass production increased significantly ($F_{1,30}$ = 5.28, P = 0.029, R^2 = 0.12; Appendix S3: Fig. S2b). Belowground biomass increased at a faster rate, but there was no change in the aboveground:belowground biomass ratio as mussel density increased ($F_{1,30}$ = 0.30, P = 0.59; Appendix S3: Fig. S2c). Pair-wise correlations between the proportional biomass of each tissue compartment (Appendix S3: Fig. S3) revealed no significant tradeoffs by *J. americana* in allocation within the aboveground biomass compartments, or between above and belowground. However, a strong shift occurred within the belowground biomass. Allocation to sediment surface runners versus subsurface roots (runner:root ratio) increased with mussel density ($F_{1,30}$ = 5.13, P = 0.03, R^2 = 0.12; Fig 1d).

High mussel density alters plant tissue composition – Mean C:N, C:P, and N:P ratios, and % C, N, and P for tissue compartments are presented in Appendix S3: Table S2. δ^{15}N signatures are detailed in Appendix S3: Table S3. Mean δ^{15}N for leaves, stems, and roots was significantly higher after exposure to mussels ($P < 0.05$ for each); runners weren't compared because they were destroyed during initial field sample collection. Tissue compartments also differed significantly from one another ($P < 0.05$ for each). However, when we compared non-mussel controls to mussel mesocosms, we found that δ^{15}N of aboveground tissues were not significantly different in the mussel-exposed mesocosms (leaf P = 0.44, stem P = 0.63). Root δ^{15}N, on the other hand, was significantly higher in mussel mesocosms than controls (P = 0.014), and while runners were not significantly higher in ^{15}N than non-mussel runners (P = 0.14), the mean was slightly (about 7 %) higher (Appendix S3: Tables S1 and S3). Mussel density was positively related to δ^{15}N enrichment in roots ($F_{1,30}$ = 15.82, $P < 0.001$, R^2 = 0.32; Fig 1e) and runners ($F_{1,23}$

=5.42, $P = 0.03$, $R^2 = 0.16$; Fig. 1f), but did not affect $\delta^{15}N$ in stems ($F_{1,30} = 0.10$, $P = 0.75$) or leaves ($F_{1,30} = 1.40$, $P = 0.25$). Variability in *J. americana* C:N:P nutrient content was not well explained by the full mussel density gradient for any of the biomass compartments sampled.

At high mussel densities (those greater than piecewise regression *BP*) SRP concentration significantly decreased *J. americana* C:P ratios in leaves ($V_{17} = 35$, $P = 0.01$; Fig. 2a), stems ($V_{17} = 30$, $P = 0.007$; Fig. 2b), and roots ($V_{17} = 37$, $P = 0.02$, Fig 2c). Runner C:P showed no relationship with SRP ($V_{13} = 85$, $P = 0.17$; Fig 2d). N:P ratios also decreased significantly in leaves ($V_{17} = 20$, $P = 0.001$; Fig 2e), stems N:P ($V_{17} = 32$, $P = 0.009$; Fig 2f) and roots ($V_{17} = 44$, $P = 0.04$; Fig 2g). Runner N:P did not respond to increasing SRP ($V_{13} = 59$, $P = 0.98$; Fig 2h).

Terrestrial vertebrate herbivores regularly consume J. americana – Of 10 motion-sensing camera traps, 5 were destroyed by flooding in August 2019. From the 5 recovered cameras, terrestrial vertebrate herbivores visited *J. americana* stands on 190 separate instances (Appendix S2: Table S1). We observed 85 herbivory events by wild vertebrates and 25 herbivory events by domestic cattle (*Bos taurus*) for a total of 110 herbivory observations. 72 % of herbivory events occurred in August, 28% in September, and 0 % in October (Appendix S2: Table S2). Of the 85 wild vertebrate herbivory events, 45% were by white-tailed deer (*Odocoileus virginianus*) and 55% were by wild boar (*Sus scrofa*).

Discussion

Our results support the hypothesis that dense aggregations of aquatic animals increase emergent macrophyte production, as increasing mussel density promoted *J. americana* biomass production. We did not find support for an increase in NH_4^+-N concentrations as mussel density increased, but SRP concentrations increased at high mussel densities, partially supporting the

hypothesis that mussels increase ambient nutrient availability. At elevated SRP concentrations, the C:P ratio of aboveground tissues decreased, indicating that animal aggregations may increase *J. americana* tissue nutrient content. In addition, increased *J. americana* biomass in response to increasing mussel biomass will result in overall higher N and P storage in *J. americana*, even where tissue nutrient content varied little. This suggests that macrophyte stands growing near animal-generated biogeochemical hotspots may store greater quantities of aquatic-derived nutrients than stands in other areas. Finally, our field observations revealed frequent herbivory by terrestrial vertebrates on *J. americana*, indicating that these animals play a significant role in transferring mussel- and macrophyte-derived resources to adjacent terrestrial ecosystems.

Although allocation to belowground *J. americana* biomass did not increase as we hypothesized, *J. americana* did alter allocation within its belowground biomass in response to mussel density – relatively more biomass to runners at the sediment-water interface than subsurface roots as mussel density increased. Terrestrial plants can grow larger runners in response to nutrient additions, enhancing acquisition of light and nutrients (Dong and de Kroon 1994, Nicholls 2011), so we suspect mussel-derived nutrients drove increased runner production. Runners help in vegetative propagation and help form the biomass network that stabilizes river sediments in *J. americana* stands. Increased runner production may enhance substrate stability in stream reaches with mussel beds, a positive feedback that would promote mussel abundance. While all biomass compartments were enriched in ^{15}N at the end of the experiment, likely due to evaporation and fractionation in our water source, roots and runners were further enriched in high density mussel treatments. Either the initial transplant into the mesocosm or mussel burrowing may have destroyed some belowground biomass and *J. americana* may have increased N uptake to regenerate these lost tissues. Furthermore, *J. americana* does not have the

ability to fix N, relying totally upon bioavailable N from the water. Root and runner regeneration would thus increase mussel-derived N in belowground tissues, contributing to a lack of response in ambient NH_4^+-N and a positive response in $\delta^{15}N$, as animal-derived N tends to be enriched in ^{15}N (Post 2002). The structural demands of regeneration may thus have prevented *J. americana* from storing excess N, which would have been necessary for tissue C:N ratios to decrease.

Consumer-driven nutrient recycling in mussel beds has well documented bottom-up effects on aquatic and riparian food webs (Allen et al. 2012, Atkinson et al. 2014). Here, the development of filamentous algae mats across treatments likely limited our ability to detect nutrient responses in both the water and *J. americana* tissues at low mussel densities. Competition between the two autotrophs (algae and *J. americana*) likely suppressed ambient concentrations of both SRP and NH_4^+-N. However, at higher mussel densities SRP availability probably exceeded the combined demand of the competing autotrophs – mussel excretion N:P ratios tend to be far lower than algal N:P ratios and the *J. americana* N:P ratios we observed here (Sterner and Elser 2002, Atkinson et al. 2013). *J. americana* would thus have relatively greater demand for N, further contributing to the absence of patterns in NH_4^+-N despite the observed increase in SRP and the corresponding decrease in C:P and N:P of *J. americana* tissues.

Our results suggest that macrophytes may form a globally distributed conduit for nutrients concentrated by animals at aquatic biogeochemical hotspots to subsidize nearby terrestrial ecosystems. We observed numerous instances of herbivory on *J. americana* by terrestrial herbivores. Nearly 45% of the wild herbivores we observed feeding on *J. americana* via game camera belonged to Family: Cervidae (*O. virginianus*). These mammals are abundant and widely distributed. *O. virginianus* populations in Oklahoma alone are estimated at 500,000-750,000 individuals (D. Barber, ODWC, pers. comm.), and the herbivore responsible for most

other herbivory events, *S. scrofa*, is a pervasive invader across the globe (Barrios-Garcia & Ballari 2012). If browsing on emergent macrophytes is as common and widespread in other systems as it is on the Kiamichi River, there is great potential for terrestrial mammalian herbivores to transfer aquatic-derived resources from *J. americana* to the surrounding landscape.

In light of the results of this study, we revisit the potential importance of macrophytes as an intermediary for aquatic-to-terrestrial resource subsidies using the quantity, quality, timing, and duration framework (Subalusky and Post 2019). Because macrophytes occur at the aquatic-terrestrial interface at a global scale (Chambers et al. 2008), the quantity of aquatic-to-terrestrial resource transfer via macrophytes is likely high. Consumer-driven nutrient recycling may add to the quantity of macrophyte biomass at animal-generated hotspots. The quality of macrophytes as a food resource is likely to be high as well, due to the high nutrient content of aquatic primary producers relative to terrestrial plants (Sterner and Elser 2002). This quality may be further increased by aquatic animals that recycle nutrients into plant-available forms. Our experiment showed an increase in plant P at high mussel densities, a key nutrient for bone and antler formation in vertebrates such as cervids and for fast-growing organisms like insects (Sterner and Elser 2002). As discussed above, cervids are widely distributed, important terrestrial game species and create a conduit for aquatic-to-terrestrial nutrient subsidies by foraging on macrophytes (Ceacero et al. 2014, Bump 2018). Although the duration of most macrophyte production in temperate zones is limited to the summer, this is the time of greatest effect for stream biogeochemical hotspots and a period of great metabolic demand for many animals. Nutrient effects generated by hotspots may subsidize this summertime demand via macrophytes.

Thus, ongoing declines in aquatic animal biomass may have bottom-up impacts that reverberate into terrestrial ecosystems (Knight et al. 2005, Dirzo et al. 2014, Schindler and Smits

2017). The multi-step linkage between biogeochemical hotspots generated by aquatic animals, macrophytes, and terrestrial herbivores needs further study, especially in the field, to draw more robust conclusions about the generality and magnitude of such resource subsidies. We must also expand our knowledge of the flexibility in elemental composition exhibited by macrophytes, for example if *J. americana* responds to altered mineral concentrations caused by the buildup of mussel shells in gravel bar sediments. Beyond N and P, mineral nutrients like sodium and calcium can influence the consumption of macrophytes (Ceacero et al. 2014). In places where macrophytes provide key nutrients and minerals in the diets of game species or livestock (e.g. Bump 2018), this may create new conservation imperatives for aquatic species. Quantitative field studies on the spatial extent and the nutrient and mineral composition of aquatic biogeochemical hotspots and macrophytes, and on the intensity and frequency of herbivory by terrestrial herbivores on aquatic plants are needed. The effects of biogeochemical hotspots on flowering and pollination in *J. americana* and other macrophytes also deserve attention as a vector for aquatic-to-terrestrial subsidies. Our results suggest that the importance of plant-animal associations that bridge ecosystem boundaries may be underappreciated, and that multi-step linkages such as the one we explored here are fundamentally important in conducting resource flows between ecosystems.

Acknowledgements

We thank T. DuBose, N. Ferreira Rodríguez, J. Hartwell and E. Higgins for help conducting the experiment. The Vaughn lab, M. Kaspari, L. Souza and two anonymous reviewers provided helpful comments. Funding was provided by a University of Oklahoma Graduate Student Senate Grant to JWL, the Oklahoma Biological Survey, and NSF DEB 1457542 to CCV. JWL, TBP, and CCV designed the experiment. JWL conducted the experiment and analyzed the data. DCA advised on and conducted stable isotope and elemental analyses. JWL wrote the initial manuscript and revised with input from all authors. This paper is part of a dissertation at the University of Oklahoma and a contribution to the program of the Oklahoma Biological Survey.

Literature cited

Allgeier, J. E., D. E. Burkepile, and C. A. Layman. 2017. Animal pee in the sea: consumer-mediated nutrient dynamics in the world's changing oceans. Global Change Biology 23:2166-2178.

Allen, D. C., and C. C. Vaughn. 2010. Complex hydraulic and substrate variables limit freshwater mussel species richness and abundance. Journal of the North American Benthological Society 29:383–394.

Allen, D. C., C. C. Vaughn, J. F. Kelly, J. T. Cooper, and M. H. Engel. 2012. Bottom-up biodiversity effects increase resource subsidy flux between ecosystems. Ecology 93:2165–2174.

Atkinson, C. L., C. C. Vaughn, K. J. Forshay, and J. T. Cooper. 2013. Aggregated filter-feeding consumers alter nutrient limitation: consequences for ecosystem and community dynamics. Ecology 94:1359–1369.

Atkinson, C. L., J. F. Kelly, and C. C. Vaughn. 2014. Tracing consumer-derived nitrogen in riverine food webs. Ecosystems 17:485–496.

Atkinson, C. L., and C. C. Vaughn. 2015. Biogeochemical hotspots: Temporal and spatial scaling of the impact of freshwater mussels on ecosystem function. Freshwater Biology 60:563–574.

Atkinson, C. L., K. A. Capps, A. T. Rugenski, and M. J. Vanni. 2017. Consumer-driven nutrient dynamics in freshwater ecosystems: from individuals to ecosystems. Biological Reviews 92:2003-2023

Barrios-Garcia, M. N., and S. A. Ballari. 2012. Impact of wild boar (*Sus scrofa*) in its introduced and native range: A review. Biological Invasions 14:2283–2300.

Baxter, C. V., K. D. Fausch, and W. C. Saunders. 2005. Tangled webs: Reciprocal flows of

invertebrate prey link streams and riparian zones. Freshwater Biology 50:201–220.

Ben-David, M., T. A. Hanley, and D. M. Schell. 1998. Fertilization of terrestrial vegetation by spawning pacific salmon: The role of flooding and predator activity. Oikos 83:47–55.

Bickel, T. O., and C. Perrett. 2016. Precise determination of aquatic plant wet mass using a salad spinner. Canadian Journal of Fisheries and Aquatic Sciences 73:1–4.

Bump, J. K. 2018. Fertilizing riparian forests: Nutrient repletion across ecotones with trophic rewilding. Philosophical Transactions of the Royal Society B: Biological Sciences 373: 20170439.

Ceacero, F., T. Landete-Castillejos, M. Miranda, A. J. García, A. Martínez, and L. Gallego. 2014. Why do cervids feed on aquatic vegetation? Behavioural Processes 103:28–34.

Cebrian, J., and J. Lartigue. 2004. Patterns of herbivory and decomposition in aquatic and terrestrial ecosystems. Ecological Monographs 74:237–259.

Chambers, P. A., P. Lacoul, K. J. Murphy, and S. M. Thomaz. 2008. Global diversity of aquatic macrophytes in freshwater. Hydrobiologia 595:9–26.

Dick, G. O., M. R. Smart, and J. K. Smith. 2004. Aquatic Vegetation Restoration in Cooper Lake, Texas: A Case Study. U.S.A.C.E., Report ERDC/EL TR-05-5, Vicksburg, MS.

Dirzo, R., H. S. Young, M. Galetti, G. Ceballos, N. J. B. Isaac, and B. Collen. 2014. Defaunation in the Anthropocene. Science 345:401–406.

Dong, M., and H. de Kroon. 1994. Plasticity in morphology and biomass allocation in *Cynodon dactylon*, a grass species forming stolons and rhizomes. Oikos 70:99–106.

Fritz, K. M., M. M. Gangloff, and J. W. Feminella. 2004a. Habitat modification by the stream macrophyte *Justicia americana* and its effects on biota. Oecologia 140:388–397.

Fritz, K. M., M. A. Evans, and J. W. Feminella. 2004b. Factors affecting biomass allocation in

the riverine macrophyte Justicia americana. Aquatic Botany 78:279–288.

Junk, W. J., P. B. Bayley, and R. E. Sparks. 1989. The flood pulse concept in river-floodplain systems. Canadian Special Publication of Fisheries and Aquatic Sciences 106:110-127

Knight, T. M., M. W. McCoy, J. M. Chase, K. A. McCoy, and R. D. Holt. 2005. Trophic cascades across ecosystems. Nature 437:880–883.

McNaughton, S. J., R. W. Ruess, and S. W. Seagle. 1988. Large Mammals and Process Dynamics in African Ecosystems. BioScience 38:794–800.

Müller, I., B. Schmid, and J. Weiner. 2000. The effect of nutrient availability on biomass allocation patterns in 27 species of herbaceous plants. Perspectives in Plant Ecology, Evolution and Systematics 3:115–127.

Nicholls, A. M. 2011. Size-dependent analysis of allocation to sexual and clonal reproduction in *Penthorum sedoides* under contrasting nutrient levels. International Journal of Plant Sciences 172:1077–1086.

Parr T.B., C.C. Vaughn, K.B. Gido. 2019. Animal effects on dissolved organic carbon bioavailability in an algal controlled ecosystem. Freshwater Biology DOI:10.1111/fwb13438.

Post, David, M. 2002. Using stable isotopes to estimate trophic position: Models, methods, and assumptions. Ecology 83:703–718.

Schindler, D. E., and A. P. Smits. 2017. Subsidies of aquatic resources in terrestrial ecosystems. Ecosystems 20:78–93.

Sterner, R.W., and J.J. Elser. Ecological Stoichiometry: The Biology of The Elements from Molecules to The Biosphere. Princeton University Press, Princeton, New Jersey, USA.

Subalusky, A. L., and D. M. Post. 2019. Context dependency of animal resource subsidies. Biological Reviews 94:517–538.

U.S. EPA [U.S. Environmental Protection Agency]. 1983. Methods for chemical analysis of water and wastewater. Environmental Monitoring and Support Library, Cincinnati, Ohio, USA.

Figure legends

Figure 1. The effects of increasing mussel density on ambient nutrient availability and on algal and *Justicia americana* biomass. (a) SRP concentration shows no relationship to mussel density at low mussel densities. The relationship becomes positive at approximately 301.54 g m^{-2} mussel biomass (df = 82, BP [± SE] = 301.54 ± 114.54, U [± SE] = 0.0033 ± 0.0021, R^2 = 0.11). The y axis is on a natural log scale. (b) Algae cover increased linearly as a function of mussel density ($F_{1,30}$ = 61.15, y = 0.013x – 0.24, P < 0.001, R^2 = 0.66). (c) *J. americana* biomass production over 9 weeks (Δ Biomass) as a function of mussel biomass density ($F_{1,30}$ = 5.18, P = 0.03. y = 0.0078x + 11.17, R^2 = 0.12). (d) Surface runner-to-subsurface root biomass ratio increases with mussel biomass density ($F_{1,30}$ = 5.13, P = 0.03, y = 0.00026x + 0.035, R^2 = 0.12). (e) Roots ($F_{1,30}$ = 15.82, P < 0.001, y = 0.0024x + 7.62, R^2 = 0.32) and (f) runners ($F_{1,23}$ =5.42, P = 0.03, y = 0.0025x + 9.39, R^2 = 0.16) had significantly enriched δ^{15}N with increasing mussel density. Leaf and stem δ^{15}N showed no relationship to mussel density.

Figure 2. *J. americana* C:P and N:P ratios decreased in three of the four biomass compartments sampled above the threshold in mussel density where SRP increases. As ambient SRP concentration increased, *J. americana* C:P significantly decreased in (a) leaves (V_{17} = 35, P = 0.01, y = -176x + 1266.5), (b) stems (V_{17} = 30, P < 0.01, y = -389.7x + 2758.5), and (c) roots (V_{17} = 37, P = 0.02, y = -301.9x +3560.3). C:P of runners (d) was not significantly related to SRP (V_{13} = 85, P = 0.17). As ambient SRP concentration increased, N:P of (e) leaves (V_{17} = 20, P = 0.001, y = -15.78 x + 99.1), (f) stems = (V_{17} = 32, P = 0.009, y = -9.48x + 79.83), and (g) roots (V_{17} = 44, P = 0.04, y = -4.36x + 81.271) also significantly decreased. (h) N:P of runners was not significantly related to SRP (V_{13} = 59, P = 0.98). Note the different scales on some y axes. The x axes are on a natural log scale.

Figures

Figure 1.

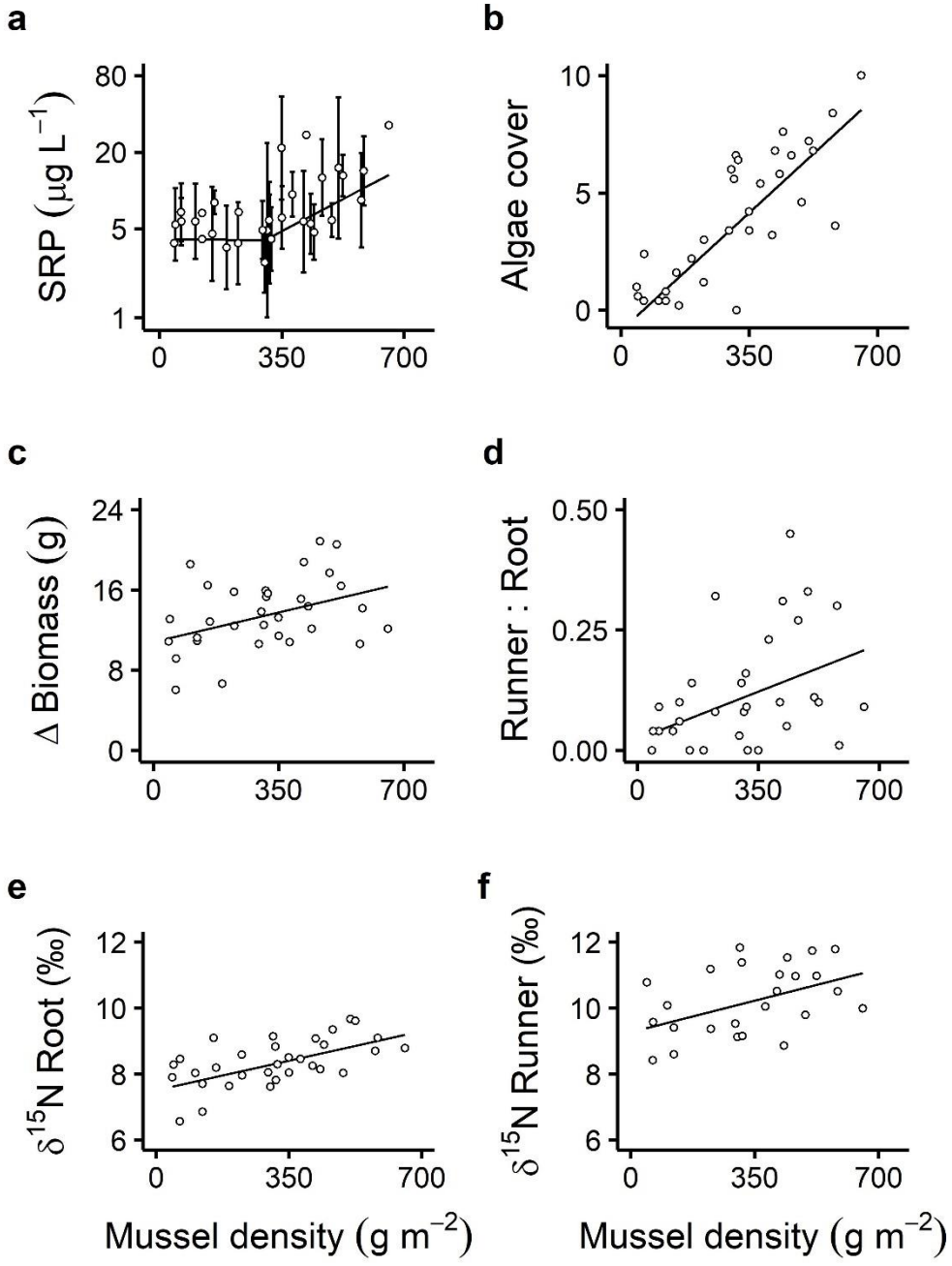

Figure 2.

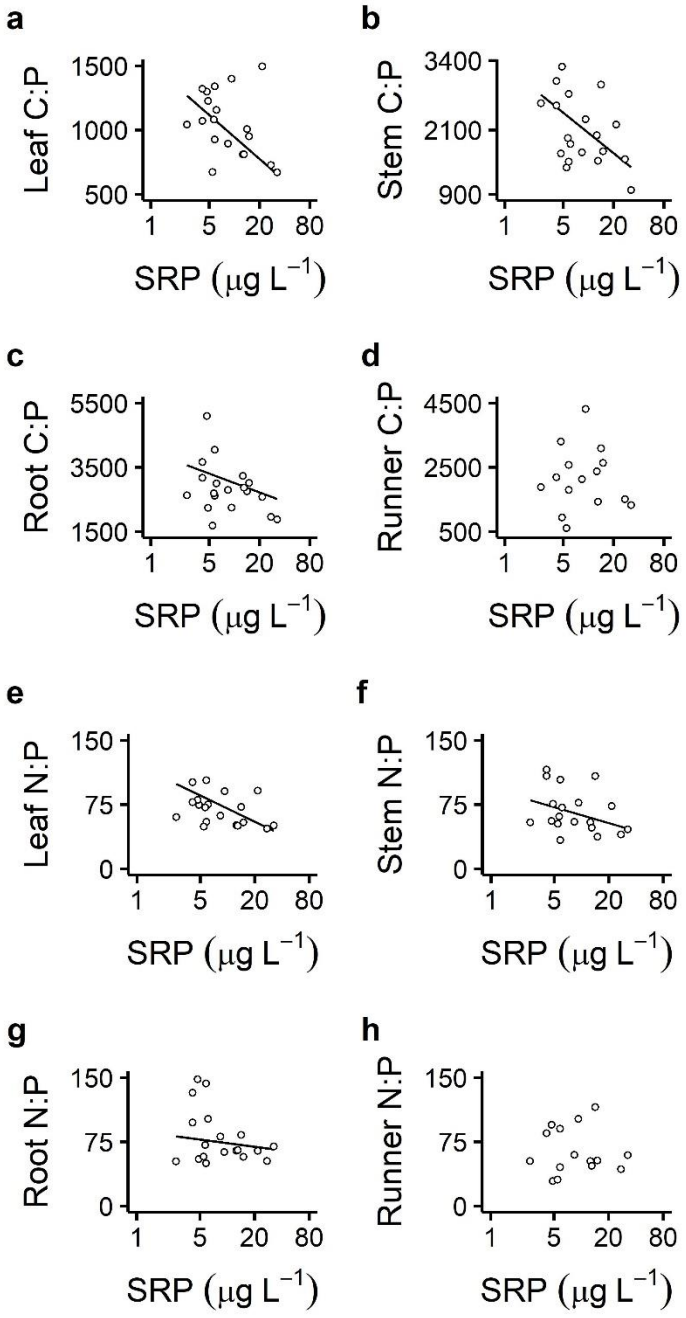
a
Leaf C:P
1500
1000
500
1
5
20
80
SRP (μg L−1)
b
Stem C:P
3400
2100
900
SRP (μg L−1)
c
Root C:P
5500
3500
1500
SRP (μg L−1)
d
Runner C:P
4500
2500
500
SRP (μg L−1)
e
Leaf N:P
150
75
0
SRP (μg L−1)
f
Stem N:P
SRP (μg L−1)
g
Root N:P
SRP (μg L−1)
h
Runner N:P
SRP (μg L−1)

Supplements

Appendix S1. Supplemental Methods.

Mesocosm design

Recirculating mesocosms (94×44 cm) consisted of molded plastic liners suspended in fiberglass basins (Appendix S1: Fig S1) that have been used successfully in other experiments examining mussel ecosystem effects to allow water circulation below and around the liner, with flow maintained by 1/32 horsepower pumps (Allen and Vaughn 2009). We added 0.5-1.5 cm diameter washed river gravel, *J. americana,* and mussels to the mesocosms to simulate field conditions during summer low flow periods. Mussels and *J. americana* were collected from the Little River, Oklahoma, in May 2018. We placed the mussels in the mesocosms two weeks prior to the start of the experiment to allow them to acclimate to experimental conditions. *J. americana* stems were separated along with a small amount of root biomass to anchor each stem. We created simulated gravel bars with an upward slope leveling off at the surface of the water (water depth of 0 cm, sediment depth of 25 cm) and transplanted 5 individual stems of *J. americana* in this area to reach a density of ~40 stems m^{-2}, which is reflective of low-density *J. americana* stands in late summer in southeastern OK (J Lopez, unpubl. data). We used 2 mussel species, *Actinonaias ligamentina* and *Amblema plicata* (in a 1:1 abundance ratio), that are dominant species in south-central US rivers, but have different thermal sensitivities, excretion rates, and stoichiometries (Spooner and Vaughn 2008), resulting in different ecosystem effects (Allen et al. 2012, Atkinson et al. 2013, 2018). Mussels were gently scrubbed to remove biofilm and placed at one end of the mesocosm at a water depth of 15 cm in gravel 10 cm deep (Appendix S1: Fig. S1). We began with a 1:1 pond water-to-well water mix, conducted weekly 50% water changes using well water, and monitored temperature with HOBO Pendants (Onset

Computer Corporation, Bourne, MA). Light availability could not be assessed due to flow patterns in the mesocosms that kept the loggers submerged, so we chose to monitor temperature because it affects mussel excretion rates (Spooner and Vaughn 2008), while also providing a general proxy for light availability. Well water chemistry was assumed to remain unchanged over the course of the experiment. The experiment was conducted over 9 weeks, from 29 May - 4 August 2018, in 38 recirculating mesocosms housed in a greenhouse at the University of Oklahoma.

We used a replicated regression design with the following treatments: 8 mussel densities each replicated 4 times (2, 4, 6, 8, 10, 12, 14, and 16 mussels/mesocosm) and 6 no-mussel controls. Densities represent a similar range as observed in mussel beds in local rivers (~10-85 mussels m^{-2}; Hopper et al. 2018) and were converted to soft tissue biomass densities (42.79-656.01 g m^{-2}) with established length-dry mass regressions (Atkinson and Vaughn 2015). Mussel growth was assumed to be negligible within the 9-week period, as adult mussels are slow-growing (Haag and Rypel 2011). Treatments were randomly assigned to mesocosms to minimize mesocosm location effects that may have resulted from different light availability, temperature, or other experimental artifacts in the greenhouse.

Literature cited

Allen, D. C., and C. C. Vaughn. 2009. Burrowing behavior of freshwater mussels in experimentally manipulated communities. Journal of the North American Benthological Society 28:93–100.

Allen, D. C., C. C. Vaughn, J. F. Kelly, J. T. Cooper, and M. H. Engel. 2012. Bottom-up biodiversity effects increase resource subsidy flux between ecosystems. Ecology

93:2165–2174.

Atkinson, C. L., C. C. Vaughn, K. J. Forshay, and J. T. Cooper. 2013. Aggregated filter-feeding consumers alter nutrient limitation: consequences for ecosystem and community dynamics. Ecology 94:1359–1369.

Atkinson, C. L., and C. C. Vaughn. 2015. Biogeochemical hotspots: Temporal and spatial scaling of the impact of freshwater mussels on ecosystem function. Freshwater Biology 60:563–574.

Atkinson, C. L., B. J. Sansom, C. C. Vaughn, and K. J. Forshay. 2018. Consumer aggregations drive nutrient dynamics and ecosystem metabolism in nutrient-limited systems. Ecosystems 21:521–535.

Haag, W. R., and A. L. Rypel. 2011. Growth and longevity in freshwater mussels: Evolutionary and conservation implications. Biological Reviews 86:225–247.

Hopper, G. W., K. B. Gido, C. C. Vaughn, T. B. Parr, T. G. Popejoy, C. L. Atkinson, and K. K. Gates. 2018. Biomass distribution of fishes and mussels mediates spatial and temporal heterogeneity in nutrient cycling in streams. Oecologia 188:1133–1144.

Spooner, D. E., and C. C. Vaughn. 2008. A trait-based approach to species' roles in stream ecosystems: Climate change, community structure, and material cycling. Oecologia 158:307–317.

Figure S1. (A) Mesocosm design showing simulated mussel bed containing *Actinonaias ligamentina* and *Amblema plicata*, with *Justicia americana* stand at the water/air interface. Filamentous algae mats are shown growing from the surface of the mussel shells. (B) Side view of mesocosm schematic showing 1/32 hp pump and inner mesocosm liner, with gravel forming mussel bed habitat and sloping up to form *J. americana* habitat.

A

B

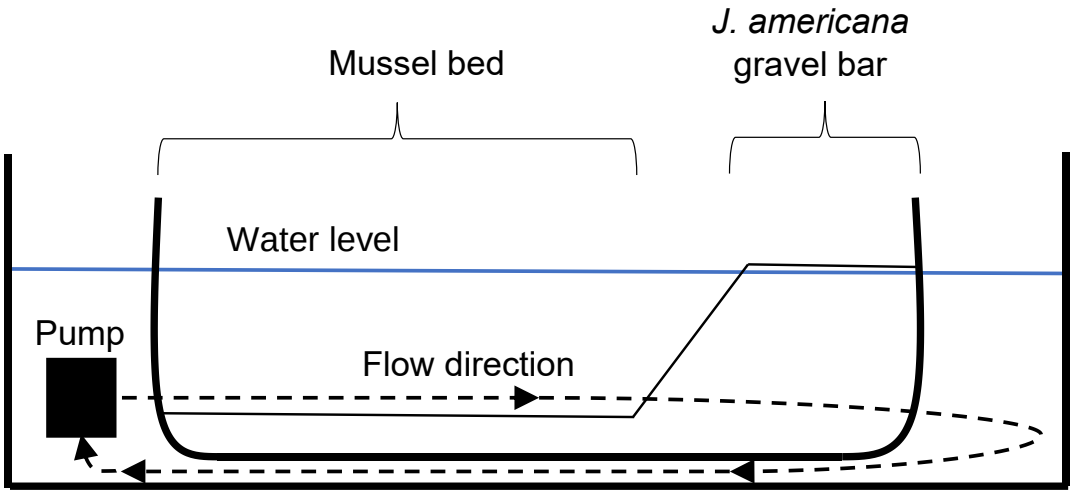

Appendix S2

Table S1. Game camera observations of terrestrial herbivores visiting *Justicia americana* stands on the Kiamichi River, OK, from 5 August – 10 October 2019. We observed four terrestrial mammal species: white-tailed deer (*Odocoileus virginianus*), wild boar (*Sus scrofa*), domestic cattle (*Bos taurus*), and elk (*Cervus elaphus*).

	Species				
Month	*O. virginianus*	*S. scrofa*	*B. taurus*	*C. elaphus*	All species
August	44	49	31	0	124
September	19	21	25	1	66
October	0	0	0	0	0
Total	63	70	56	1	190

Table S2. Game camera observations of terrestrial herbivores consuming *Justicia americana* during the visits listed in Appendix S3: Table S1 on the Kiamichi River, OK, from 5 August – 10 October 2019. We observed four terrestrial mammal species: white-tailed deer (*Odocoileus virginianus*), wild boar (*Sus scrofa*), domestic cattle (*Bos taurus*), and elk (*Cervus elaphus*). *C. elaphus* was not observed feeding on *J. americana*, only visiting the site.

	Species				
Month	*O. virginianus*	*S. scrofa*	*B. taurus*	*C. elaphus*	All species
August	28	37	14	0	79
September	9	11	11	0	31
October	0	0	0	0	0
Total	37	48	25	0	110

Figure S1. Map of motion-sensing camera trap deployment locations along the Kiamichi River from 5 August – 10 October 2019. Only cameras that were successfully recovered without damage are shown (n = 5). Red triangles in inset mark camera deployment locations. The circled marker indicates two cameras deployed within 1 km of one another.

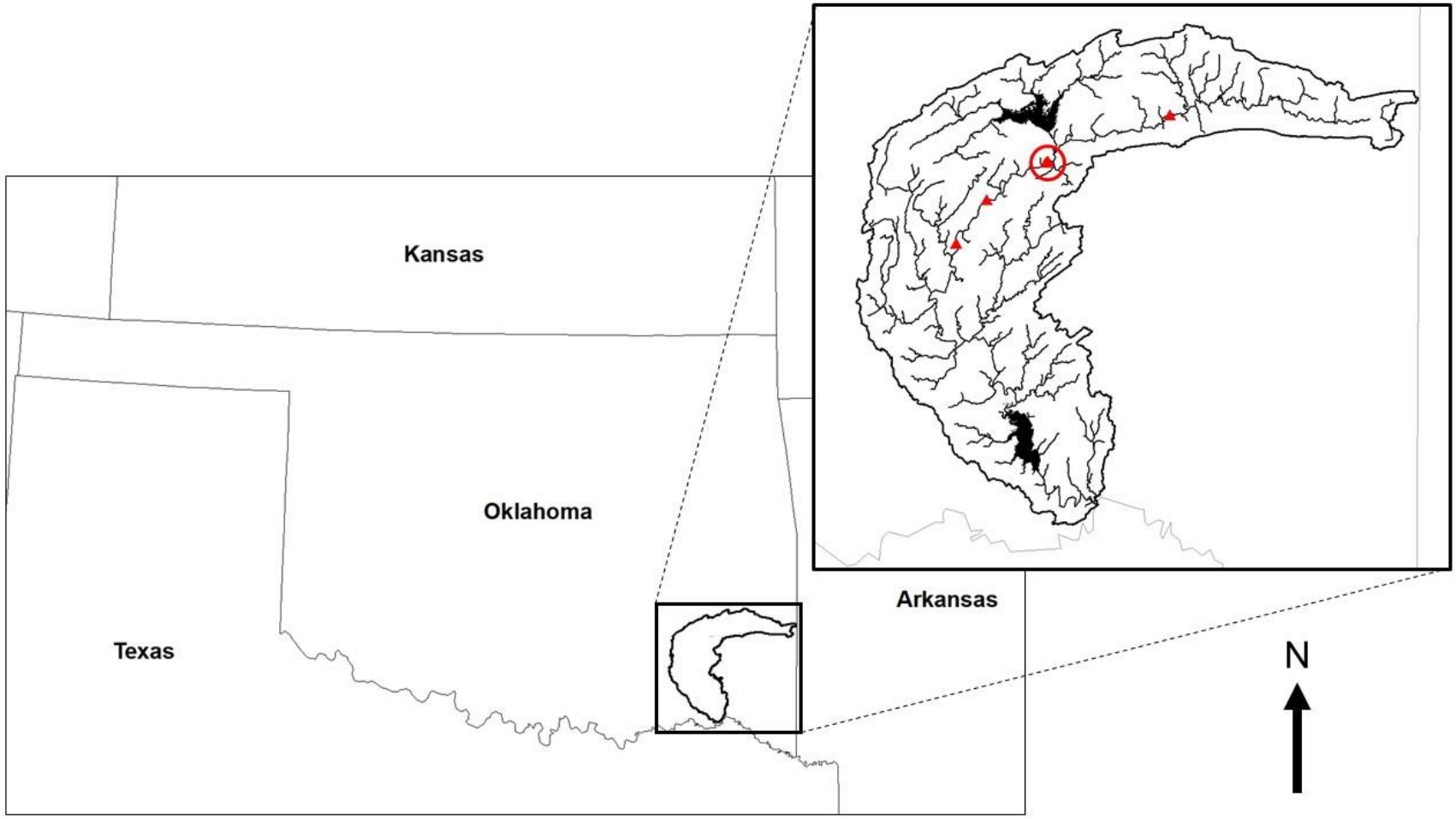

Appendix S3

Table S1. Mean (± SE) values for all water column nutrient, algae, and *Justicia americana* response variables in non-mussel control (n = 6) mesocosms.

Response variable	Non-mussel control
NH_4^+-N (µg NH_4^+-N L^{-1})	86.31 ± 16.02
SRP (µg P L^{-1})	3.44 ± 0.47
Algal cover (score)	0.60 ± 0.41
Justicia americana biomass production (g)	16.15 ± 0.66
Runner:root (biomass ratio)	0.10 ± 0.03
$C:N_{leaf}$	14.83 ± 0.23
$C:N_{stem}$	33.46 ± 1.87
$C:N_{root}$	37.50 ± 1.53
$C:N_{runner}$	34.81 ± 1.48
$C:P_{leaf}$	1060.93 ± 78.89
$C:P_{stem}$	2259.42 ± 204.05
$C:P_{root}$	2729.24 ± 325.14
$C:P_{runner}$	2042.94 ± 344.36
$N:P_{leaf}$	71.54 ± 5.09
$N:P_{stem}$	68.18 ± 6.72
$N:P_{root}$	73.80 ± 9.80
$N:P_{runner}$	59.62 ± 10.39
% C_{leaf}	40.40 ± 0.21
% C_{stem}	41.42 ± 0.22
% C_{root}	44.23 ± 0.68
% C_{runner}	43.59 ± 0.50
% N_{leaf}	3.18 ± 0.062
% N_{stem}	1.47 ± 0.096
% N_{root}	1.39 ± 0.059
% N_{runner}	1.47 ± 0.075
% P_{leaf}	0.10 ± 0.0069

% P_{stem}	0.049 ± 0.0043
% P_{root}	0.044 ± 0.0050
% P_{runner}	0.064 ± 0.014
$\delta^{15}N_{leaf}$ (‰)	11.46 ± 0.20
$\delta^{15}N_{stem}$ (‰)	9.32 ± 0.13
$\delta^{15}N_{root}$ (‰)	7.84 ± 0.06
$\delta^{15}N_{runner}$ (‰)	9.55 ± 0.33

Table S2. Mean (± SE) values for responses in *Justicia americana* tissue nutrient ratios and percentages in all four biomass compartments for all mussel density gradient mesocosms (n = 32).

	Tissue compartment			
Response variable	Leaf	Stem	Root	Runner
C:N	14.93 ± 0.31	31.75 ± 1.40	36.81 ± 1.80	32.56 ± 1.64
C:P	1027.49 ± 41.51	2050.04 ± 99.24	2799.07 ± 126.16	2185.81 ± 170.89
N:P	69.64 ± 3.16	67.47 ± 3.97	81.11 ± 5.28	68.19 ± 5.08
% C	40.04 ± 0.13	41.01 ± 0.11	44.50 ± 0.23	43.63 ± 0.18
% N	3.17 ± 0.067	1.59 ± 0.065	1.51 ± 0.066	1.66 ± 0.086
% P	0.11 ± 0.0045	0.056 ± 0.0029	0.044 ± 0.0020	0.062 ± 0.0070

Table S3. Mean (± SE) values for responses in *Justicia americana* tissue for $\delta^{15}N$ signatures of an initial subsample of *J. americana* (n = 10) taken prior to the experiment, and for the final $\delta^{15}N$ signatures of all four biomass compartments for all mussel density gradient mesocosms (n = 32) following the experiment. We were not able to take an initial subsample of runner biomass because runners were destroyed during initial sample collection in the field.

Compartment	Initial $\delta^{15}N$ (‰)	Final $\delta^{15}N$ (‰)
Leaf	7.10 ± 0.12	11.63 ± 0.10
Stem	5.04 ± 0.15	8.97 ± 0.24
Root	5.55 ± 0.25	8.36 ± 0.12
Runner	N/A	10.24 ± 0.21

Figure S1. Water column NH_4^+-N concentration showed no response to mussel density ($P > 0.05$).

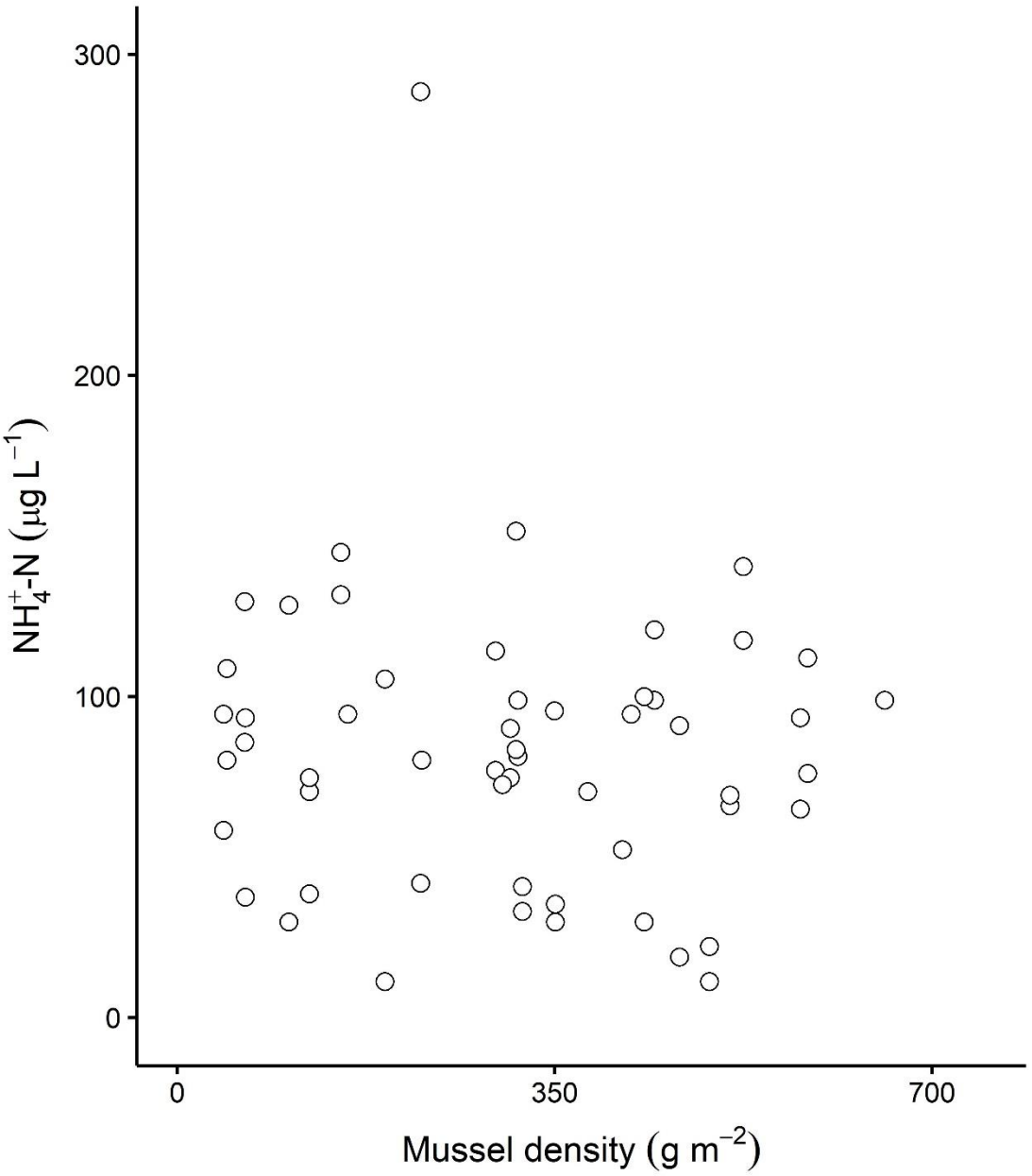

Figure S2. The effects of increasing mussel density on *Justicia americana* biomass production over 9 weeks for **(a)** aboveground biomass (AG Δ Biomass), **(b)** belowground biomass (BG Δ Biomass), and **(c)** *J. americana* relative allocation to aboveground versus belowground biomass production (AG:BG). **(a)** Aboveground biomass increased marginally as a linear function of mussel density ($F_{1,30}$ = 3.39, y = 0.0014x + 2.43, P = 0.076, R^2 = 0.08). **(b)** Belowground biomass increased significantly as a linear function of mussel density ($F_{1,30}$ = 5.28, y = 0.0065x + 8.74, P = 0.029, R^2 = 0.12). **(c)** Ratio of aboveground-to-belowground biomass allocation showed no relationship to mussel density ($F_{1,30}$ = 0.30, P = 0.59).

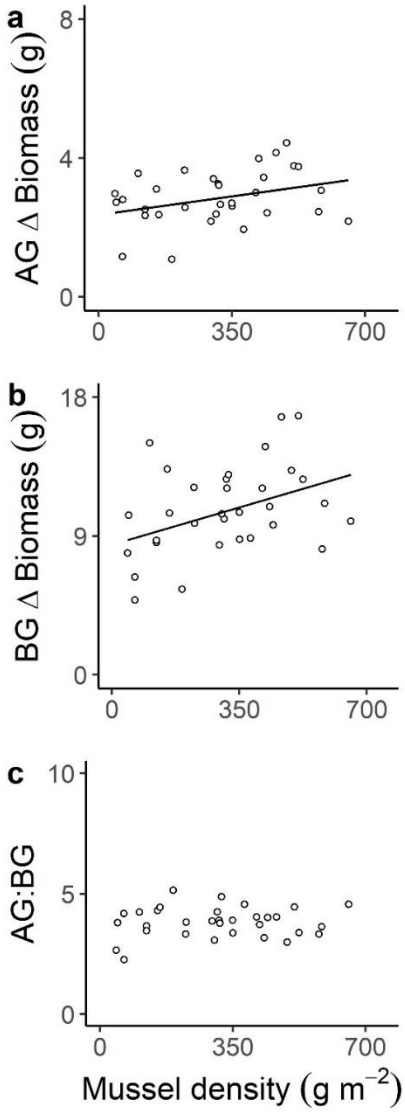

Figure S3. Pairwise Spearman correlation matrix showing the relationships in biomass allocation for different compartments of *Justicia americana* tissue. Red boxes show positive correlations, blue boxes show negative correlations. Darker shading represents stronger correlations, with actual correlation coefficients shown within each box. An asterisk (*) in the upper right corner of a box denotes a statistically significant ($P < 0.05$) correlation.

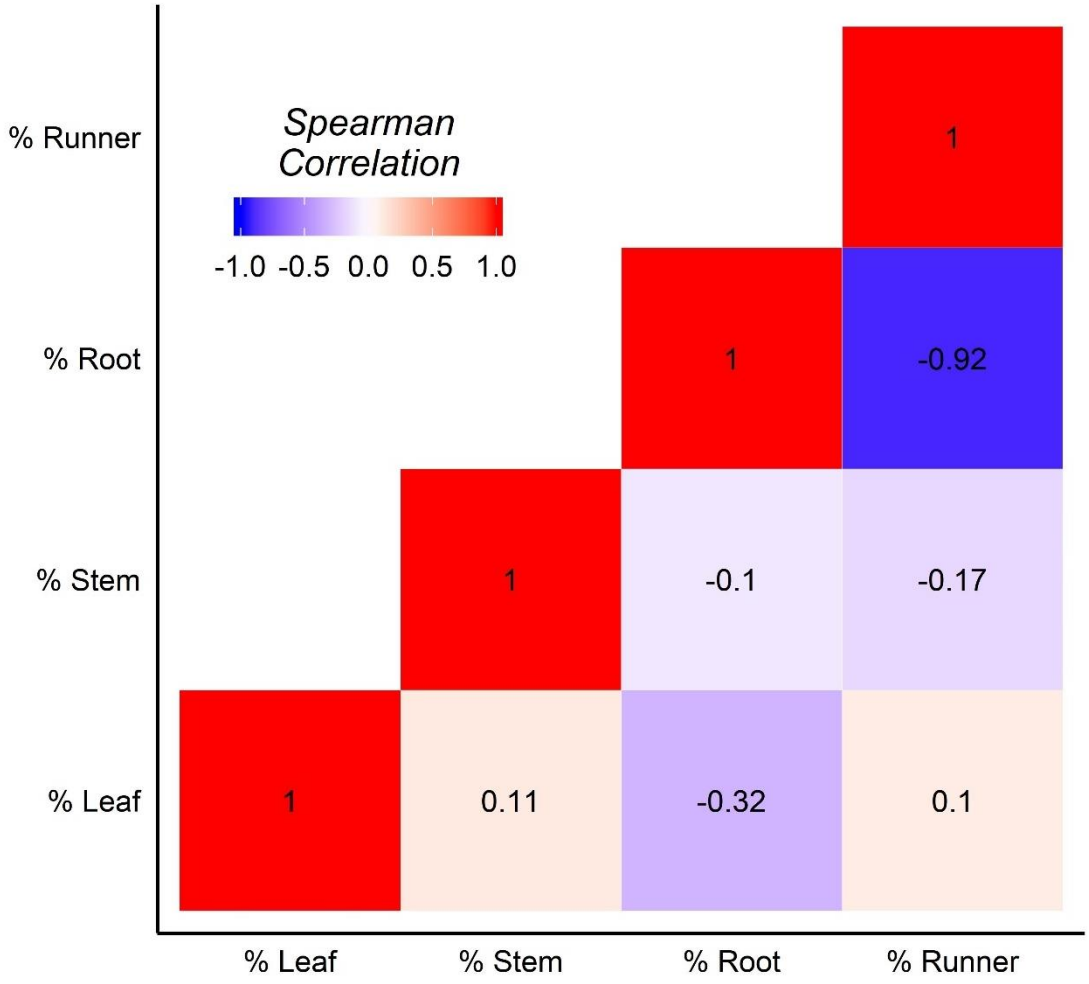

CHAPTER TWO

Ecosystem bioelement variability is associated with freshwater animal aggregations at the aquatic-terrestrial interface

Keywords:

ionome, calcium, trace element, bivalve, freshwater mussel

Formatted for submission to *Oecologia*

Authors: Jonathan W. Lopez, Rachel N. Hartnett, Thomas B. Parr, Caryn C. Vaughn

Abstract

The impacts of animals on the biogeochemical cycles of major bioelements like C, N, and P are well-studied across ecosystem types. However, more than 20 elements are necessary for life. The feedbacks between animals and the biogeochemical cycles of the other bioelements are an emerging research priority. We explored whether freshwater mussels (Bivalvia: Unionoida) are related to variability in ecosystem pools of 10 of these bioelements (Ca, Cu, Fe, K, Mn, Na, Mg, P, S and Zn) in streams containing a natural mussel density gradient in the US Interior Highlands. We conducted two studies of the concentrations of these bioelements across the aquatic-terrestrial interface – in the water column, riverine gravel bar subsurface, and the emergent macrophyte *Justicia americana*. Higher mussel density was associated with increased calcium in gravel bars and macrophytes. Mussel density also correlated with variability in iron and other redox-sensitive trace elements in gravel bars and macrophytes, although this relationship was mediated by sediment grain size. There were no clear associations between water column bioelement concentrations and mussel density. We suggest that (1) increased calcium availability in gravel bars near denser mussel aggregations is a product of the buildup and dissolution of shells in the gravel bar, and (2) mussels alter redox conditions in gravel bars with fine sediments, either behaviorally or through physical structure provided by shell material. Maintaining and conserving the roles that animals play in mediating a wider range of biogeochemical cycles is thus necessary to preserve the societal value of freshwater ecosystems.

Introduction

Bioelements comprise the matter portion of the ecological economy: they construct the various structures of life and perform all its complex chemical reactions. Decades of study have revealed the ecological importance of three of the most abundant bioelements, carbon (C), nitrogen (N), and phosphorus (P). Organisms actively seek out nutrient bioelements like N and P, which are relatively less common in the environment than C and other structural bioelements such as oxygen (O), hydrogen (H) and sulfur (S). Nutrient utilization drives many ecological patterns and processes and organismal behaviors, so understanding the biogeochemical cycles of these elements is necessary for ecological comprehension and forecasting. However, life requires many more elements than C, H, O, N, S, and P (Peñuelas et al. 2019, Kaspari 2021). For instance, calcium (Ca) works with P to construct bone in vertebrates and shells in mollusks; iron (Fe) forms hemoglobin in mammals and can limit primary production in marine ecosystems (Boyd et al. 2000); zinc (Zn), manganese (Mn) and other transition metals bind to proteins to catalyze metabolic reactions; magnesium (Mg) is the central atom of chlorophyll molecules and helps support the phosphate backbone of DNA. To unravel ecological patterns and processes, we must explore the exchanges of matter underlying ecosystems and the organisms within them.

The ionome concept – defined as the mineral and trace element composition of an organism – was developed by studying the elemental compositions of plants and microbes and changes to that composition in response to physiological, developmental, or genetic factors (Salt et al. 2008), and the concept has recently been extended to animals (Peñuelas et al. 2019). While the role of animals in the biogeochemical cycling of the major bioelements, especially C, N, and P, is now recognized across terrestrial, marine, and freshwater ecosystems (McNaughton 1985, Vanni 2002, Allgeier et al. 2017, Schmitz et al. 2018, Parr et al. 2019), animal effects on the

cycles of other elements and the ecological responses to such effects have received less attention (Jeyasingh and Pulkkinen 2019, Prater et al. 2019, Hopper et al. 2021).

Animals influence biogeochemical cycles in distinct ways from plants, fungi, and microbes (Schmitz et al. 2018). Compared with these other taxa, animals exhibit more complex behaviors and larger scales of movement and produce chemically distinct specialized tissues. Further, animals' behavior can mediate their impacts on biogeochemical cycles. Animals may alter the physical environment, for example by trampling soils and creating grazing lawns in terrestrial systems (McNaughton 1985, Schmitz et al. 2018) or by bioturbation – the reworking of sediments by burrowing that occurs across ecosystem types (Meysman et al. 2006). Animals also influence the forms and distributions of bioelements in the ecosystem when they aggregate to breed, rest, or feed, and when they move or migrate across ecosystems (Polis and Hurd 1996, Subalusky and Post 2019). Mobile animals with large body size or high abundances can quickly transport large pools of bioelements through space, and can cross ecosystem boundaries within and between marine, freshwater, and terrestrial environments (Ben-David et al. 1998, Roman et al. 2014, Bump 2018). Vertebrates and mollusks concentrate large amounts of Ca and P in their bones and shells respectively and release these elements slowly into the environment upon their death (Strayer and Malcom 2007, Subalusky et al. 2017). All animals also rely on a range of electrolytes – metals that dissociate in solution to form ions that conduct electrical currents – and trace elements to maintain homeostasis and perform physiological processes such as biosynthesis, immune responses, and metabolism (Harrison et al. 1936, Yatoo et al. 2013).

Full comprehension and evaluation of the ecosystem functions and services provided by animals requires an integrated understanding of their behavioral and biogeochemical effects on the ecosystems they inhabit. In both freshwater and marine ecosystems, bivalves play important

functional roles and possess many of the physiological and behavioral characteristics discussed above that may uniquely influence the cycling of a wide range of bioelements (Vaughn and Hoellein 2018). Where they occur, bivalves can be the dominant component of freshwater benthic zone biomass, especially in streams (Strayer and Smith 1994). Freshwater mussels (Bivalvia: Unionoida, hereafter "mussels") filter large amounts of particulate matter from the water column and egest or excrete excess nutrients, forming biogeochemical hotpots of nutrient recycling (Atkinson and Vaughn 2015). Mussel-derived N and P from these hotspots can drive variation in overall ecosystem nutrient limitation and in algal and aquatic macrophyte production (Atkinson et al. 2013, Lopez et al. 2020). However, mussel physiology suggests these animals should interact with a wide range of other bioelements (Table 1).

Mussels produce calcium carbonate-based shells – even in Ca-poor waters, mussels sequester Ca (Strayer 1993). Like other freshwater animals, mussels have evolved to take up and concentrate electrolyte-forming metals – which include Ca and Mg, as well as sodium (Na), and potassium (K) – selectively from the environment to prevent diffusive loss of solutes (Dietz 1978, Scheide and Dietz 1982, Larsen et al. 2014) . Most mussel species concentrate copper (Cu) in their hemolymph – the invertebrate analog of blood – in the form of hemocyanin. Here, Cu serves the same purpose as Fe does in vertebrate hemoglobin by binding and transporting O_2 (Nugroho and Frank 2011). The bioavailability and ionic form of trace metals like Cu and Fe are influenced by many factors, but they depend strongly on environmental redox conditions (Zhang et al. 2014). For example, mussels create bioturbation effects that increase oxygen penetration into aquatic sediments and alter the oxidation states of trace metals, inhibiting the buildup of reduced states such as the divalent (+2) cations Fe^{2+} and Mn^{2+}, in favor of more oxidized states – like Fe^{3+} and Mn^{3+} – which are less soluble (Matisoff et al. 1985, Aller 1990). Dead, empty

shells also create structure in the sediment and may increase oxygen penetration by creating larger pore spaces (Vaughn and Hoellein 2018, Bódis et al. 2014). Oxidation of the sediment may increase or decrease trace element availability depending on microbial metabolism and whether oxidation shifts trace metals toward or away from their bioavailable states (Zhang et al. 2014). Demand for bioelements and alteration of the environment suggest mussels should interact with a wide range of ecologically important biogeochemical pools and cycles.

Mussel-derived bioelements may have nutritional effects on higher trophic levels and even influence adjacent terrestrial ecosystems. For example, mussels increase emergence of flying insects from aquatic larval stages, and they often inhabit stream reaches next to gravel bars that provide access to food and water for terrestrial animals (Allen et al. 2012, Lopez et al. 2020). In eastern North American rivers, dense aggregations of mussels – mussel beds – are found near gravel bars formed by the emergent macrophyte *Justicia americana*. Mussels seem to benefit from substrate stability provided by dense *J. americana* root networks (Fritz et al. 2004), and in turn the macrophytes gain mussel-derived nutrients (Atkinson et al. 2014). Mussels primarily inhabit the permanently wetted part of the stream channel, where they directly interact with water column biogeochemistry. However, they also burrow up to the margins of these gravel bars and even among the roots of *J. americana* (J. Lopez, pers. obs.) At low flows, gravel bars and associated macrophytes are exposed as part of the riparian environment, obtaining nutrients from subsurface porewater. However, at high flows, gravel bars are submerged, and mussels can be dislodged from their beds and washed onto the adjacent gravel bars. When the water retreats, many mussels die, and their shells – and the nutrients therein – decompose into the gravel bar sediment (Sousa et al. 2012). Mussel bioturbation (when flows are high enough) and subsequent mortality (when flows recede) may therefore influence gravel bar porewater

biogeochemistry. Gravel bar porewater composition may correlate with the composition of *J. americana* tissue because the elemental composition of autotrophs is flexible (Sterner and Elser 2002). The correlation between elemental concentration in resources and plants may be positive if plants exhibit luxury consumption of abundant elements (Sterner and Elser 2002), or negative if plants exhibit preferential bioaccumulation of relatively rare trace elements (Kaspari 2021).

We asked whether variability in the density of freshwater mussel aggregations is associated with the concentrations of a suite of ten bioelements across three biogeochemical pools: the water column, gravel bar porewater, and the macrophyte *J. americana* (Figure 1). We focused primarily on Ca because of its importance in mussel shell formation, but also sampled for trace metals (Cu, Fe, Mn, Zn), the other electrolyte-forming metals (K, Mg, Na), and two more major bioelements (S, P). We assessed the following hypotheses: **H1**—environmental Ca concentrations are (a) unrelated to mussel density in the water column due to mussels' efficiency in sequestering Ca, and (b) positively related to mussel density in gravel bar porewater and macrophytes due to the buildup and dissolution of shell material; **H2**—the concentrations of redox-sensitive bioelements (Cu, Fe, Mn, Zn, S, and P) covary with mussel density (a) in the water column because of physiological demand for trace elements and because of mussel excretion of P, and (b) in gravel bar porewater and macrophytes for all six redox-sensitive bioelements because of sediment oxygen penetration caused by mussel effects on substrate structure; **H3**—electrolyte-forming metals other than Ca (K, Mg, Na) (a) covary with mussel density in the water column due to physiological demand for osmoregulation and (b) are unrelated to mussel density in gravel bars because they are not redox-sensitive. We tested these hypotheses by conducting two field studies across a naturally occurring mussel density gradient.

Methods

We studied associations between freshwater mussel aggregations and ecosystem bioelement concentrations in the Ouachita Highlands and Gulf Coastal plain regions of Oklahoma, USA, in three adjacent rivers within the Red River drainage. The Kiamichi and Little Rivers are tributaries to the Red River, and the Glover is a tributary of the Little River. The Little River is the largest drainage at 10,720 km^2 and is the most hydrologically stable. The Kiamichi has a drainage area of 4,500 km^2 and is more hydrologically stable than the Glover, which has a drainage area of 828 km^2. These rivers have similar physico-chemical conditions (OWRB 2021) and well-studied mussel communities from a shared regional species pool (Vaughn 2003, Allen et al. 2013). Mussels have similar effects on ecosystem function across the three drainages (Atkinson and Vaughn 2015, Hopper et al. 2018). To test the hypothesized association between mussel density and environmental Ca concentrations and to test for additional covariation between mussels and other bioelements, we conducted a pilot study using soil ion exchange probes, followed by a stream reach-scale study of major bioelement pools. Bioelement concentrations and references to the elements in this study refer to the total soluble or exchangeable element concentrations; specific oxidation states where not measured. We had 15 sites (Figure S1) across the two field studies, and each consisted of stream reaches of approximately 100 m in length, with either no mussels (0 ind m^{-2}) or a mussel bed occupying the channel surrounding the gravel bar with a density of ~10-38 ind m^{-2} (Table 2). Mussel density was determined using 0.25 m^{-2} quadrat surveys described in Hopper et al. (2018). Sites less than 1 km apart were blocked together and defined as a “site block” during data analysis to account for autocorrelation. Both studies were conducted at baseflow so discharge would not affect elemental concentrations.

Soil probe pilot study – In 2018, we evaluated the plant-available concentrations of the selected bioelements in gravel bar sediments within *J. americana* beds at 8 sites in the Kiamichi and Little Rivers using Plant Root Simulator (PRS)® soil probes (Western Ag Innovations, Saskatoon, SK, Canada). PRS® probes consist of a resin ion exchange membrane encased in plastic and provide a time integrated measurement of ion adsorption designed to simulate the availability of nutrients in the sediment to plants. 6 sites were in the Kiamichi River and 2 were in the Little River (Table 2; Figure S1).

We buried the soil probes from 06-Aug-2018 to 30-Aug-2018. We randomly placed three soil probe samples <0.5 m from the water's edge at each site, along a transect running parallel to the upstream edge of the gravel bar. Intended burial duration was 7 d, based on a test burial conducted in May-2018 (J. Lopez, unpubl. data). However, a storm event, which peaked at ~300 times baseflow occurred on the scheduled day of removal (13-Aug-2018) for half of the sites (USGS Gage #07335790). These probes were subjected to different hydrologic conditions, as we were forced to extend the burial duration until conditions allowed for retrieval (23 d). We statistically accounted for potential flooding effects (e.g., groundwater or allochthonous inputs). Upon retrieval, PRS® probes were rinsed with deionized water and refrigerated until shipping to Western Ag Innovations for analysis via inductively coupled plasma optical emission spectrometry (ICP-OES) for Ca, Cu, Fe, K, Mg, Mn, P, S, and Zn.

Stream reach study – In 2020 we sampled bioelement concentrations in the stream water column, gravel bar porewater, and *J. americana* aboveground biomass at 12 sites in the Kiamichi and Glover Rivers. This included 10 sites on the Kiamichi River and 2 sites on the Glover River (Table 2; Figure S1). We used Wolman pebble counts to determine the median sediment grain size in each gravel bar (Wolman 1954). Sediment grain size is an important covariate that affects

the activity and availability of some bioelements in porewater by altering redox conditions and sediment binding sites (Horowitz and Elrick 1987). Wolman's method uses categorical classifications for grains ≤ 2 mm ("sand") and grains ≥ 257 mm ("boulders"), so we coded these categories as 0 mm for sand and 257 mm for boulders while calculating medians. There were no sites with median sediment size ≥ 257 mm. When the median sediment size value for a site was 0 mm (sand), we assumed the functional difference between 0-2 mm to be negligible at the scale we sampled.

We sampled water column elemental concentrations by taking duplicate water samples from the center of the stream channel using a syringe filter and glass fiber filters (GF/F; 0.7 µm pore size) and stored them frozen until processing. Duplicate sample results were averaged prior to statistical analysis. We sampled gravel bar porewater by inserting a porewater sampler into the gravel bar in two locations: the upstream end and the downstream end. We took duplicate samples at each location. Bioelement concentrations in samples from upstream and downstream ends did not differ statistically, so we averaged them to get composite concentrations for gravel bar porewater. Porewater samples were too high in sediment to filter in the field and were stored unfiltered and frozen until just prior to analysis, at which point we thawed and decanted them into a syringe filter. We filtered the decanted samples using cellulose acetate membrane filters (CA; 0.7 µm pore size). All water samples were analyzed using ICP-OES.

We also quantitatively sampled the bioelement content of *J. americana* at each site to explore the potential role of emergent macrophytes in transferring aquatic-derived bioelements to terrestrial herbivores. We placed transects perpendicular to the direction of flow in the adjacent river. We sampled one transect per 10 m of river length when *J. americana* beds were greater than 20 m long, and every 5 m when beds were 20 m or less. On each transect we placed three

equidistant 0.25 m^2 quadrats spanning the entire breadth of the macrophyte bed and harvested the aboveground biomass in each plot. The biomass from each plot was dried at 70ºC for 72 h and ground in preparation for acid digestion and ICP-OES analysis.

ICP-OES analysis – We subsampled approximately 50 mg of *J. americana* biomass for each plot and combusted it for 4 h at 500°C to remove complex hydrocarbons such as lignin that interfere with plant tissue digestion. We digested the remaining mineral ash in a 2:1 v/v solution of HNO_3:H_2O_2 (BDH Aristar® Plus, VWR International, Radnor, PA) in polypropylene tubes and diluted the digested sample to 3-5% HNO_3. We analyzed digested *J. americana* samples using ICP-OES (Thermo Scientific iCAP 7400, Waltham, MA). Sample elemental concentrations were determined using standard curves from multi-element standards (CCV standards 1A & 1B, CPI International, Santa Rosa, CA) and calibrated using an internal yttrium standard (Peak Performance Inorganic Y Standard, CPI International, Santa Rosa, CA). Filtered water samples were also diluted to 3-5% HNO_3; GF/F filtered samples and CA filtered samples were analyzed separately using filtered deionized water blanks for each filter type. We analyzed water samples and GF/F and CA filter blanks using the same standards and instruments listed above. Of the 10 elements that we sampled, we removed those that had analytical uncertainties (i.e., those with CCV standard concentration values that drifted over a given sample run) or interferences that caused the instrument to return an "N/A" value from further analysis.

Data analysis – We conducted all analyses in R v4.0.4 (R Core Team 2021). We used linear models to test for associations between mussel density and bioelement availability and concentrations. Stream water column and gravel bar porewater samples were collected at the site level, so we used OLS regression to model bioelement concentrations as a function of mussel density. When OLS residuals deviated strongly from normality based on a Shapiro-Wilks test

and histogram inspection, we used a nonparametric robust regression – Siegel's repeated medians method (Siegel 1982; package: *mblm*). When analyzing porewater and macrophyte samples for redox-sensitive elements we included median sediment grain size and its interaction with mussel density as covariates. In the soil probe study and in macrophyte samples we modelled bioelement associations with mussel density using linear mixed effects (LME) models. We included site block (sites < 1 km apart) as a random intercept in the models (package: *lme4*). For our soil probe study, we also included fixed effects for the flooding event and the interaction between the flood event and mussel density. We tested LME model terms for statistical significance with type III Wald Chi-squared tests (fixed effects) and likelihood ratio tests (random effects). We used *F* tests for OLS regression models with *t* tests for individual parameter slopes. For robust regression slopes, we used a Wilcoxon *V* statistic and calculated Spearman correlation coefficients (ρ) because robust regression does not calculate R^2.

Results

Soil probe pilot study – In our PRS® soil probe study we found that the flooding event was not associated with elemental availability in gravel bars, and that Ca, Fe, K, and P concentrations were spatially variable between site blocks (Figure 2, Table S1). Ca and Fe were associated with mussel density. Mean Ca availability was 1562 ± 79 μg cm^{-2} and Ca increased as mussel density increased ($\chi^2 = 7.48$, $P = 0.006$; Figure 2a). Mean Fe availability was 1586 ± 165 μg cm^{-2} but in contrast to Ca, Fe decreased as mussel density increased ($\chi^2 = 12.41$, $P < 0.001$, Figure 2b). Mn, Cu, Zn, K, Mg, P, and S did not covary with mussel density (Figure 2c-i, Table S1), and their mean elemental availabilities are shown in Table S2.

Stream reach study: Water column and gravel bar porewater – Variability in stream

water column sample bioelement concentrations was not related to mussel density (Figure 3, Table S3). Median sediment grain size varied from <2 mm-48.5 mm, with a mean of 24.01 ± 4.81 across sites (Table 2). Gravel bar porewater concentrations of Ca, Fe, and Mn covaried with mussel density (Figure 4, Table S3). Mean porewater Ca concentration in gravel bar porewater was 12888 ± 3371 µg L^{-1} and increased as mussel density increased (V_{10} = 64, P = 0.055, ρ = 0.28; Figure 4a). Mean porewater Fe concentration was 136 ± 58 µg L^{-1} and the relationship between Fe and mussel density was mediated by sediment grain size ($F_{3,8}$ = 3.74, P = 0.060, R^2_{adj} = 0.43; Figure 4b). Fe decreased as mussel density increased (t_8 = -2.33, P = 0.048, *partial* R^2_{adj} = 0.33) and as sediment size increased (t_8 = -3.09, P = 0.015, *partial* R^2_{adj} = 0.49), with a mussel-sediment interaction (t_8 = 1.92, P = 0.091, *partial* R^2_{adj} = 0.23). In fine sediments, Fe concentrations were negatively related to mussel density when sediment grain size was small, but as sediment size increased the association between mussels and Fe grew weaker and became positive (Figure 4b). Mean porewater Mn concentration was 1015 ± 505 µg L^{-1} and showed a similar pattern to Fe. At fine sediment sizes, mussels and Mn were negatively related, and as sediment size increased, the association was negligible or positive (Figure 4c). Although the linear model predicting Mn concentrations did not explain a statistically significant amount of variation in Mn concentrations ($F_{3,8}$ = 2.39, P = 0.144, R^2_{adj} = 0.28), increases in sediment size (t_8 = -2.61, P = 0.031, *partial* R^2_{adj} = 0.39), and mussel density (t_8 = -1.98, P = 0.083, *partial* R^2_{adj} = 0.25) were related to decreases in porewater Mn, with an interaction between the mussel density and sediment size (t_8 = 1.96, P = 0.086, *partial* R^2_{adj} = 0.24). Variation in porewater Cu, Zn, K, Mg, and Na were not related to mussel density nor sediment size (Figure 4d-h, Table S3).

Stream reach study: Macrophyte samples – The elemental composition of *J. americana* varied among site blocks for Ca, Cu, Fe, Mn, Na, and Zn (Figure 5, Table S4). As with gravel

bar porewater concentrations, the content of Ca and several trace metals (Fe, Cu, Zn) in *J. americana* biomass covaried with mussel density. Mean macrophyte Ca content was 21360 ± 483 µg g^{-1}. As in gravel bar porewater, Ca and mussel density were positively related (χ^2 = 6.97, P = 0.008; Figure 5a). Mean macrophyte Fe content was 25747 ± 232 µg g^{-1}. Mussel density was positively associated with Fe content (χ^2 = 36.86, P < 0.001) and sediment size was negatively associated with Fe content (χ^2 = 9.71, P = 0.002), with an interaction between mussel density and sediment grain size (χ^2 = 29.91, P < 0.001). In contrast to the patterns found in our porewater samples, macrophyte biomass Fe was positively associated with mussel density when sediments were fine, but weakly or negatively associated with mussel density when sediments were coarse (Figure 5b). Mean macrophyte Mn was 1407 ± 68 µg g^{-1}, but this variation was not associated with mussel density (χ^2 = 0.85, P = 0.357; Figure 5c). However, there was a decrease in Mn content as sediment grain size increased (χ^2 = 3.67, P = 0.055) and an interaction effect between sediment size and mussel density (χ^2 = 4.23, P = 0.040). Cu and Zn were associated with mussel density, sediment size, and their interaction. Mean macrophyte Cu content was 12.35 ± 0.35 µg g^{-1} and was positively associated with mussel density (χ^2 = 9.00, P = 0.003) as well as sediment grain size (χ^2 = 17.39, P < 0.001) and was related to the mussel-sediment interaction (χ^2= 16.49, P < 0.001). Mean macrophyte Zn content was 30.51 µg g^{-1} and increased in association with mussel density (χ^2 = 21.75, P < 0.001; Figure 5e) and sediment grain size (χ^2 = 4.10, P = 0.043), with a significant mussel-sediment interaction (χ^2 = 22.05, P = < 0.001). Like Fe, macrophyte Cu and Zn were both positively associated with mussel density when sediments were fine, but negatively associated with mussel density when sediments were coarse. Mean macrophyte Na content was 249 ± 30 µg g^{-1} but was not related to mussel density (Figure 5f, Table S4). Mean elemental concentrations for the stream reach study are presented in Table S5.

Discussion

Calcium availability – Mussel density was associated with elevated Ca concentrations in the gravel bar substrate and in emergent macrophytes, supporting the hypothesis that mussel aggregations covary with Ca at the aquatic-terrestrial interface (**H1**). Plant-available Ca, dissolved Ca in gravel bar porewater, and Ca in *J. americana* tissues all increased in association with mussel density. We hypothesize that the observed patterns in plant-available Ca and porewater Ca are due to the buildup and dissolution of Ca from mussel shells. The positive relationship between mussel density and macrophyte Ca content is also consistent with our hypothesis. We suggest this positive relationship occurs because Ca is relatively bioavailable when dissolved as a divalent cation (Ca^{2+}) and plants have a high demand for Ca, so it benefits the plant to take up and store as much Ca as possible (i.e., luxury consumption; Sterner and Elser 2002). Our study was not designed to disambiguate whether mussel density is driving elevated Ca concentrations versus responding to naturally elevated Ca concentrations. However, if mussels were responding to naturally elevated Ca, we would expect mussel density to be related to water column Ca, as dissolved Ca is the primary source of Ca for mussels (Pynnönen 1991). As such, we conclude that it is more likely that mussels are driving the associations with Ca.

Trace metals in gravel bar porewater – The hypothesis that mussels were associated with variability in redox-sensitive trace metals was also supported (**H2**). There was no evidence that mussels were related to water column trace metal concentrations, but mussels were negatively related to gravel bar porewater concentrations of Fe and Mn. These relationships were mediated by sediment grain size. The interaction between sediment and mussel density meant there was a stronger and more negative association of mussels with Fe and Mn in finer sediments. The likely

driver of this pattern is some form of physico-chemical structuring of the sediments that is associated with mussels (Matisoff et al. 1985, Aller 1990). Increases in oxygen penetration to the substrate should be most pronounced in finer sediments where conditions are more likely to be anoxic. Increased oxygen penetration should preclude microbial reduction of Fe and Mn, allowing oxidation of Fe^{2+} and Mn^{2+} to less soluble oxidation states (e.g., Fe^{3+}, Mn^{3+}), and precipitation as solid metal oxides (Zhang et al. 2014). As with gravel bar Ca concentrations, we suggest the association between mussels and trace metals is best explained by the buildup of shell material in the environment. Shell fragments are incorporated into the substrate as large particles, and we would expect them to create spaces which increase oxygen penetration and oxidize sediments (Bódis et al. 2014), decreasing Fe and Mn bioavailability. Furthermore, $CaCO_3$ from shell decay should buffer the acidity of gravel bar sediments. Acidic conditions tend to increase bioavailability of trace metals to plants, so carbonate buffering should decrease Fe and Mn availability (Graham and Stangoulis 2003). We find the alternative explanation, that bioturbation of the sediment drives variation in trace metal concentrations, to be less likely. Bioturbation occurs primarily at the margins of the macrophyte bed and in the stream channel, but we saw no patterns in trace element availability in the water column. However, we cannot rule out the possibility that mussel bioturbation provides lasting structure to gravel bar substrates when the gravel bar is submerged, and mussels are washed onto them. Mussels may rework sediments in ways that persist after the water has retreated. However, we believe that physical structure and the buffering effect caused by shell buildup provide a more plausible explanation for decreases in concentrations of Fe and Mn in gravel bar porewater.

Trace metals in macrophytes – Variation in the trace metal content of *J. americana* tissues was also associated with mussel density (**H2**). In contrast to porewater concentrations,

trace metals (Fe, Cu, and Zn) in *J. americana* biomass tended to increase with mussel density. The contrasting patterns in trace metal concentrations between porewater and macrophytes align with the hypothesis that plants preferentially adsorb bioelements that are scarce in the environment (Kaspari 2021). Plants are known to increase Fe uptake when they are deficient, suggesting that the macrophytes may preferentially take up Fe as it becomes scarcer in the porewater. The same mechanisms that plants use to upregulate Fe adsorption also promote the uptake of Zn, Cu, and Mn as a byproduct – regardless of Zn, Cu, and Mn concentration (Graham and Stangoulis 2003). Decreases in porewater Fe may thus cause *J. americana* to acquire excess Fe, Cu, and Zn, despite their scarcity, resulting in increased macrophyte Fe, Cu and Zn content.

Two results are more difficult to explain: why were macrophyte Fe and Mn content negatively related to sediment size while Cu and Zn were positively related, and why there was no detectable positive relationship between macrophyte Mn content as there was in the other trace metals? Macrophyte Fe and Mn may be negatively related to sediment size because both have +3 or greater oxidation states that can be reduced to the divalent +2 states favored by plants. Finer sediments with more reduced Fe and Mn might therefore create less incentive for macrophytes to increase metal uptake. Cu on the other hand exists in +1 or +2 states, while Zn only has the +2 form. As a result, porewater Cu and Zn concentrations may be less sensitive to changes in oxygen penetration or buffering in the sediment – especially since they are not used in microbial reduction. We might even expect increases in natural availability of Cu or Zn to plants if oxidation from the monovalent or elemental forms to the divalent forms occurs with increased sediment size. The lack of a detectable increase in macrophyte Mn may have occurred due to an interaction between the plants to decreased Fe and decreased porewater Mn that occurred with increasing mussel density and sediment size. Even if Mn uptake increased as a byproduct of the

plants' trace metal uptake response, the correlated decreases in porewater Mn may prevent the plant from taking up enough Mn to detect. Verifying the causes of the observed relationships between mussels and trace elements will require additional research. A factorial approach where mussel density, shell presence, and sediment grain size are systematically varied would be a good starting point to disentangling how mussels may alter trace element chemistry.

Electrolytes – Except for Ca, our hypothesis that mussels would be related to electrolyte-forming metals was not supported (**H3**). Although recent findings in terrestrial ecosystems demonstrate that low Na concentrations can limit grassland invertebrates (Welti et al. 2019), we found no clear associations between Na and mussel aggregations, nor did we find evidence for covariation between mussel density and the other electrolyte-forming metals we sampled (K and Mg). Because freshwater organisms must maintain internal electrolyte concentrations higher than ambient concentrations (Larsen et al. 2014), we had hypothesized an association between electrolyte-forming metals and mussel density. Ca, Na, K, Mg, and Cl all play roles in freshwater mussel osmoregulation (Dietz 1978, Scheide and Dietz 1982, Dietz et al. 1994). We suggest the lack of an association is due to the constant turnover of matter within streams. Although stream electrolyte concentrations are low, consistent delivery of Ca, Na, K, and Mg, along with efficient osmoregulatory mechanisms probably led to the lack of a relationship between electrolyte-forming metals and mussel aggregations in our study system. This constant delivery of bioelements is also the most likely explanation for the lack of associations between other water column bioelements concentrations and mussel densities. A more fruitful way of exploring mussel associations with stream biogeochemistry might be to explore the relationship between mussels and the turnover rates of bioelements in the water column, rather than static pools.

Conclusions – Taken together, our findings indicate that freshwater mussels have diverse

relationships with biogeochemical cycles across a breadth of bioelements beyond the well-studied C, N, and P pathways. The strongest relationship we found is that mussel density and environmental Ca were positively associated. Ca plays critical roles across many taxa. In plants, Ca helps comprise the cell wall and is used in nutrient uptake and other cellular processes such as signaling pathways and cell division (Hepler 2005). Vertebrates and bivalves sequester large amounts of Ca in their bones and shells respectively (Sterner and Elser 2002). We also saw associations between trace metal concentrations and mussels. Cu, Fe, and Zn are all important to animal growth, immune function, and reproduction (Hollingsworth et al. 2021). Thus, the elevated concentrations of Ca, Cu, Fe, and Zn in macrophytes that we saw correlated with mussel density may have implications for herbivores that feed on the macrophytes.

Because our study macrophyte, *J. americana*, is consumed regularly by game species and livestock (Lopez et al. 2020), elevated Ca levels in *J. americana* resulting from dense mussel beds probably confer nutritional benefits to these economically important animals. Indeed, some terrestrial herbivores are thought to seek out aquatic vegetation actively for its elevated mineral content relative to terrestrial plants (Ceacero et al. 2014). Ca has specifically been hypothesized as a driver of spatial patterns in the consumption of macrophytes by terrestrial herbivores (Labisky et al. 2003, Bergman and Bump 2015). The nutritional benefit of macrophytes associated with dense mussel beds may be further enhanced by elevated concentrations of Fe and other trace metals used to catalyze metabolic reactions. When terrestrial animals return to the uplands, they transport the nutrients and minerals that they consume in aquatic and riparian habitats to terrestrial ecosystems (Bump 2018). As such, our findings are important evidence supporting the value of healthy freshwater ecosystems, and further indicate the importance of conserving freshwater mussels considering their highly imperiled status (Strayer and Dudgeon

2010, Böhm et al. 2020).

Terrestrial ecologists have begun to investigate the synergistic, additive, and individual effects of multiple bioelements (Kaspari et al. 2016, Prather et al. 2020), but dynamic nature of aquatic systems, especially flowing systems, makes designing rigorous experiments to evaluate bioelement dynamics challenging. Our study represents the type of basic ecosystem research that is needed to develop an improved understanding of how animals exert control over biogeochemical cycles in freshwater ecosystems. Once patterns in elemental availability such as the ones we have quantified here are identified, the mechanisms that drive them can be more rigorously tested. Comprehension and prediction of animal-driven variability in bioelement dynamics is inextricably linked to broader applications in conservation and socio-ecological systems. Successful conservation and management initiatives require information on the elemental resources available to and required by an organism, or its "biogeochemical niche" (*sensu* Peñuelas et al. 2019). The broader implications of ecosystem bioelement dynamics center around the idea that maintaining healthy and sustainable biogeochemical cycles improves conditions for socially and economically important parts of the ecosystem, such as the game and livestock species that eat macrophytes. Maintaining and conserving these biogeochemical pathways is thus necessary to preserve the societal value of freshwater ecosystems.

Acknowledgements

We thank A. Franzen, E. Higgins, the members of the Vaughn Lab, A. Cooper, and M. Spikes for assistance. We thank L. Souza and M. Kaspari for comments that improved the manuscript. J. Hartwell designed Figure 1. We also thank the landowners that allowed us access to our study rivers through their property. This paper is part of a dissertation at the University of Oklahoma and a contribution to the program of the Oklahoma Biological Survey.

Literature cited

Allen DC, Galbraith HS, Vaughn CC, Spooner DE (2013) A tale of two rivers: Implications of water management practices for mussel biodiversity outcomes during droughts. Ambio 42:881–891. https://doi.org/10.1007/s13280-013-0420-8

Allen DC, Vaughn CC, Kelly JF, et al (2012) Bottom-up biodiversity effects increase resource subsidy flux between ecosystems. Ecology 93:2165–2174. https://doi.org/10.1890/11-1541.1

Aller R (1990) Bioturbation and manganese cycling in hemipelagic sediments. Philos Trans R Soc Lond Ser Math Phys Sci 331:51–68. https://doi.org/10.1098/rsta.1990.0056

Allgeier JE, Burkepile DE, Layman CA (2017) Animal pee in the sea: consumer-mediated nutrient dynamics in the world's changing oceans. Glob Change Biol 23:2166–2178. https://doi.org/10.1111/gcb.13625

Atkinson CL, Vaughn CC (2015) Biogeochemical hotspots: Temporal and spatial scaling of the impact of freshwater mussels on ecosystem function. Freshw Biol 60:563–574. https://doi.org/10.1111/fwb.12498

Atkinson CL, Vaughn CC, Forshay KJ, Cooper JT (2013) Aggregated filter-feeding consumers alter nutrient limitation: consequences for ecosystem and community dynamics. Ecology 94:1359–1369. https://doi.org/10.1108/JKM-08-2015-0312

Ben-David M, Hanley TA, Schell DM (1998) Fertilization of terrestrial vegetation by spawning Pacific salmon: The role of flooding and predator activity. Oikos 83:47–55

Bergman BG, Bump JK (2015) Experimental evidence that the ecosystem effects of aquatic herbivory by moose and beaver may be contingent on water body type. Freshw Biol 60:1635–1646. https://doi.org/10.1111/fwb.12595

Bódis E, Tóth B, Szekeres J, et al (2014) Empty native and invasive bivalve shells as benthic

habitat modifiers in a large river. Limnologica 49:1–9. https://doi.org/10.1016/j.limno.2014.07.002

Böhm M, Dewhurst-Richman NI, Seddon M, et al (2020) The conservation status of the world's freshwater molluscs. Hydrobiologia 0123456789: https://doi.org/10.1007/s10750-020-04385-w

Boyd PW, Watson AJ, Law CS, et al (2000) A mesoscale phytoplankton bloom in the polar Southern Ocean stimulated by iron fertilization. Nature 407:695–702. https://doi.org/10.1038/35037500

Bump JK (2018) Fertilizing riparian forests: Nutrient repletion across ecotones with trophic rewilding. Philos Trans R Soc B Biol Sci 373:. https://doi.org/10.1098/rstb.2017.0439

Ceacero F, Landete-Castillejos T, Miranda M, et al (2014) Why do cervids feed on aquatic vegetation? Behav Processes 103:28–34. https://doi.org/10.1016/j.beproc.2013.10.008

Dietz TH (1978) Sodium transport in the freshwater mussel, Carunculina texasensis (Lea). Am J Physiol 235:35–40

Dietz TH, Lessard D, Silverman H, Lynn JW (1994) Osmoregulation in Dreissena polymorpha: The importance of Na, Cl, K, and particularly Mg. Biol Bull 187:76–83. https://doi.org/10.2307/1542167

Fritz KM, Gangloff MM, Feminella JW (2004) Habitat modification by the stream macrophyte Justicia americana and its effects on biota. Oecologia 140:388–397. https://doi.org/10.1007/s00442-004-1594-3

Graham RD, Stangoulis JCR (2003) Trace element uptake and distribution in plants. J Nutr 133:1502S-1505S

Harrison HE, Darrow DC, Yannet H (1936) The total electrolyte content of animals and its

probable relation To the distribution of body water. J Biol Chem 113:515–529. https://doi.org/10.1016/s0021-9258(18)74873-4

Hepler PK (2005) Calcium: A Central Regulator of Plant Growth and Development. Plant Cell Online 17:2142–2155. https://doi.org/10.1105/tpc.105.032508

Hollinsworth KA, Shively RD, Light JE, et al (2021) Trace mineral supplies for populations of little and large herbivores. PLoS ONE. 16: e0248204. https://dx.plos.org/10.1371/journal.pone.0248204

Hopper GW, Dickinson GK, Atkinson CL (2021) Associations among elements in freshwater mussel shells (Unionidae) and their relation to morphology and life history. Freshw Biol 00:1–12. https://doi.org/10.1111/fwb.13807

Hopper GW, Gido KB, Vaughn CC, et al (2018) Biomass distribution of fishes and mussels mediates spatial and temporal heterogeneity in nutrient cycling in streams. Oecologia 188:1133–1144. https://doi.org/10.1007/s00442-018-4277-1

Horowitz AJ, Elrick KA (1987) The relation of stream sediment surface area, grain size and composition to trace element chemistry. Appl Geochem 2:437–451. https://doi.org/10.1016/0883-2927(87)90027-8

Jeyasingh PD, Pulkkinen K (2019) Does differential iron supply to algae affect Daphnia life history? An ionome-wide study. Oecologia 191:51–60. https://doi.org/10.1007/s00442-019-04482-1

Kaspari M (2021) The invisible hand of the periodic table: How micronutrients shape ecology. Annu Rev Ecol Evol Syst 52:199–219

Kaspari M, Roeder KA, Benson B, et al (2016) Sodium co-limits and catalyzes macronutrients in a prairie food web. Ecology 98:315–320. https://doi.org/10.1002/ecy.1677

Labisky RF, Hurd CC, Oli MK, Barwick RS (2003) Foods of White-Tailed Deer in the Florida Everglades : The Significance of Crinum. Southeast Nat 2:261–270

Larsen EH, Deaton LE, Onken H, et al (2014) Osmoregulation and excretion. Compr Physiol 4:405–573. https://doi.org/10.1002/cphy.c130004

Lopez JW, Parr TB, Allen DC, Vaughn CC (2020) Animal aggregations promote emergent aquatic plant production at the aquatic–terrestrial interface. Ecology 101:1–8. https://doi.org/10.1002/ecy.3126

Matisoff G, Fisher JB, Matis S (1985) Effects of benthic macroinvertebrates on the exchange of solutes between sediments and freshwater. Hydrobiologia 122:19–33. https://doi.org/10.1007/BF00018956

McNaughton SJ (1985) Ecology of a grazing ecosystem: The Serengeti. Ecol Monogr 55:259–294

Meysman FJR, Middelburg JJ, Heip CHR (2006) Bioturbation: a fresh look at Darwin's last idea. Trends Ecol Evol 21:688–695. https://doi.org/10.1016/j.tree.2006.08.002

Nugroho AP, Frank H (2011) Uptake, distribution, and bioaccumulation of copper in the freshwater mussel Anodonta anatina. Toxicol Environ Chem 93:1838–1850. https://doi.org/10.1080/02772248.2011.582989

Parr TB, Vaughn CC, Gido KB (2019) Animal effects on dissolved organic carbon bioavailability in an algal controlled ecosystem. Freshw Biol 1–13. https://doi.org/10.1111/fwb.13438

Peñuelas J, Fernández-Martínez M, Ciais P, et al (2019) The bioelements, the elementome, and the biogeochemical niche. Ecology 100:1–15. https://doi.org/10.1002/ecy.2652

Polis GA, Hurd SD (1996) Linking marine and terrestrial food webs: Allochthonous input from

the ocean supports high secondary productivity on small Islands and coastal land communities. Am Nat 147:396–423. https://doi.org/10.1086/285858

Prater C, Scott DE, Lance SL, et al (2019) Understanding variation in salamander ionomes: A nutrient balance approach. Freshw Biol 64:294–305. https://doi.org/10.1111/fwb.13216

Prather RM, Castillioni K, Kaspari M, et al (2020) Micronutrients enhance macronutrient effects in a meta-analysis of grassland arthropod abundance. Glob Ecol Biogeogr 29:2273–2288. https://doi.org/10.1111/geb.13196

Pynnönen K (1991) Accumulation of 45Ca in the freshwater unionids Anodonta anatina and Unio tumidus, as influenced by water hardness, protons, and aluminum. J Exp Zool 260:18–27. https://doi.org/10.1002/jez.1402600103

Roman J, Estes JA, Morissette L, et al (2014) Whales as marine ecosystem engineers. Front Ecol Environ 12:377–385. https://doi.org/10.1890/130220

Salt DE, Baxter I, Lahner B (2008) Ionomics and the Study of the Plant Ionome. Annu Rev Plant Biol 59:709–733. https://doi.org/10.1146/annurev.arplant.59.032607.092942

Scheide JI, Dietz TH (1982) The effects of independent sodium and chloride depletion on ion balance in freshwater mussels. Can J Zool 60:1676–1682. https://doi.org/10.1139/z82-220

Schmitz OJ, Wilmers CC, Leroux SJ, et al (2018) Animals and the zoogeochemistry of the carbon cycle. Science 362:. https://doi.org/10.1126/science.aar3213

Siegel AF (1982) Robust Regression Using Repeated Medians. Biometrika 69:242–244

Sousa R, Varandas S, Cortes R, et al (2012) Massive die-offs of freshwater bivalves as resource pulses. Ann Limnol - Int J Limnol 48:105–112. https://doi.org/10.1051/limn/2012003

Sterner RW, Elser JJ (2002) Ecological stoichiometry: The biology of elements from molecules to the biosphere. Princeton University Press, Princeton, New Jersey, USA

Strayer D, Smith L (1994) Distribution, abundance, and roles of freshwater clams (Bivalvia, Unionidae) in the freshwater tidal Hudson River. Freshw Biol 31:239–248. https://doi.org/10.1111/j.1365-2427.1994.tb00858.x

Strayer DL (1993) Macrohabitats of Freshwater Mussels (Bivalvia : Unionacea) in Streams of the Northern Atlantic Slope. J North Am Benthol Soc 12:236–246

Strayer DL, Dudgeon D (2010) Freshwater biodiversity conservation: Recent progress and future challenges. J North Am Benthol Soc 29:344–358. https://doi.org/10.1899/08-171.1

Strayer DL, Malcom HM (2007) Shell decay rates of native and alien freshwater bivalves and implications for habitat engineering. Freshw Biol 52:1611–1617. https://doi.org/10.1111/j.1365-2427.2007.01792.x

Subalusky AL, Dutton CL, Rosi EJ, Post DM (2017) Annual mass drownings of the Serengeti wildebeest migration influence nutrient cycling and storage in the Mara River. Proc Natl Acad Sci U S A 114:7647–7652. https://doi.org/10.1073/pnas.1614778114

Subalusky AL, Post DM (2019) Context dependency of animal resource subsidies. Biol Rev 94:517–538. https://doi.org/10.1111/brv.12465

Vanni MJ (2002) Nutrient cycling by animals in freshwater ecosystems. Annu Rev Ecol Syst 33:341–370. https://doi.org/10.1146/annurev.ecolsys.33.010802.150519

Vaughn C (2003) The Mussel Fauna of the Glover River, Oklahoma. Proc Okla Acad Sci 83:1–6

Vaughn CC, Hoellein TJ (2018) Bivalve Impacts in Freshwater and Marine Ecosystems. Annu Rev Ecol Evol Syst 49:annurev-ecolsys-110617-062703. https://doi.org/10.1146/annurev-ecolsys-110617-062703

Welti EAR, Sanders NJ, de Beurs KM, Kaspari M (2019) A distributed experiment demonstrates widespread sodium limitation in grassland food webs. Ecology 100:1–7.

https://doi.org/10.1002/ecy.2600

Wolman MG (1954) A method of sampling coarse river-bed material. Trans Am Geophys Union 35:951–956

Yatoo MI, Saxena A, Deepa PM, et al (2013) Role of trace elements in animals: A review. Vet World 6:963–967. https://doi.org/10.14202/vetworld.2013.963-967

Zhang C, Yu Z, Zeng G, et al (2014) Effects of sediment geochemical properties on heavy metal bioavailability. Environ Int 73:270–281. https://doi.org/10.1016/j.envint.2014.08.01

Tables

Table 1. Physiological roles of ten bioelements present in freshwater mussels. These elements were selected based on our hypothesized associations between freshwater mussels and the concentrations of these elements in the environment. The physiological roles of the elements are classified into three major freshwater mussel tissue types: shells, soft tissues, and fluids (hemolymph & extrapallial fluid (EPF)). Selected references are included as footnotes (Full citations can be found in Table S6).

	Element									
Tissue type	Ca	Cu	Fe	K	Mg	Mn	Na	P	S	Zn
Shell	Primary structural component in form of $CaCO_3$.[a,b,c,d]	Divalent ion substituted for Ca in shell formation[b,c]	Divalent ion substituted for Ca in shell formation[c]	N/A – no examples found	Divalent ion substituted for Ca in shell formation[d]	Divalent ion substituted for Ca in shell formation[a,b,d]	Unclear – likely substitution into $CaCO_3$ matrix or organic matrix[e]	Nutrient storage/sequestration[f]	Amino acids within organic matrices[g,h]	Divalent ion substituted for Ca in shell formation[b,c]
Soft tissues (gills, mantle, foot)	Present in granular extracellular concretions[a,i,j,k]	Storage and biosynthesis – especially of hemocyanin[l]	Storage and biosynthesis; present in granular extracellular concretions[i, j,k,m]	Present, but function not clear[k,n]	Present, but function not clear[k]	Present in granular extracellular concretions[i, j,k]	Present in granular extracellular concretions[i,j]	Broad range of functions – e.g., concretions, nucleic acids, structure[f,i,j, n]	Present in amino acids and foot tissue[u]	Present in granular extracellular concretions[j]
Hemolymph & EPF	Present as an ion in solution for transport and osmotic balance – EPF uses for shell formation[o,p,q,r]	Present as an ion in solution for transport and in the form of O_2-transporting hemocyanin[l]	Present at low concentrations as an ion in solution for transport[m,s]	Present as an ion in solution for transport and osmotic balance[o,q]	Present as an ion in solution for transport and osmotic balance[q,r]	Present at low concentrations as an ion in solution for transport[t]	Present as an ion in solution for transport and osmotic balance[o,p,q,t]	Present in nucleic acids and as an ion in solution (PO_4^{3-}) for transport and osmotic balance[q,r]	Rarely assessed (but see ref. s); present in amino acids and possibly in solution (SO_4^{2-})	Present at low concentrations as an ion in solution for transport[s]

[a]Ravera et al. 2003; [b]Zhao et al. 2017; [c]Binkowski et al. 2019; [d]Geeza et al. 2019; [e]O'Neil and Gillikin 2014; [f]Atkinson and Vaughn 2015; [g]Tamenori and Yoshimura 2018; [h]Dauphin et al. 2018; [i]Silverman et al. 1983; [j]Pynnönen et al. 1987; [k]Zieritz et al. 2018; [l]Nugroho and Frank 2011; [m]Hobden 1970; [n]Sohail et al. 2016; [o]Scheide and Dietz 1982; [p]Dietz et al. 1994; [q]Gustafson et al. 2005a, [r]Gustafson et al. 2005b; [s]Hemelraad et al. 1990; [t]Dietz 1978; [u]Newton et al. 2013

Table 2. Mussel density and median sediment grain size of the gravel bars at each of the 15 sites used in the two field studies. Mussel densities are rounded to the nearest whole number. Sediment grain size data was not collected at sites during the soil probe pilot study. Whether each site was sampled in the soil probe pilot study, or the stream reach study is indicated by an "x" if the site was sampled.

Site	Mussel density (ind. m^{-2})	Median sediment grain size (mm)	Soil probe pilot study	Stream reach study
GLM	29	<2		x
GLN	0	34.9		x
KMU	0	23.3		x
KBD	11	41.55		x
K2N	0	<2	x	x
K2M	9	<2	x	x
K3C	34	22.95		x
KTM	38	14.55	x	x
KTN	0	48.5	x	x
KSM	24	48.45	x	x
KSN	0	-	x	
K7M	24	26.7		x
K7B	0	34.5		x
LYM	22	-	x	
LYN	17	-	x	

Figure legends

Figures

Figure 1. Freshwater mussels interact with the environmental concentrations of bioavailable minerals and micronutrients in stream ecosystems. Mussels directly interact with the overlying water column and with gravel bar sediments during high flows. Water column and gravel bar porewater chemistry may interact with each other through diffusion or subsurface flows. Emergent aquatic plants such as Justicia americana inhabit riverine gravel bars and acquire nutrients directly from the porewater. Plants may reflect variation in porewater chemistry in their tissues. Changes in plant nutritional status may affect herbivores that consume aquatic plants.

Figure 2. Estimates of plant-available ion concentrations ([a] calcium, [b] iron, [c] manganese, [d] copper, [e] zinc, [f] potassium, [g] magnesium, [h] phosphorus, [i] sulfur) in 8 gravel bars spanning a gradient of freshwater mussel density in the Kiamichi and Little Rivers, Oklahoma, USA. Site block is indicated by color. Overlapping points are slightly jittered for visibility. Intercepts of the lines and 95% confidence bands shown were calculated using the average intercepts across site blocks from linear mixed-effects models. Line presence indicates statistical significance of the mussel-bioelement slope at $P < 0.05$.

Figure 3. Stream channel water column concentrations of bioelements ([a] calcium, [b] iron, [c] manganese, [d] copper, [e] zinc, [f] potassium, [g] magnesium, [h] sodium, [i] phosphorus) at 12 sites spanning a gradient of freshwater mussel density in the Kiamichi and Glover Rivers, Oklahoma, USA. Overlapping points are slightly jittered for visibility.

Figure 4. Gravel bar porewater concentrations of bioelements ([a] calcium, [b] iron, [c] manganese, [d] copper, [e] zinc, [f] potassium, [g] magnesium, [h] sodium) at 12 sites spanning a gradient of freshwater mussel density in the Kiamichi and Glover Rivers, Oklahoma, USA.

Overlapping points are slightly jittered for visibility. Panels with multiple lines and 95% confidence bands show the interaction between sediment size (indicated by darkness of the line shading) and mussel density. Line type indicates statistical significance level of the mussel-bioelement slope from OLS or robust regressions: solid lines represent $P < 0.05$, and dashed lines represent $P < 0.10$.

Figure 5. Tissue bioelement content of *Justicia americana* aboveground biomass ([a] calcium, [b] iron, [c] manganese, [d] copper, [e] zinc, [f] sodium) at 12 sites spanning a gradient of freshwater mussel density in the Kiamichi and Glover Rivers, Oklahoma, USA. Boxes show median and IQR, with whiskers corresponding to 1.5x the IQR at each site and outliers indicated by points. Color indicates sit block (see overlaid key in panel f). Overlapping boxes are slightly jittered for visibility. Panels with multiple lines and 95% confidence bands show the interaction between sediment size (indicated by darkness of the line shading) and mussel density. Intercepts of the lines and 95% confidence bands shown were calculated using the average intercepts across site blocks from linear mixed-effects models. Solid lines indicate statistical significance of the mussel-bioelement slope at $P < 0.05$.

Figures

Figure 1.

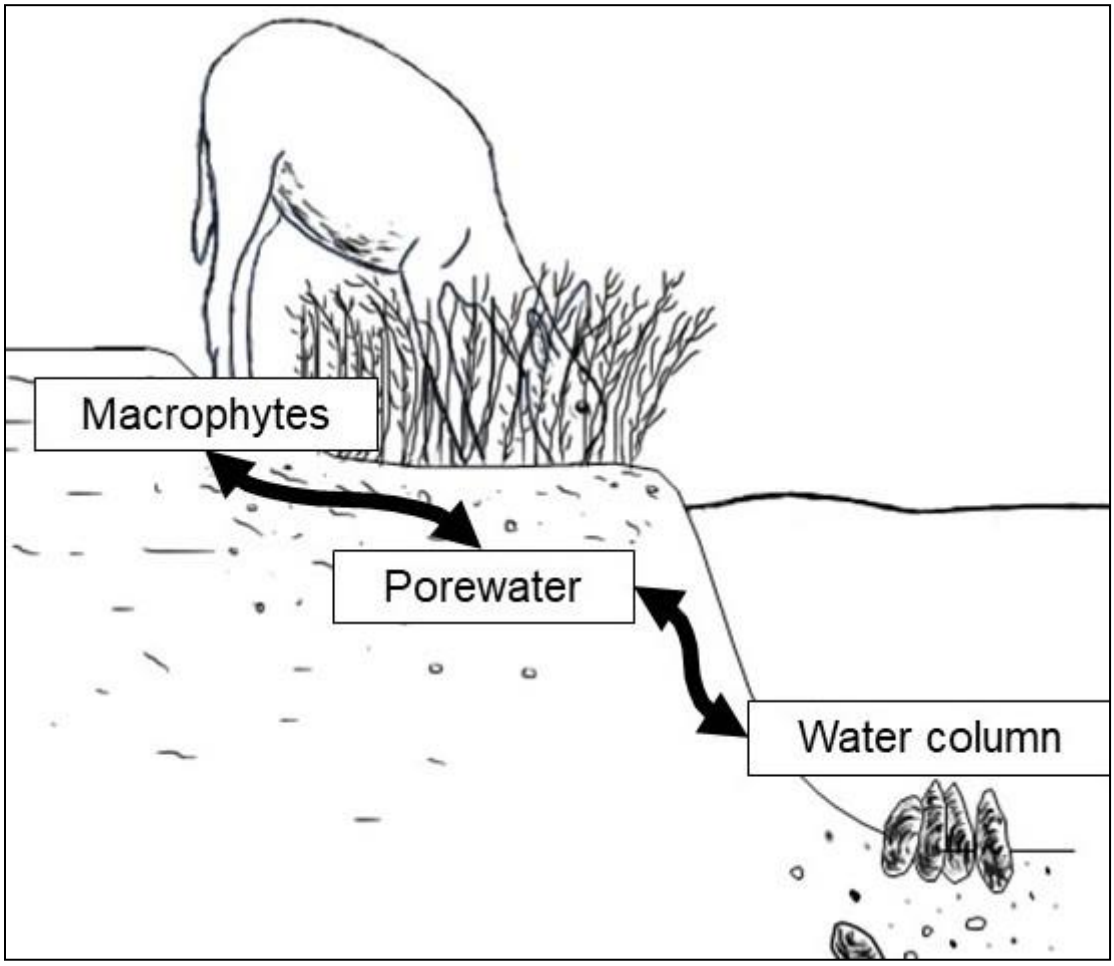

Figure 2.

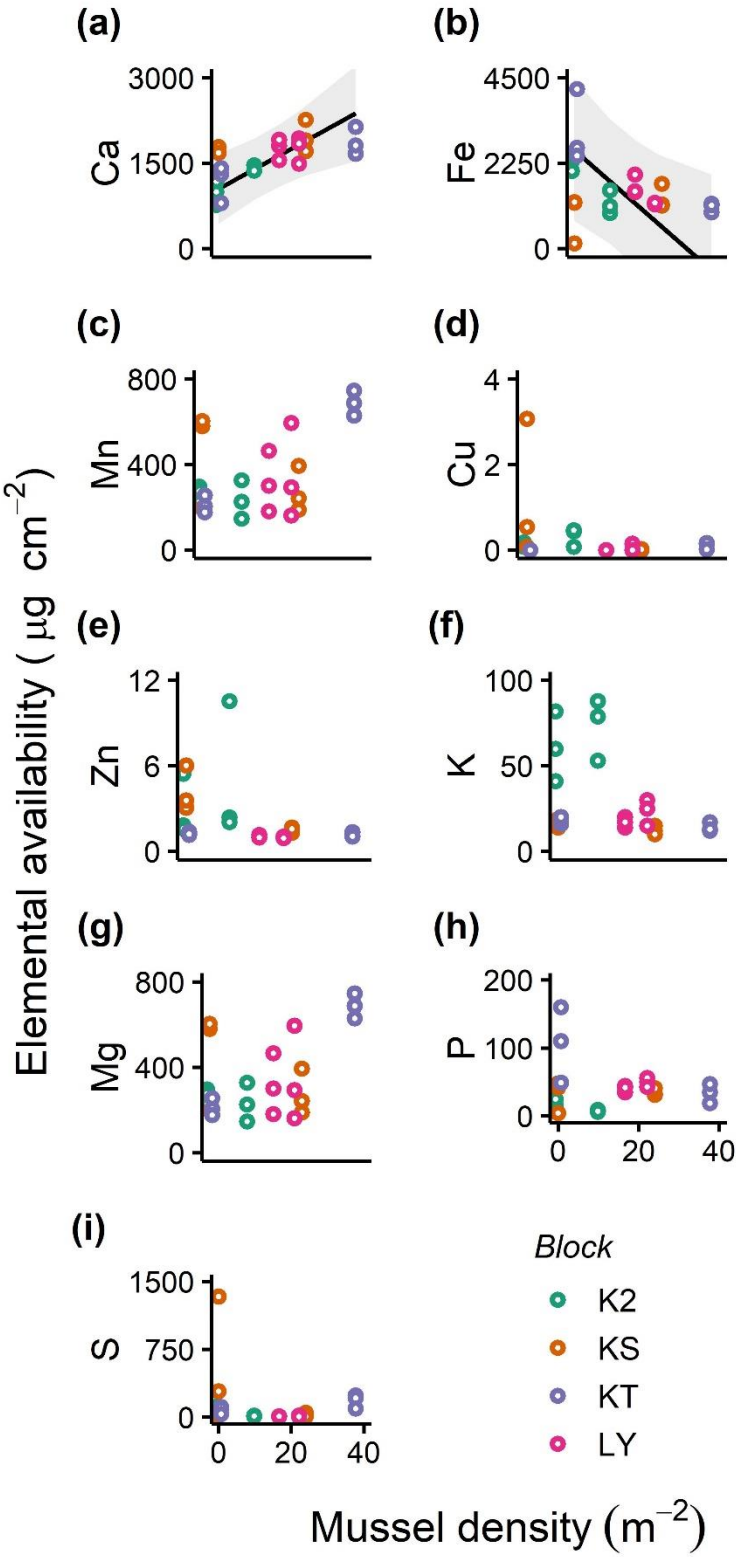
(a)
Ca
3000
1500
0
(b)
Fe
4500
2250
0
(c)
Mn
800
400
0
(d)
Cu
4
2
0
(e)
Zn
12
6
0
(f)
K
100
50
0
(g)
Mg
800
400
0
(h)
P
200
100
0
0
20
40
(i)
S
1500
750
0
0
20
40
Block
K2
KS
KT
LY
Elemental availability (μg cm^{-2})
Mussel density (m^{-2})

Figure 3.

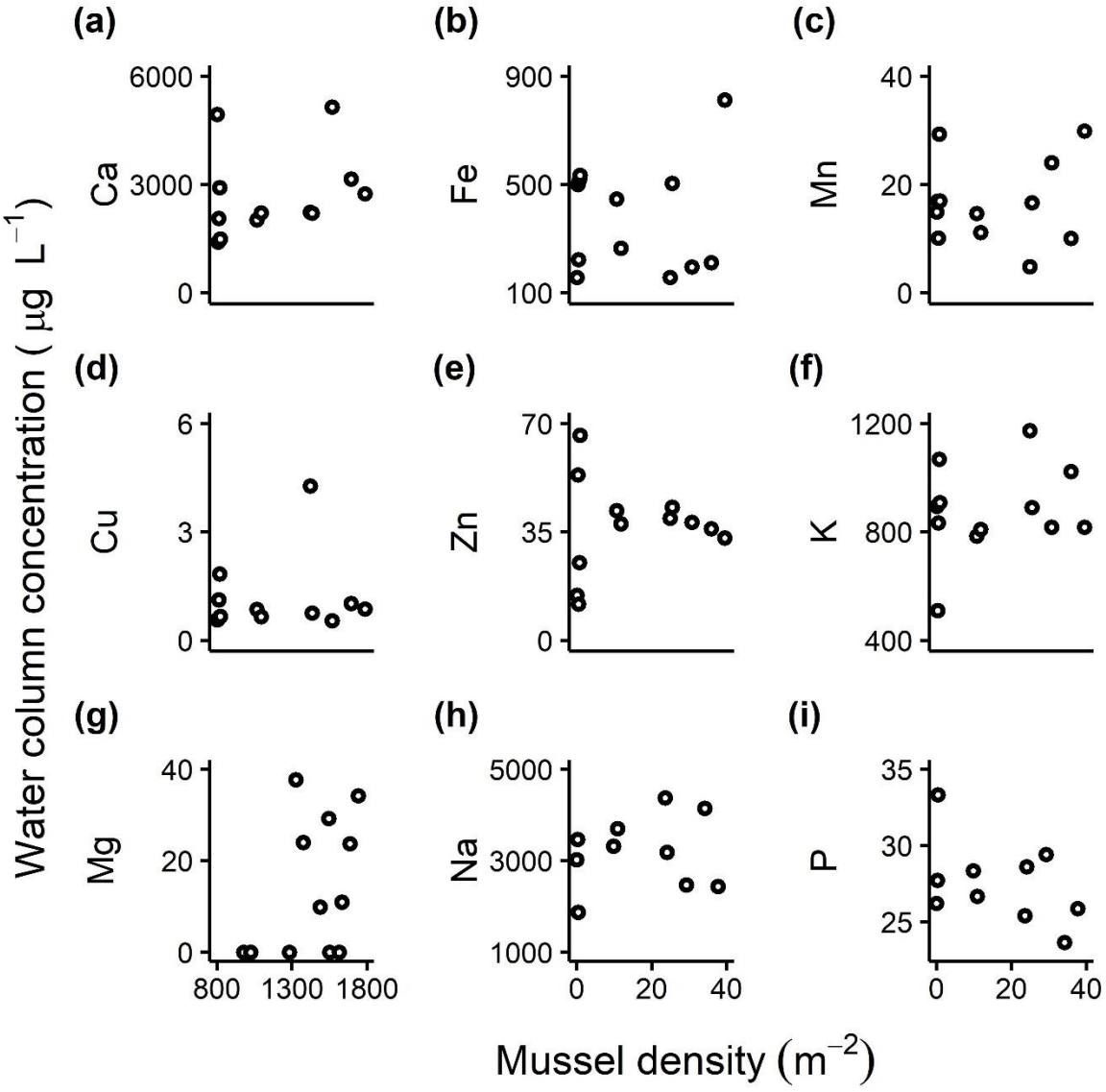
(a)
(b)
(c)
(d)
(e)
(f)
(g)
(h)
(i)
Ca
Fe
Mn
Cu
Zn
K
Mg
Na
P
Water column concentration (µg L^{-1})
Mussel density (m^{-2})

Figure 4.

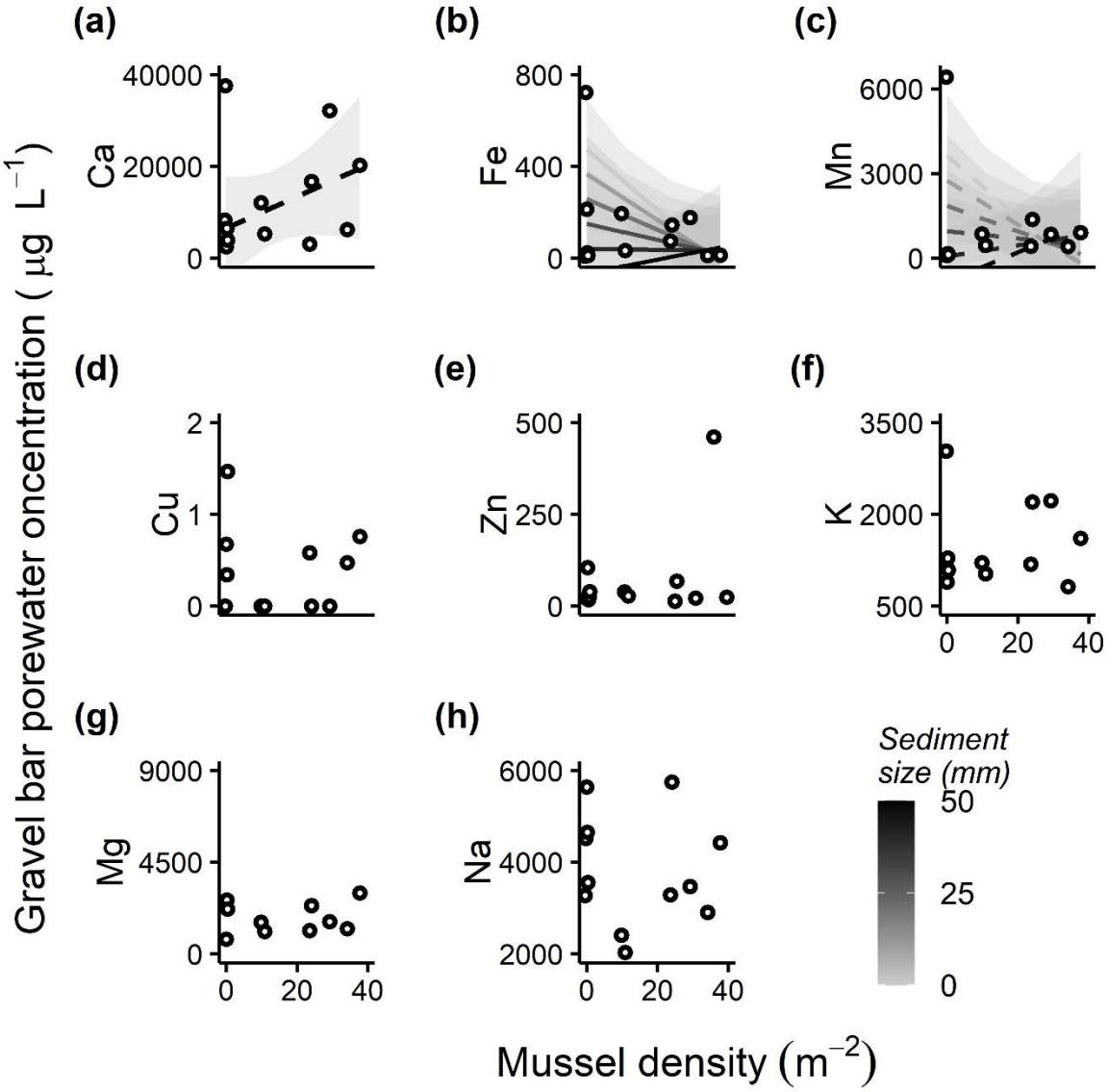
(a)
(b)
(c)
(d)
(e)
(f)
(g)
(h)
Ca
Fe
Mn
Cu
Zn
K
Mg
Na
Gravel bar porewater oncentration (μg L−1)
Mussel density (m−2)
Sediment size (mm)
50
25
0

Figure 5.

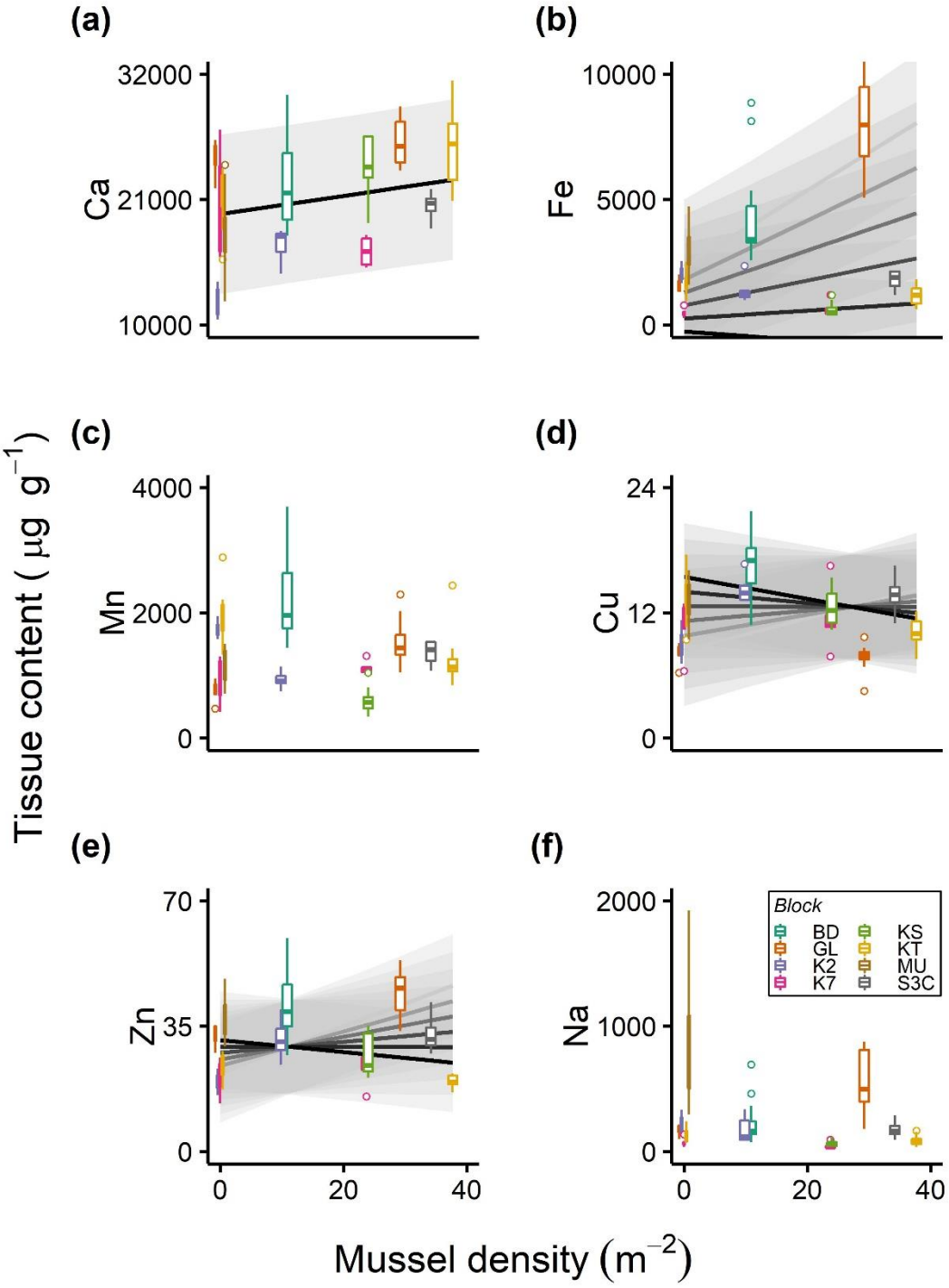
(a)
(b)
(c)
(d)
(e)
(f)
Ca
Fe
Mn
Cu
Zn
Na
32000
21000
10000
5000
0
4000
2000
24
12
70
35
20
40
Block
BD
GL
K2
K7
KS
KT
MU
S3C
Tissue content (µg g^{-1})
Mussel density (m^{-2})

Supplements

Figure S1. Map of study rivers with labelled site locations.

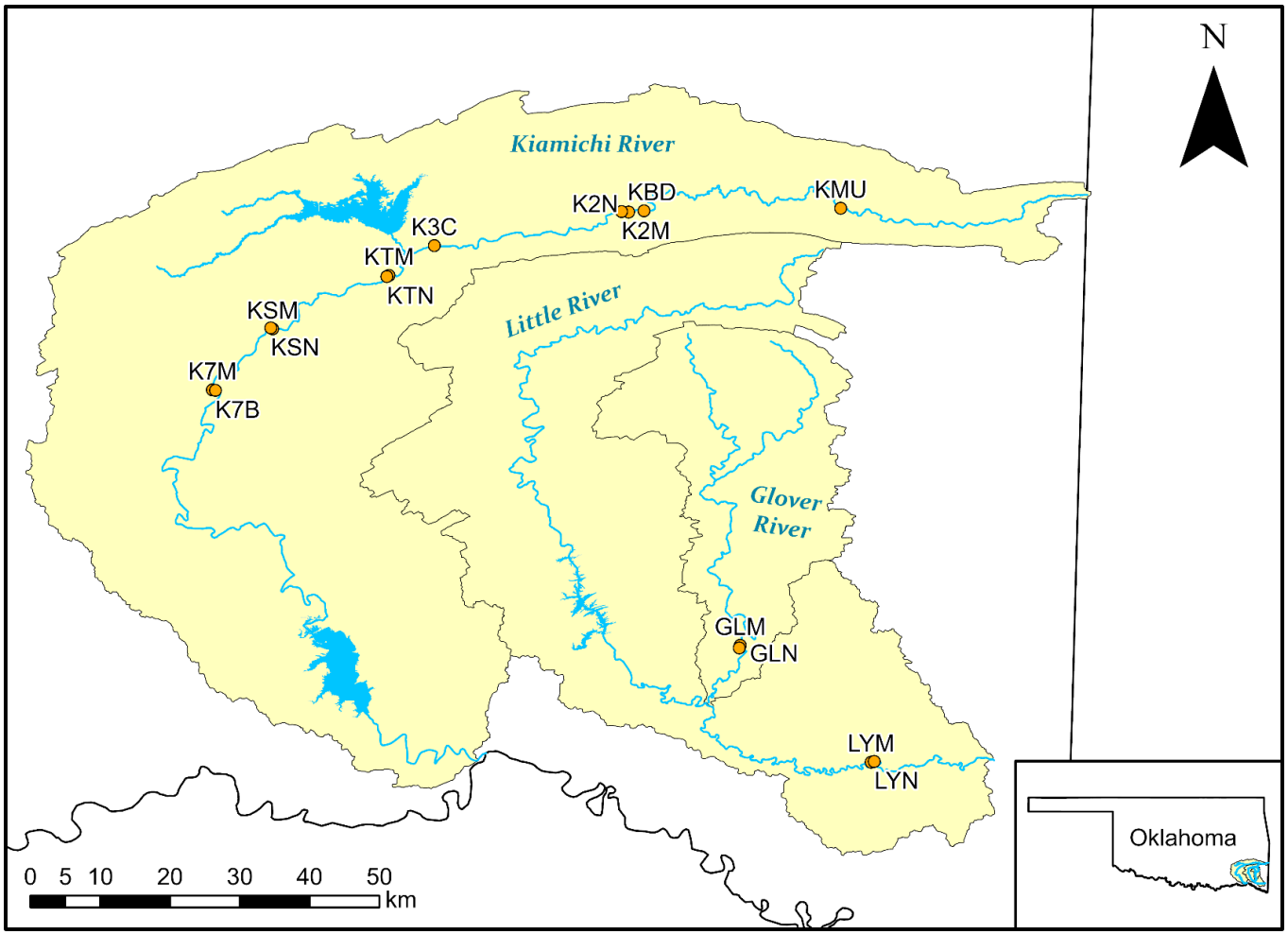

Table S1. ANOVA table for LME models of bioelement availability in the soil probe study. Random effect statistics are not shown for models where the blocking variable did not explain variance in the response.

	Mussel density		Flood effect		Mussel*Flood interaction		Site block	
Bioelement response	χ^2	*P*	χ^2	*P*	χ^2	*P*	λ_{RT}	*P*
Ca	7.48	0.006	1.59	0.21	1.82	0.178	3.30	0.069
Cu	0.02	0.892	0.77	0.381	0.18	0.673	0.087	0.768
Fe	4.77	0.029	0.29	0.591	1.72	0.190	6.15	0.013
K	2.14	0.143	0.18	0.667	2.60	0.110	11.20	8.2e-4
Mg	1.53	0.216	0.49	0.486	0.15	0.698	-	-
Mn	0.51	0.473	0.31	0.575	0.18	0.674	-	-
P	0.03	0.87	1.68	0.196	0.95	0.330	4.96	0.026
S	0.09	0.765	1.76	0.185	0.05	0.82	-	-
Zn	0.072	0.789	0.04	0.850	0.30	0.583	0.93	0.34

Table S2. Mean (SE) concentrations of plant-available mineral nutrients (μg cm^{-2}) of 9 elements in soil probe study across sites the Kiamichi and Little Rivers.

Element	Availability (μg cm^{-2})
Ca	1562 (79)
Cu	0.23 (0.13)
Fe	1586 (165)
K	30 (5)
Mg	217 (23)
Mn	350 (38)
P	40 (7)
S	120 (55)
Zn	2.26 (0.45)

Table S3. Linear model results for stream reach study water samples. Stream water column and gravel bar porewater model results are presented from OLS regression models when parametric assumptions were met, and from robust regression models when OLS assumptions were not met. Only model statistics are presented for simple regression models, but parameter statistics are shown for multiple regression models. Regression equations are not shown for models when R^2, r^2, or $\rho \leq 0.05$.

		Mussel density ($x_{[1]}$)			Sediment effect (x_2)			Mussel*Sediment interaction (x_3)			Model statistics			
Sample type	Bioelement response	*t*	*P*	*partial* R^2_{adj}	*t*	*P*	*partial* R^2_{adj}	*t*	*P*	*partial* R^2_{adj}	*Test statistic*	*P*	*Effect*	Equation
Water column	Ca										$V_{10} = 20.02$	0.108	$\rho = 0.44$	$y = 19.59x + 1873.34$
	Cu										$V_{10} = 51$	0.367	$\rho = 0.08$	$y = 0.011x + 0.66$
	Fe										$F_{1,10} = 0.07$	0.799	$r^2_{adj} = 0$	-
	K										$F_{1,10} = 0.64$	0.444	$r^2_{adj} = 0$	-
	Mg										$F_{1,10} = 2.00$	0.188	$r^2_{adj} = 0.08$	$y = 6.83x + 1341.69$
	Mn										$F_{1,10} = 0.11$	0.742	$r^2_{adj} = 0$	-
	Na										$F_{1,10} = 0.97$	0.349	$r^2_{adj} = 0$	-
	P										$F_{1,10} = 1.75$	0.215	$r^2_{adj} = 0.06$	$y = -0.06x + 28.33$
	Zn										$F_{1,10} = 0.04$	0.837	$r^2_{adj} = 0$	-
Gravel bar porewater	Ca										$V_{10} = 64$	0.055	$\rho = 0.28$	$y = 345.60x + 6515.10$
	Cu	-0.06	0.950	0	1.27	0.241	0.06	0.04	0.967	0	$F_{3,8} = 1.08$	0.412	$R^2_{adj} = 0.02$	-
	Fe	-2.33	0.048	0.33	-3.09	0.015	0.49	1.92	0.091	0.23	$F_{3,8} = 3.74$	0.060	$R^2_{adj} = 0.43$	$y = -3.20x_1 - 10.83x_2 + 0.32x_3 + 474.62$
	K										$V_{10} = 50$	0.410	$\rho = 0.12$	$y = 3.67x + 1176.06$
	Mg										$V_{10} = 26$	0.326	$\rho = 0.28$	$y = -24.68x + 2199.81$
	Mn	-1.98	0.083	0.25	-2.61	0.031	0.39	1.96	0.086	0.24	$F_{3,8} = 2.39$	0.144	$R^2_{adj} = 0.28$	$y = -109.88x_1 - 89.45x_2 + 3.24x_3 + 3639.19$
	Na										$F_{1,10} = 0.11$	0.752	$r^2_{adj} = 0$	-
	Zn	1.29	0.235	0	-0.02	0.984	0	-0.73	0.484	0	$F_{3,8} = 0.87$	0.494	$R^2_{adj} = 0$	-

Table S4. LME model parameters for stream reach study emergent macrophyte (*Justicia americana*) samples.

	Mussel density		Sediment effect		Mussel*Sediment interaction		Site block	
Bioelement response	χ^2	*P*	χ^2	*P*	χ^2	*P*	λ_{RT}	*P*
Ca	6.97	0.008					34.08	5.3e-9
Cu	9.00	0.003	17.39	3.0e-5	16.49	4.9e-5	65.74	5.1e-16
Fe	36.86	1.3e-9	9.71	0.002	29.91	4.5e-8	68.58	<2.2e-16
Mn	0.85	0.357	3.67	0.055	4.23	0.040	48.31	3.6e-12
Na	0.34	0.557					50.02	1.5e-12
Zn	21.75	3.1e-6	4.10	0.043	22.05	2.7e-6	34.36	4.6e-9

Table S5. Mean (SE) concentrations of 10 elements sampled in macrophyte tissue (µg g^{-1}), the stream channel water column (µg L^{-1}), and gravel bar porewater (µg L^{-1}) in the Kiamichi and Glover Rivers. N/A values represent those with analytical uncertainties or interferences that were excluded from analysis.

Element	Macrophyte tissue	Main channel	Porewater
Ca	21360 (483)	2715 (348)	12888 (3371)
Cu	12.35 (0.35)	1.14 (0.30)	0.36 (0.13)
Fe	2547 (232)	377 (59)	136 (58)
K	N/A	878 (48)	1479 (193)
Mg	N/A	1438 (71)	2364 (589)
Mn	1407 (68)	17 (2)	1015 (505)
Na	249 (30)	3077 (221)	3827 (341)
P	N/A	27 (1)	N/A
Zn	30.51 (1.04)	36.66 (4.35)	71.57 (36.17)

Table S6. Full citations used in Table 1.

Full citation
Atkinson CL, Vaughn CC. 2015. Biogeochemical hotspots: Temporal and spatial scaling of the impact of freshwater mussels on ecosystem function. Freshw Biol 60:563–74.
Binkowski ŁJ, Błaszczyk M, Przystupińska A, Ożgo M, Massanyi P. 2019. Metal concentrations in archaeological and contemporary mussel shells (Unionidae): Reconstruction of past environmental conditions and the present state. Chemosphere 228:756–61.
Dauphin Y, Luquet G, Salome M, Bellot-Gurlet L, Cuif JP. 2018. Structure and composition of Unio pictorum shell: arguments for the diversity of the nacroprismatic arrangement in molluscs. J Microsc 270:156–69.
Dietz TH. 1978. Sodium transport in the freshwater mussel, Carunculina texasensis (Lea). Am J Physiol 235:35–40.
Dietz TH, Lessard D, Silverman H, Lynn JW. 1994. Osmoregulation in Dreissena polymorpha: The importance of Na, Cl, K, and particularly Mg. Biol Bull 187:76–83.
Geeza TJ, Gillikin DP, Goodwin DH, Evans SD, Watters T, Warner NR. 2019. Controls on magnesium, manganese, strontium, and barium concentrations recorded in freshwater mussel shells from Ohio. Chem Geol 526:142–52. https://doi.org/10.1016/j.chemgeo.2018.01.001
Gustafson LL, Stoskopf MK, Bogan AE, Showers W, Kwak TJ, Hanlon S, Levine JF. 2005a. Evaluation of a nonlethal technique for hemolymph collection in Elliptio complanata, a freshwater bivalve (Mollusca: Unionidae). Dis Aquat Organ 65:159–65.
Gustafson LL, Stoskopf MK, Showers W, Cope G, Eads C, Linnehan R, Kwak TJ, Andersen B, Levine JF. 2005b. Reference ranges for hemolymph chemistries from Elliptio complanata of North Carolina. Dis Aquat Organ 65:167–76.
Hemelraad J, Holwerda DA, Herwig HJ, Zandee DI. 1990. Effects of cadmium in freshwater clams. I. Interaction with energy metabolism in Anodonta cygnea. Arch Environ Contam Toxicol 19:699–703.
Hobden DJ. 1970. Aspects of iron metabolism in a freshwater mussel. Can J Zool 48:83–6.
Newton TJ, Vaughn CC, Spooner DE, Nichols SJ, Arts MT. 2013. Profiles of biochemical tracers in unionid mussels across a broad geographical range. J Shellfish Res 32:497–507.
Nugroho AP, Frank H. 2011. Uptake, distribution, and bioaccumulation of copper in the freshwater mussel Anodonta anatina. Toxicol Environ Chem 93:1838–50.
O'Neil DD, Gillikin DP. 2014. Do freshwater mussel shells record road-salt pollution? Sci Rep 4:1–6.
Pynnönen K, Holwerda DA, Zandee DI. 1987. Occurrence of calcium concretions in various tissues of freshwater mussels, and their capacity for cadmium sequestration. Aquat Toxicol 10:101–14.
Ravera O, Cenci R, Beone GM, Dantas M, Lodigiani P. 2003. Trace element concentrations in freshwater mussels and macrophytes as related to those in their environment. J Limnol 62:61–70.
Scheide JI, Dietz TH. 1982. The effects of independent sodium and chloride depletion on ion balance in freshwater mussels. Can J Zool 60:1676–82.
Silverman H, Steffens WL, Dietz TH. 1983. Calcium concretions in the gills of a freshwater mussel serve as a calcium reservoir during periods of hypoxia. J Exp Zool 227:177–89.
Sohail M, Khan MN, Chaudhry AS, Shahzad K. 2016. Proximate composition and elemental analysis in soft tissues of freshwater mussels (Anodonta anatina) from the Chashma Lake, River Indus Pakistan. Front Biol (Beijing) 11:331–7.
Tamenori Y, Yoshimura T. 2018. Sulfur speciation in growth layers of shell cross section of the long-lived bivalve Margaritifera laevis using synchrotron spectromicroscopy analysis. Geochim Cosmochim Acta 237:357–69. https://doi.org/10.1016/j.gca.2018.07.002
Zhao L, Schöne BR, Mertz-Kraus R. 2017. Delineating the role of calcium in shell formation and elemental composition of Corbicula fluminea (Bivalvia). Hydrobiologia 790:259–72.
Zieritz A, Azam-Ali S, Marriott AL, Nasire NA binti M, Razak NAABA, Watts M. 2018. Biochemical composition of freshwater mussels in Malaysia: a neglected nutrient source for rural communities. J Food Compos Anal 72:104–14.

CHAPTER THREE

Animal-generated biogeochemical hotspots promote aquatic-to-terrestrial subsidies via mammalian herbivory on macrophytes

Keywords:

aquatic-terrestrial linkage, nutrient subsidy, freshwater mussel, bivalve, aquatic plant, deer, cervid, stream, riparian

Formatted for submission to *Ecology*

Authors: Jonathan W. Lopez, Daniel C. Allen, Caryn C. Vaughn

Abstract

Trophic interactions between mobile animals and their food sources often vector resource flows across ecosystem boundaries. However, the quality and quantity of such ecological subsidies may be altered by indirect interactions between seemingly unconnected taxa. We studied a multi-step resource flow pathway from biogeochemical hotspots created by sedentary aquatic animal aggregations, to emergent aquatic macrophytes, and to terrestrial herbivores. We tested (1) whether the density and nutrient content of the macrophyte *Justicia americana* increase in association with dense aggregations of freshwater mussels, and (2) whether terrestrial herbivores preferentially consume macrophytes from mussel-generated hotspots, promoting aquatic-to-terrestrial subsidies. Mussel density did not have strong effects on N and P concentrations in sediment porewater or on macrophyte growth, but N isotopes in *J. americana* leaves indicated assimilation of mussel-derived nutrients. Data from motion-sensing camera surveys indicated that terrestrial herbivores fed more frequently at mussel-generated hotspots. C and N isotopes in white-tailed deer *(Odocoileus virginianus)* feces suggested that deer receive nutritional benefits from macrophyte consumption and convey nutrients from *J. americana* into terrestrial ecosystems. Thus, emergent macrophytes mediate a subsidy from nutrient-rich aquatic biogeochemical hotspots to nearby terrestrial habitats that are relatively nutrient limited.

Introduction

Ecosystem structure and function constantly respond to the exchange of resources across ecosystem boundaries ("subsidies"). Animals play important roles in conveying resource subsidies in all ecosystem types (McNaughton et al. 1988, Polis and Hurd 1996, Nakano and Murakami 2001). Mobile animals may feed in one ecosystem and subsidize another ecosystem via either waste production or mortality. Seabirds subsidize coastal ecosystems by excreting marine-derived nutrients around their nests (Polis and Hurd 1996), African hippopotami subsidize rivers via waste production after feeding in grasslands (Subalusky et al. 2015), and moose convey subsidies from aquatic to terrestrial ecosystems by feeding on aquatic macrophytes (Bump 2018). These direct plant-herbivore and predator-prey relationships, each based on a mobile animal species, represent fundamental resource subsidies. However, multi-step resource subsidies created by indirect effects between organisms remain much less explored.

Animal-derived resource subsidies are often characterized by animal movement across ecosystem boundaries. Yet, immobile animals can alter resource availability as well. When animal consumers aggregate, they create spatial-temporal biogeochemical hotspots of nutrient recycling and availability (McNaughton et al. 1988, Vanni 2002, Allgeier et al. 2017). These include sedentary or sessile animals that consume food resources from their immediate surroundings, digest that food, and excrete or egest excess nutrients as bioavailable inorganic wastes (Aquilino et al. 2009, Atkinson et al. 2017). This, in turn, increases local inorganic nutrient availability and thus primary production (Peterson and Heck 1999, Atkinson et al. 2013). Primary producer biomass is predicted to increase in nutrient content as ambient nutrients increase, and production that is more nutrient-rich is more likely to be consumed by herbivores (Sterner and Elser 2002, Cebrian and Lartigue 2004). As a result, large aggregations of sedentary

animals may generate biogeochemical hotspots that initiate multi-step nutrient subsidies which flow from their excreta, through primary producers, into herbivores, and are then exported to more resource limited ecosystems.

Freshwater mussels (Unionoida: Bivalvia; hereafter "mussels") form sedentary aggregations that can create biogeochemical hotspots of nitrogen (N) and phosphorus (P) cycling in river ecosystems (Atkinson and Vaughn 2015). Mussel presence thus results in increased primary production by algae and macrophytes (Vaughn et al. 2007, Crane et al. 2020, Lopez et al. 2020). North American mussels have a mutually beneficial relationship with American water willow (*Justicia americana*) – an emergent macrophyte that improves mussel habitat by stabilizing nearby sediments, while mussel excretion helps meet the plant's nutrient demands (Fritz et al. 2004, Atkinson et al. 2014). Mussel-derived nutrients are most concentrated in the summer when flows are low and temperatures are high, leading to increased volumetric excretion rates by mussels (Spooner and Vaughn 2008, Atkinson and Vaughn 2015).

Macrophytes, such as *J. americana*, provide a nutritional resource for terrestrial animals like white-tailed deer (*Odocoileus virginianus*; Ceacero et al. 2014). While *O. virginianus* do not rely on aquatic ecosystems to the extent that other members of the family Cervidae do (e.g., moose, swamp deer), they access wetlands and rivers to drink and feed on aquatic macrophytes (Labisky et al. 2003, Lopez et al. 2020; Figure 1a). It is thought that cervids eat macrophytes because they are richer in nutrients and minerals than most terrestrial plants (Jordan et al. 1973, Ceacero et al. 2014). Aquatic ecosystems tend to be richer in nutrients than terrestrial ecosystems (Shurin et al. 2006, Schindler and Smits 2017), so grazing by cervids on aquatic macrophytes represents a potential uphill, aquatic-to-terrestrial resource subsidy. If mussel-generated biogeochemical hotspots increase productivity or nutritional content in macrophytes, this may

result in increased herbivory by *O. virginianus*. This would further increase the magnitude of cervid-driven nutrient subsidies from aquatic to terrestrial ecosystems, especially during the summer, when nutritional demand in the recipient ecosystem is high.

Here, we assess whether aquatic consumer-generated biogeochemical hotspots support terrestrial ecosystems via a multi-step pathway from aquatic animal excreta through emergent macrophytes into terrestrial herbivores (Figure 1b). We conducted a field study to determine the effects of mussel-generated biogeochemical hotspots on gravel bar nutrient availability, *J. americana* and *O. virginianus*. We sampled the density and nutrient composition of *J. americana* – metrics of the quantity and quality of this macrophyte as a food source. We used stable isotopes ($\delta^{13}C$ and $\delta^{15}N$) and nutrient stoichiometry from *J. americana* tissue and *O. virginianus* fecal pellets to infer the source of nutrients in both organisms. We also used motion-sensing cameras to evaluate whether terrestrial herbivores forage more frequently on *J. americana* at biogeochemical hotspots. We tested the following hypotheses: (**H1**) that mussel density would increase ambient N and P concentrations via excretion, which would in turn promote *J. americana* density and/or the relative N and P content of *J. americana* tissues; (**H2**) regardless of nutrient concentrations, *J. americana* tissue $\delta^{15}N$ values will increase as mussel density increases because more of the available N will be animal-derived; (**H3**) terrestrial herbivores preferentially consume *J. americana* from mussel sites compared to other stream segments and terrestrial vegetation because it is higher in quantity and quality; and (**H4**) *O. virginianus* fecal samples collected from riparian zones would have relatively higher N and P content than those collected from upland ridges bounding the watershed because of access to nutrient-rich macrophytes.

Methods

We sampled nine gravel bars with *J. americana* beds along a natural mussel density gradient from 10 July – 14 August 2019. Eight sites were along an ~118 km stretch of the Kiamichi River (U.S.) between Muse and Eubanks, OK; one site was on North Jackfork Creek – a major tributary of the Kiamichi that is dammed to form Lake Sardis near Clayton, OK (Appendix S1: Figure S1). Four sites contained no mussels, and five contained mussel beds (~3-38 ind m^{-2}).

Nutrient and macrophyte sampling – To test the effect of mussels on ambient nutrients, we estimated gravel bar porewater nutrient concentrations at each site. We sampled ammonium (NH_4^+-N) by the phenol-hypochlorite method and soluble reactive phosphorus (SRP) using the molybdate blue method (U.S. Environmental Protection Agency 1983). We chose these forms because they are highly bioavailable and are the forms of N and P excreted by mussels. We took a composite sample from the upstream and the downstream end of each site. The samples were too high in sediment to filter in the field and were frozen until analysis, when we thawed and decanted them into a syringe filter. We filtered the decanted samples using GF/F filters (0.7 µm).

To test the effects of mussels on *J. americana* density and tissue nutrient and isotope composition, we established 0.25 m^2 plots across a representative spatial distribution of the *J. americana* bed at each site and sampled macrophyte density and nutrient composition within them. We determined plot density by measuring the length of each *J. americana* bed parallel to the direction of stream flow (range = 13 – 113.4 m) and sampled a minimum of one plot per 15 m (range = 2 – 10 plots). We also sampled environmental covariates that can influence plant growth and nutrient composition: light availability (percent shade using a spherical densiometer), and the median sediment grain size by measuring the length of the medial axis of 50 individual grains (Wolman 1954). At each plot, we counted the total density of *J. americana* stems, then

counted the proportion of stems that showed physical damage as a proxy for herbivore effects. We used density rather than biomass as an indicator of *J. americana* growth because herbivory and nutrient enrichment tend to have counteracting effects of similar magnitude on producer biomass (Gruner et al. 2008). We then harvested all aboveground biomass in each plot by clipping the stems at their base and harvested belowground biomass by excavating down to a depth of ~10 cm. Aboveground biomass was separated into leaf and stem tissue; all biomass was dried at 70ºC for 72 h then ground in a knife mill. In leaf, stem, and root tissues, we assessed C:N:P stoichiometry using molar ratios and the $\delta^{13}C$ and $\delta^{15}N$ isotopic signature. We quantified C and N content and isotopes using a Thermo Isolink CN Elemental Analyzer integrated with a Thermo Delta V Advantage IRMS through a Conflo IV (Thermo Fischer Scientific, West Palm Beach, FL, USA). $\delta^{13}C$ and $\delta^{15}N$ values were calibrated using externally certified standards (USGS 40 and 41a for $\delta^{15}N$ relative to air and $\delta^{13}C$ relative to VPDB, and an Algae [*Spirulina*] standard [Elemental Microanalysis Limited, Devon, UK] for C and N content). The Algae [*Spirulina*] standard was used for QA/QC and had an average standard deviation of less than 0.2 ‰ for both $\delta^{13}C$ and $\delta^{15}N$ between sample runs. Total P content was estimated by combustion at 500° C and acid-digestion at 105° C followed by SRP analysis by the molybdate blue method (U.S. Environmental Protection Agency 1983).

Terrestrial herbivore sampling – To test whether terrestrial herbivores preferentially consumed macrophytes at mussel-generated hotspots, we analyzed data collected during a motion-sensing game camera survey (Model# TR10i35A-7, Wildgame Innovations, Grand Prairie, TX) originally described, but not analyzed in Lopez et al. (2020). Briefly, we identified terrestrial vertebrate herbivores that visited *J. americana* beds, triggering a 30 s time-stamped video, and whether they were observed consuming *J. americana*. We placed cameras at 10

stream reaches, but flooding caused the loss of five cameras, leaving us with only four stream reaches at which we could compare herbivore activity; two cameras overlooking stream reaches that contained mussels and two reaches with no mussels. We compared differences in the frequencies with which terrestrial herbivores visited and foraged at mussel reaches (sites KTM and KS7M) and non-mussel reaches (sites K2N and KTN).

To test for differences in diet between riparian and upland deer populations, we collected 23 *O. virginianus* fecal samples from game trails surrounding feeding areas from 26 July – 1 August 2019 and 16 June – 4 August 2021. During this period, there were never more than 21 consecutive days without a rain event (USGS gage 07335700), so we verified that fecal samples were less than 24 days old by excluding samples eroded by precipitation (Jenks et al. 1990). We compared 14 samples collected from trails and gravel bars along the Kiamichi River (riparian samples) to 9 samples collected from trails running to and from wildlife clearings in the Ouachita National Forest along Pashubbe Trailhead (upland samples). Riparian samples represent *O. virginianus* populations that have access to the Kiamichi River, where macrophyte and mussel beds are abundant. Upland samples represent populations that only have access to high-gradient tributaries with no large macrophyte beds or mussels. We analyzed C:N:P stoichiometry, $\delta^{13}C$ and $\delta^{15}N$ of the fecal samples by drying them to a constant weight, then using the methods described above. We also analyzed the $\delta^{13}C$ and $\delta^{15}N$ composition of 10 greenbriar (*Smilax spp.*) leaf samples collected at the same locations as the upland fecal samples. *Smilax spp.* are a preferred food source of *O. virginianus* in the Ouachita Forest (Segelquist and Pennington 1968), and are the dominant understory vegetation, along with poison ivy (*Toxicodendron radicans*). We compared the isotopic and nutrient composition of *Smilax spp.* and *J. americana* leaves to upland and riparian feces to determine the role of macrophytes in *O. virginianus* diet.

Data analysis –We averaged all data at the site level to test our hypotheses across all study sites (Appendix S1: Table S1). We used linear regression models to assess the response of *J. americana* density, nutrient stoichiometry, and isotopic composition to mussel density and the biotic and abiotic covariates described below. To determine what variables drove porewater nutrient concentrations, as well as *J. americana* density and stoichiometry, we used ordinary least squares regression due to the method's flexibility to include multiple predictors. We selected potential drivers using best subsets regression. We selected from mussel density and median sediment grain size as drivers in the models of porewater nutrient concentrations. We selected from percent shade (light effects), proportion of damaged or clipped stems (herbivore effects), sediment size (physical effects) and porewater NH_4^+-N:SRP ratio (nutrient effects) as drivers of *J. americana* density and stoichiometry. We selected the best model based on differences in Akaike Information Criterion with correction for small sample size (ΔAIC_c). Due to the large number of models tested, when multiple models for a given response variable had ΔAIC_c values < 2 (indicating similar fit), we presented only the model yielding the highest adjusted R^2 value. To test *J. americana* $\delta^{15}N$ response to mussel density, we only had one driver to consider, so we used Seigel's robust regression (package *mblm*) to decrease the influence of high-leverage points in this small dataset. The parameters and statistics describing each regression model are reported in Appendix S1: Table S2.

We used Wilcoxon rank sum tests to compare the counts of terrestrial herbivores observed at the two paired sites with motion-sensing cameras, the frequency with which they were seen feeding on *J. americana,* and the stoichiometry of *O. virginianus* fecal samples between upland and riparian habitats. Mean (± SE) values for site-level *J. americana* and *Smilax spp.* leaf tissue, and *O. virginianus* fecal pellet stoichiometry and isotopes are reported in

Appendix S1: Table S3. Finally, we plotted the isotopic niche of the fecal samples in relation to *Smilax spp.* and *J. americana* to assess whether *J. americana* contributes more to the diet of riparian than upland *O. virginianus* populations. We applied trophic enrichment factors of +3 ‰ for $\delta^{15}N$ and -0.8 ‰ for $\delta^{13}C$ to the fecal samples (Sponheimer et al. 2003b, 2003a). We chose not to use a mixing model to test this hypothesis because we could not reasonably assume the two food resources that we sampled comprise the entire diet of *O. virginianus* (Phillips et al. 2014). Instead, we used a PERMANOVA (package *vegan*) to test if the isotopic composition of riparian and upland *O. virginianus* fecal pellets indicated significant differences in diet.

Results

Gravel bar porewater P, but not N, increases with mussel density – Partially consistent with H1, porewater SRP (soluble reactive phosphorus) was associated with increasing mussel density (Figure 2a). SRP increased by 62% across the mussel density gradient ($\beta = 0.04$, $F_{1,7} = 4.44$, $P = 0.073$, $R^2 = 0.30$). Porewater NH_4^+-N did not strongly covary with mussel density or sediment size (Figure 2b; Appendix S1: Table S2).

Light and porewater stoichiometry co-limit stem density – Also consistent with H1, *J. americana* stem density varied with porewater nutrient availability. Stem density varied 6-fold among sites; density increased with porewater NH_4^+-N:SRP ratio ($\beta_1 = 1.24$, *partial* $R^2 = 0.56$), but was constrained by the negative effect of percent shade ($\beta_2 = -4.75$, *partial* $R^2 = 0.58$). The model with these drivers explained much of the variance in *J. americana* density ($F_{2,6} = 10.86$, $P = 0.010$, $R^2 = 0.71$), suggesting potential co-limitation of *J. americana* growth by light and N (Figure 3).

Porewater stoichiometry did not drive macrophyte stoichiometry – In contrast, *J.*

americana tissue stoichiometry did not respond to porewater nutrient stoichiometry and did not support H1. Rather, the environmental covariates we tested appeared to drive *J. americana* stoichiometry. Increasing median sediment size tended to increase carbon content. Leaf C:P varied by 65% across sites, increasing with sediment size (β_1 = 2.67, *partial* R^2 = 0.63) but constrained by percent shade (β_2 = -3.34, *partial* R^2 = 0.67 [model: $F_{2,6,}$= 8.68, P = 0.017, R^2 = 0.66]). Increases in sediment size were also associated with increases of 42% in stem C:N (β = 0.26, $F_{1,7}$ = 11.34, P = 0.012, R^2 = 0.56) and 35% in root C:N (β = 0.20, $F_{1,7}$ = 8.68, P = 0.020, R^2= 0.49). No other tissue types varied consistently with the drivers we tested (Appendix S1: Table S2).

Leaf δ15N increases with mussel density – Increasing mussel density corresponded to a 49% enrichment in δ^{15}N in *J. americana* leaf tissues, thus supporting H2 (β = 0.02, V_7 = 42, P = 0.020; Figure 4). This was not true for stems and roots (Appendix S1: Table S2).

Terrestrial herbivores feed on macrophytes more frequently at mussel-generated hotspots – We captured four terrestrial herbivore species (*Bos taurus* [cows], *Sus scrofa* [feral hogs], *Cervus canadensis*[elk], and *O. virginianus*) at the four sites with motion-sensing cameras. The number of herbivores counted per video at mussel sites (3.35 ± 0.35) was 74% higher than non-mussel sites (1.93 ± 0.21 [W = 886, P = 0.032; Figure 5a]). Furthermore, we observed a nearly 4-fold higher average frequency of herbivory on *J. americana* at mussel sites (2.58 ± 0.48) than non-mussel sites (0.69 ± 0.13 [W = 1043.5, P < 0.001; Figure 5b]), a pattern consistent with H3.

J. americana is prevalent in O. virginianus diet – *O. virginianus* fecal nutrient stoichiometry and isotopes supported H3 & H4. Samples collected from the Kiamichi River riparian zone had 3% lower C:N (W = 29, P = 0.033; Figure 6a) and 20% lower C:P ratios (W = 22, P = 0.009; Figure 6b) than fecal samples from the Kiamichi Valley uplands, consistent with

higher diet quality in *O. virginianus* populations accessing the riparian zone. Riparian samples also had 26 % higher N:P ratios ($W = 29$, $P = 0.033$), indicating the egestion of more excess N relative to P. After being corrected for fractionation, riparian and upland fecal samples differed in isotopic composition ($F_{1,21} = 73.25$, $P = 0.001$; Figure 6c). Upland fecal samples clustered close to *Smilax spp.* but were depleted in ^{15}N compared to *Smilax spp.* indicating that we are either missing an additional dietary source for upland deer or that the fractionation factor we used was too large. However, riparian fecal samples clustered between *Smilax spp.* and *J. americana* in isotopic space, indicating higher prevalence of *J. americana* in the riparian deer diet.

Discussion

This study demonstrates that terrestrial herbivores in riparian habitats have more nutrient-rich diets than herbivores feeding in upland habitats because they benefit from aquatic macrophyte-derived resource subsidies. Herbivores preferentially feed on macrophytes at biogeochemical hotspots, but this pattern does not seem to be generated by N and P dynamics. Rather, the preference for macrophytes growing at hotspots is likely driven by previously identified patterns in mineral dynamics, namely calcium that has been concentrated in mussel shell material.

Contrary to our expectations, mussel-generated biogeochemical hotspots did not have strong effects on N and P dynamics. SRP in gravel bar porewater only marginally increased with mussel density and models suggested that NH_4^+-N concentration was more related to sediment grain size (H1). Our data suggest that the observed positive effect of mussels on SRP was weak across a nine-site sample. NH_4^+-N concentrations varied over a much larger range than mussels

have been shown to affect (Trentman et al. 2018), so NH_4^+-N dynamics within our study gravel bars are likely controlled by a combination of physical and microbial processes (Zarnetske et al. 2011). Macrophyte density increased significantly with porewater NH_4^+-N:SRP ratio (H1). This may align with previous work demonstrating that primary production in the Kiamichi River is N-limited (Vaughn et al. 2007, Atkinson et al. 2013). However, we also found that porewater NH_4^+-N:SRP exceeded the N:P of *J. americana* tissues in most cases – a pattern more consistent with P limitation. It is possible that at high NH_4^+-N:SRP, *J. americana* becomes more P limited and preferentially adsorbs P, further increasing sediment NH_4^+-N:SRP and creating the misleading appearance of N limitation. Experimental nutrient additions might reveal whether *J. americana* growth is truly N limited in this system. Macrophyte C:N:P stoichiometry responded to some environmental factors in a few cases, but was mostly invariant between sites, despite the fact that NH_4^+-N:SRP ratios varied over an order of magnitude (H1). Ecological syntheses suggest that vascular plants are likely more homeostatic in their nutrient composition that previously thought (Demars and Edwards 2007, Elser et al. 2010, Borer et al. 2013), and our results support this notion. Yet *J. americana* leaves became enriched in $\delta^{15}N$ as mussels became denser, indicating that *J. americana* was using mussel-derived N (H2). We are confident in this hypothesis because macrophyte N isotopic composition is mainly a function of the nutrient's source, rather than to hydrologic or temporal variability (Chang et al. 2009, Pastor et al. 2014). However, elevated $\delta^{15}N$ levels were not reflected in roots or stems, likely because the N content of *J. americana* leaves was much higher than roots and stems. Because leaves incorporated more ^{15}N from the environment, effect sizes of $\delta^{15}N$ enrichment in the smaller root and stem N pools would have to have been larger to be detected.

Despite the apparent lack of strong mussel-derived effects on N and P dynamics,

terrestrial herbivores did feed on *J. americana* more frequently at mussel-generated hotspots than non-mussel sites (H3). In a prior study of the availability of a suite of 10 minerals and micronutrients conducted at the same sites, *J. americana* calcium content increased significantly as mussel density increased, probably due to the buildup of calcium carbonate mussel shells in the sediment (Lopez et al. *unpubl.*). We propose that increased feeding by *O. virginianus* at mussel sites is driven by elevated concentrations of this mineral. Calcium is especially important to cervids, and demand for calcium has been proposed as a driver of spatial feeding patterns in moose (Bergman and Bump 2015). Beyond the standard mammalian needs for bone and milk production, annual calcium demand for antler formation in male cervids is so extreme it may cause resorption of calcium from existing bone (Moen and Pastor 1998, Ceacero et al. 2014). However, we observed mostly female *O. virginianus* eating *J. americana*. Female *O. virginianus* in the Florida Everglades have a higher proportion of aquatic plants in their diet, which likely improves reproductive success (Labisky et al. 2003). We suggest that calcium-rich *J. americana* serves a similar role in our study system during gestation and lactation in the summer months.

O. virginianus feces were also enriched in nutrients and had isotopic signatures closer to those of *J. americana* in riparian areas compared to terrestrial vegetation (H3 & H4). C:N and C:P ratios were significantly lower in riparian fecal samples, consistent with higher diet quality (Leslie et al. 2008). Alternatively, one might expect microbial and fungal mineralization to influence nutrient content depending on sample age or the surrounding habitat. However, fecal N mineralization in cervids is relatively consistent between riparian and upland habitats, and N content is stable across 24+ days of exposure (Jenks et al. 1990, Guernsey et al. 2015). Isotopic differences in *O. virginianus* fecal samples between upland and riparian habitats indicated a preference for macrophyte consumption. Upland fecal samples clustered very close to the

signature of *Smilax spp.* and riparian samples formed a second cluster in between *Smilax spp.* and *J. americana*. Aquatic macrophytes are generally higher in nutrients and lower in C than terrestrial plants (Elser et al. 2000, Gruner et al. 2008); this held true in our study when comparing *Smilax spp.* and *J. americana*. Cervids, including *O. virginianus*, seek out food resources that maximize quality and digestibility (Vangilder et al. 1982, Mcarthur et al. 1993). The isotopic and stoichiometric composition of the fecal samples analyzed here strongly suggest that that *O. virginianus* prefer macrophytes in their diet when they are available.

We have demonstrated that although mussel-generated biogeochemical hotspots may not increase the magnitude of aquatic-to-terrestrial nutrient flows through the mechanisms we predicted, *O. virginianus* is still a vector for aquatic-derived resource subsidies. Because dense mussel beds create elevated levels of calcium in macrophyte tissues – which appears to draw cervids to consume macrophytes – healthy mussel beds should promote the redistribution of aquatic-derived nutrients from streams back uphill into the surrounding landscape. Mussels, macrophytes and cervids are all globally distributed (Graf and Cummings 2007, Chambers et al. 2008, Heywood 2010). Thus, the relationship between these taxa may represent a significant vector for nutrients to flow across the aquatic-terrestrial transition. The deposition of nutrient- and mineral-rich material from aquatic source ecosystems should have important functional implications for the recipient terrestrial ecosystems, as resource flows in terrestrial habitats tend to be less concentrated than aquatic ones (Schindler and Smits 2017, Subalusky and Post 2019).

Our results reveal a multi-step pathway of resource exchange driven by animals and mediated by plants. Nutrient subsidies from aquatic animal-generated biogeochemical hotspots traverse the aquatic-terrestrial interface in the tissues of emergent macrophytes and are ultimately transported into the terrestrial environment by mobile herbivores. However, the often-studied

nutrients N and P were insufficient to explain the patterns we observed. Ecological stoichiometry has now begun to move beyond N and P to a more comprehensive approach that includes the balance of all the 20+ elements necessary for life (Peñuelas et al. 2019, Kaspari 2021). In this study, we were fortunate to have prior research on ten other elements across the same sites and species that informed our interpretation of the patterns we found (Lopez et al. *unpubl.*). Without a broader understanding of the interactions between animals and elemental cycles, we cannot expect to disentangle the stoichiometric imbalances that drive trophic interactions and underpin resource flows within and between ecosystems. There is a need for exploratory studies that describe the ecological stoichiometry of elements beyond C, N, and P (Jeyasingh and Pulkkinen 2019, Prater et al. 2019, Hopper et al. 2021). In addition to calcium, minerals such as iron, iodine, cobalt, selenium, and sodium have all been proposed as key drivers of ecological processes (Orians and Milewski 2007, Kaspari et al. 2010, Welti et al. 2019). Such mineral elements may be important determinants of animal-driven ecological subsidies because they are scarce in the environment and in plants, but essential to animal physiology.

Animal-driven resource subsidies are integral to understanding biogeochemical flows. Although animals have traditionally been thought of as negligible players in global elemental cycles, we now know that they have radiating effects on the entire ecosystem and significantly alter elemental dynamics at large spatial scales (Doughty et al. 2015, Schmitz et al. 2018). However, range contractions and loss of animal biomass have altered, and threaten to irreversibly damage the resource flows that support ecosystems (Laliberte and Ripple 2004, Estes et al. 2011). Comprehensive understanding of the roles that animals play in concentrating and translocating nutrient and mineral resources provides the opportunity for targeted conservation or restoration actions that may help preserve or repair the biogeochemical pillars of

earth’s ecosystems.

Acknowledgements

We thank T.P. DuBose, A. Franzen, A. Cooper, H. Stanfield, J. Ahpeatone, and A. Mehta for help in the field, and M. Kaspari and L. Souza for comments that improved this manuscript. We thank the U.S. Forest Service, R. Bastarache, and J. Ford for assistance with work conducted in the Ouachita National Forest. This work was funded by NSF DEB 1457542 to CCV, the Oklahoma Department of Wildlife Conservation (F19AF00247), the University of Oklahoma Department of Biology, and the University of Oklahoma Graduate Student Senate. DCA conducted C and N elemental analyses. JWL wrote the initial manuscript and revised with input from all authors. This paper is part of a dissertation at the University of Oklahoma and a contribution to the program of the Oklahoma Biological Survey.

Literature cited

Allgeier, J. E., D. E. Burkepile, and C. A. Layman. 2017. Animal pee in the sea: consumer-mediated nutrient dynamics in the world's changing oceans. Global Change Biology 23:2166–2178.

Aquilino, K. M., M. E. S. Bracken, M. N. Faubel, and J. J. Stachowicz. 2009. Local-scale nutrient regeneration facilitates seaweed growth on wave-exposed rocky shores in an upwelling system. Limnology and Oceanography 54:309–317.

Atkinson, C. L., J. F. Kelly, and C. C. Vaughn. 2014. Tracing Consumer-Derived Nitrogen in Riverine Food Webs. Ecosystems 17:485–496.

Atkinson, C. L., B. J. Sansom, C. C. Vaughn, and K. J. Forshay. 2017. Consumer aggregations drive nutrient dynamics and ecosystem metabolism in nutrient-limited systems. Ecosystems 21:521–535.

Atkinson, C. L., and C. C. Vaughn. 2015. Biogeochemical hotspots: Temporal and spatial scaling of the impact of freshwater mussels on ecosystem function. Freshwater Biology 60:563–574.

Atkinson, C. L., C. C. Vaughn, K. J. Forshay, and J. T. Cooper. 2013. Aggregated filter-feeding consumers alter nutrient limitation: consequences for ecosystem and community dynamics. Ecology 94:1359–1369.

Bergman, B. G., and J. K. Bump. 2015. Experimental evidence that the ecosystem effects of aquatic herbivory by moose and beaver may be contingent on water body type. Freshwater Biology 60:1635–1646.

Borer, E. T., M. E. S. Bracken, E. W. Seabloom, J. E. Smith, J. Cebrian, E. E. Cleland, J. J. Elser, W. F. Fagan, D. S. Gruner, W. S. Harpole, H. Hillebrand, A. J. Kerkhoff, and J. T. Ngai. 2013. Global biogeography of autotroph chemistry: Is insolation a driving force? Oikos

122:1121–1130.

Bump, J. K. 2018. Fertilizing riparian forests: Nutrient repletion across ecotones with trophic rewilding. Philosophical Transactions of the Royal Society B: Biological Sciences 373.

Ceacero, F., T. Landete-Castillejos, M. Miranda, A. J. García, A. Martínez, and L. Gallego. 2014. Why do cervids feed on aquatic vegetation? Behavioural Processes 103:28–34.

Cebrian, J., and J. Lartigue. 2004. Patterns of herbivory and decomposition in aquatic and terrestrial ecosystems. Ecological Monographs 74:237–259.

Chambers, P. A., P. Lacoul, K. J. Murphy, and S. M. Thomaz. 2008. Global diversity of aquatic macrophytes in freshwater. Hydrobiologia 595:9–26.

Chang, C.C.Y., P.V. McCormick, S. Newman, E.M. Elliot. 2009. Isotopic indicatiors of environmental change in a subtropical wetland. Ecological Indicators. 9: 825–836.

Crane, K., N. E. Coughlan, R. N. Cuthbert, J. T. A. Dick, L. Kregting, A. Ricciardi, H. J. Macisaac, and N. Reid. 2020. Friends of mine: An invasive freshwater mussel facilitates growth of invasive macrophytes and mediates their competitive interactions. Freshwater Biology:1–10.

Demars, B. O. L., and A. C. Edwards. 2007. Tissue nutrient concentrations in freshwater aquatic macrophytes: High inter-taxon differences and low phenotypic response to nutrient supply. Freshwater Biology 52:2073–2086.

Doughty, C. E., J. Roman, S. Faurby, A. Wolf, A. Haque, E. S. Bakker, Y. Malhi, J. B. Dunning, and J. C. Svenning. 2015. Global nutrient transport in a world of giants. Proceedings of the National Academy of Sciences 113:868–873.

Elser, J. J., W. F. Fagan, R. F. Denno, D. R. Dobberfuhl, A. Folarin, A. Huberty, S. Interlandi, S. S. Kilham, E. McCauley, K. L. Schulz, E. H. Siemann, and R. W. Sterner. 2000. Nutritional

constraints in terrestrial and freshwater food webs. Nature 408:578–580.

Elser, J. J., W. F. Fagan, A. J. Kerkhoff, N. G. Swenson, and B. J. Enquist. 2010. Biological stoichiometry of plant production: Metabolism, scaling and ecological response to global change. New Phytologist 186:593–608.

Estes, J. A., J. Terborgh, J. S. Brashares, M. E. Power, J. Berger, W. J. Bond, S. R. Carpenter, T. E. Essington, R. D. Holt, J. B. C. Jackson, R. J. Marquis, L. Oksanen, T. Oksanen, R. T. Paine, E. K. Pikitch, W. J. Ripple, S. A. Sandin, M. Scheffer, T. W. Schoener, J. B. Shurin, A. R. E. Sinclair, M. E. Soulé, R. Virtanen, and D. A. Wardle. 2011. Trophic downgrading of planet earth. Science 333:301–306.

Fritz, K. M., M. M. Gangloff, and J. W. Feminella. 2004. Habitat modification by the stream macrophyte Justicia americana and its effects on biota. Oecologia 140:388–397.

Graf, D. L., and K. S. Cummings. 2007. Review of the systematics and global diversity of freshwater mussel species (Bivalvia: Unionoida). Journal of Molluscan Studies 73:291–314.

Gruner, D. S., J. E. Smith, E. W. Seabloom, S. A. Sandin, J. T. Ngai, H. Hillebrand, W. S. Harpole, J. J. Elser, E. E. Cleland, M. E. S. Bracken, E. T. Borer, and B. M. Bolker. 2008. A cross-system synthesis of consumer and nutrient resource control on producer biomass. Ecology Letters 11:740–755.

Guernsey, N. C., K. A. Lohse, and R. T. Bowyer. 2015. Rates of decomposition and nutrient release of herbivore inputs are driven by habitat microsite characteristics. Ecological Research 30:951–961.

Heywood, J. J. N. 2010. Explaining patterns in modern ruminant diversity: contingency or constraint?

Hopper, G. W., G. K. Dickinson, and C. L. Atkinson. 2021. Associations among elements in

freshwater mussel shells (Unionidae) and their relation to morphology and life history. Freshwater Biology 00:1–12.

Jenks, J. A., R. B. Soper, R. L. Lochmiller, and D. M. Leslie. 1990. Effect of exposure on nitrogen and fiber characteristics of white-tailed deer feces. The Journal of Wildlife Management 54:389–391.

Jeyasingh, P. D., and K. Pulkkinen. 2019. Does differential iron supply to algae affect Daphnia life history? An ionome-wide study. Oecologia 191:51–60.

Jordan, P. A., D. B. Botkin, A. S. Dominski, H. S. Lowendorf, and G. E. Belovsky. 1973. Sodium as a critical nutrient for the moose of Isle Royale. Page North American Moose Workshop.

Kaspari, M. 2021. The invisible hand of the periodic table: How micronutrients shape ecology. Annual Review of Ecology, Evolution, and Systematics 52:199–219.

Kaspari, M., C. Chang, and J. Weaver. 2010. Salted roads and sodium limitation in a northern forest ant community. Ecological Entomology 35:543–548.

Labisky, R. F., C. C. Hurd, M. K. Oli, Barwick, and Robert S. 2003. Foods of white-tailed deer in the Florida Everglades: The significance of Crinum. Southeastern Naturalist 2:261–270.

Laliberte, A. S., and W. J. Ripple. 2004. Range contractions of North American carnivores and ungulates. Page BioScience.

Leslie, D. M., R. T. Bowyer, and J. A. Jenks. 2008. Facts from feces: Nitrogen still measures up as a nutritional index for mammalian herbivores. Journal of Wildlife Management 72:1420–1433.

Lopez, J. W., T. B. Parr, D. C. Allen, and C. C. Vaughn. 2020. Animal aggregations promote emergent aquatic plant production at the aquatic–terrestrial interface. Ecology 101:1–8.

Mcarthur, C., C. T. Robbins, A. E. Hagerman, and T. A. Hanley. 1993. Diet selection by a ruminant generalist browser in relation to plant chemistry. Canadian Journal of Zoology 71:2236–2243.

McNaughton, S. J., R. W. Ruess, and S. W. Seagle. 1988. Large mammals and process dynamics in African ecosystems. BioScience 38:794–800.

Moen, R., and J. Pastor. 1998. A model to predict nutritional requirements for antler growth in moose. Alces 34:59–74.

Nakano, S., and M. Murakami. 2001. Reciprocal subsidies: Dynamic interdependence. PNAS 98:166–170.

Orians, G. H., and A. v. Milewski. 2007. Ecology of Australia: The effects of nutrient-poor soils and intense fires. Biological Reviews 82:393–423.

Pastor, A., J.L. Riera, M. Peipoch, L. Cañas, M. Ribot, E. Gacia, E. Martí, F. Sabater. 2014. Temporal variability of nitrogen stable isotopes in primary uptake compartments in four streams differing in human impacts. Environmental Science and Technology. 48: 6612–6619.

Peñuelas, J., M. Fernández-Martínez, P. Ciais, D. Jou, S. Piao, M. Obersteiner, S. Vicca, I. A. Janssens, and J. Sardans. 2019. The bioelements, the elementome, and the biogeochemical niche. Ecology 100:1–15.

Peterson, B. J., and K. L. Heck. 1999. The potential for suspension feeding bivalves to increase seagrass productivity. Journal of Experimental Marine Biology and Ecology 240:37–52.

Phillips, D. L., R. Inger, S. Bearhop, A. L. Jackson, J. W. Moore, A. C. Parnell, B. X. Semmens, and E. J. Ward. 2014. Best practices for use of stable isotope mixing models in food-web studies. Canadian Journal of Zoology 92:823–835.

Polis, G. A., and S. D. Hurd. 1996. Linking Marine and Terrestrial Food Webs: Allochthonous

Input from the Ocean Supports High Secondary Productivity on Small Islands and Coastal Land Communities. The American Naturalist 147:396–423.

Prater, C., D. E. Scott, S. L. Lance, S. O. Nunziata, R. Sherman, N. Tomczyk, K. A. Capps, and P. D. Jeyasingh. 2019. Understanding variation in salamander ionomes: A nutrient balance approach. Freshwater Biology 64:294–305.

Schindler, D. E., and A. P. Smits. 2017. Subsidies of aquatic resources in terrestrial ecosystems. Ecosystems 20:78–93.

Schmitz, O. J., C. C. Wilmers, S. J. Leroux, C. E. Doughty, T. B. Atwood, M. Galetti, A. B. Davies, and S. J. Goetz. 2018. Animals and the zoogeochemistry of the carbon cycle. Science 362:eaar3213.

Segelquist, C. A., and R. E. Pennington. 1968. Deer browse in the Ouachita Forest in Oklahoma. The Journal of Wildlife Management 32:623–626.

Shurin, J. B., D. S. Gruner, and H. Hillebrand. 2006. All wet or dried up? Real differences between aquatic and terrestrial food webs. Proceedings of the Royal Society B: Biological Sciences 273:1–9.

Sponheimer, M., T. Robinson, L. Ayliffe, B. Passey, B. Roeder, L. Shipley, E. Lopez, T. Cerling, D. Dearing, and J. Ehleringer. 2003a. An experimental study of carbon-isotope fractionation between diet, hair, and feces of mammalian herbivores. Canadian Journal of Zoology 81:871–876.

Sponheimer, M., T. F. Robinson, B. L. Roeder, B. H. Passey, L. K. Ayliffe, T. E. Cerling, M. D. Dearing, and J. R. Ehleringer. 2003b. An experimental study of nitrogen flux in llamas: Is 14N preferentially excreted? Journal of Archaeological Science 30:1649–1655.

Spooner, D. E., and C. C. Vaughn. 2008. A trait-based approach to species' roles in stream

ecosystems: Climate change, community structure, and material cycling. Oecologia 158:307–317.

Sterner, R. W., and J. J. Elser. 2002. Ecological stoichiometry: The biology of elements from molecules to the biosphere. Princeton University Press, Princeton, New Jersey, USA.

Subalusky, A. L., C. L. Dutton, E. J. Rosi-Marshall, and D. M. Post. 2015. The hippopotamus conveyor belt: Vectors of carbon and nutrients from terrestrial grasslands to aquatic systems in sub-Saharan Africa. Freshwater Biology 60:512–525.

Subalusky, A. L., and D. M. Post. 2019. Context dependency of animal resource subsidies. Biological Reviews 94:517–538.

Trentman, M. T., C. L. Atkinson, and J. D. Brant. 2018. Native freshwater mussel effects on nitrogen cycling: impacts of nutrient limitation and biomass dependency. Freshwater Science 37:000–000.

U.S. Environmental Protection Agency. 1983. Methods for Chemical Analysis of Water and Wastes. Cincinatti, Ohio, USA.

Vangilder, L. D., O. Torgerson, and W. R. Porath. 1982. Factors influencing diet selection by white-tailed deer. Source: The Journal of Wildlife Management 46:711–718.

Vanni, M. J. 2002. Nutrient cycling by animals in freshwater ecosystems. Annual Review of Ecology and Systematics 33:341–370.

Vaughn, C. C., D. E. Spooner, and H. S. Galbraith. 2007. Context-dependent species identity effects within a functional group of filter-feeding bivalves. Ecology 88:1654–1662.

Welti, E. A. R., N. J. Sanders, K. M. de Beurs, and M. Kaspari. 2019. A distributed experiment demonstrates widespread sodium limitation in grassland food webs. Ecology 100:1–7.

Wolman, M. G. 1954. A method of sampling coarse river-bed material. Transactions of the

American Geophysical Union 35:951–956.

Zarnetske, J. P., R. Haggerty, S. M. Wondzell, and M. A. Baker. 2011. Dynamics of nitrate production and removal as a function of residence time in the hyporheic zone. Journal of Geophysical Research: Biogeosciences 116.

Figure legends

Figure 1. (a) White-tailed deer (*Odocoileus virginianus*) feeding on emergent macrophytes (*Justicia americana*) on a gravel bar bordering the Kiamichi River, Oklahoma, USA. (b) Conceptual diagram of the hypothesized pathway along which biogeochemical hotspots generated by freshwater mussels may create indirect aquatic-to-terrestrial nutrient subsidies.

Figure 2.(a) Increased freshwater mussel density was associated with increased porewater SRP concentrations ($y = 0.04x + 4.38$). (b) NH_4^+-N concentrations did not change in association with mussel density.

Figure 3. Porewater NH_4^+-N:SRP (x_1) and shade (x_2) co-limit macrophyte density ($y = 1.24x_1 + -4.75x_2 + 248.98$). The regression plane shows the gradient of low *Justicia americana* stem density in the gray to high stem density in dark green.

Figure 4. $\delta^{15}N$ values in *Justicia americana* leaf tissues increase with mussel density ($y = 0.02x + 4.98$), likely indicating an increase in animal-derived N being assimilated.

Figure 5. Video observations of terrestrial herbivores at *Justicia americana* beds. (a) Herbivores visited mussel sites more frequently than non-mussel sites. (b) Herbivores *consumed J. americana* more frequently mussel sites than non-mussel sites.

Figure 6. Comparison of the stoichiometric and isotopic composition of *Odocoileus virginianus* fecal samples from riparian and upland populations. Riparian samples had significantly lower (a) C:N and (b) C:P ratios than upland samples, indicating a more nutrient-rich diet. (c) Isotope biplot comparing Justicia americana and Smilax spp. as potential food sources. Black points with error bars show mean (± SD) values of food sources. Colored points show fecal samples with 95% CI ellipses. O. virginianus diets in the riparian habitats were significantly different from upland habitats ($F_{1,21} = 73.25$, $P = 0.001$).

Figures

Figure 1.

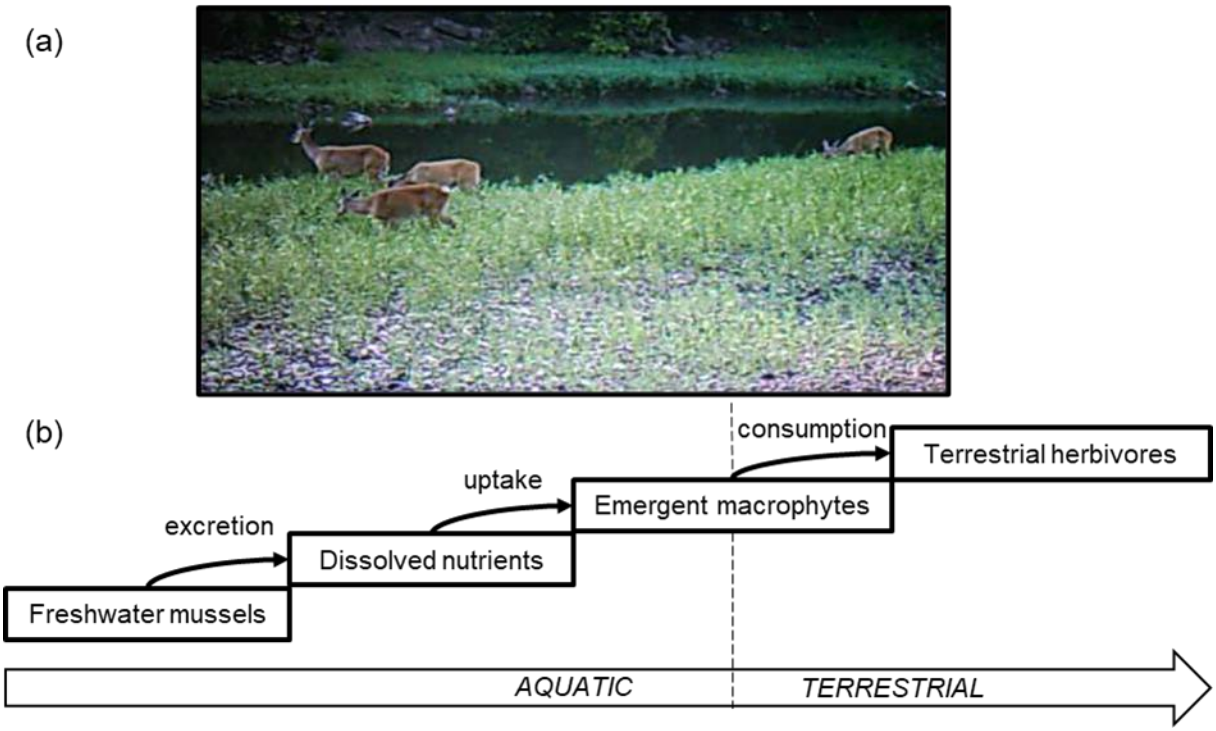

Figure 2.

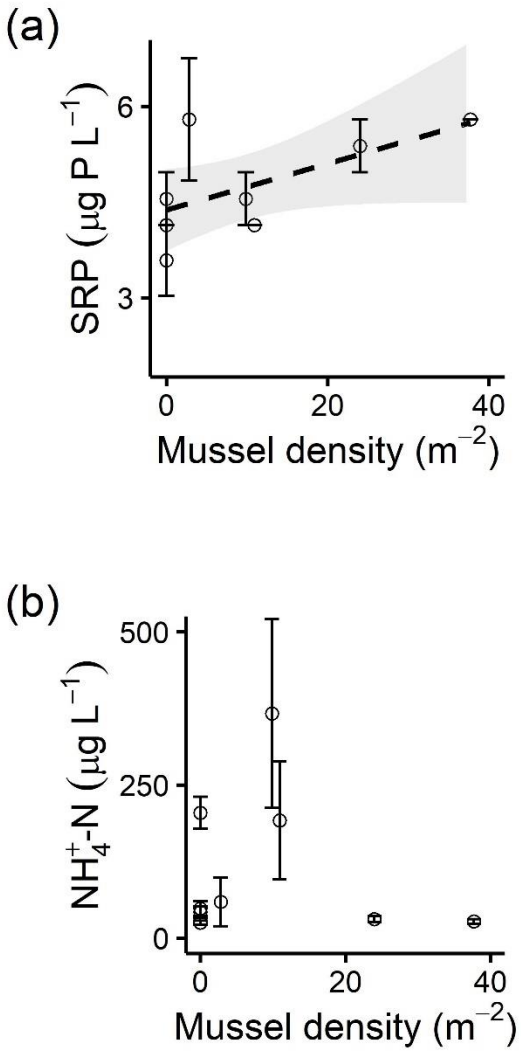
(a)
SRP (µg P L^{-1})
6
3
0
20
40
Mussel density (m^{-2})
(b)
NH_4^+-N (µg L^{-1})
500
250
0
0
20
40
Mussel density (m^{-2})

Figure 3.

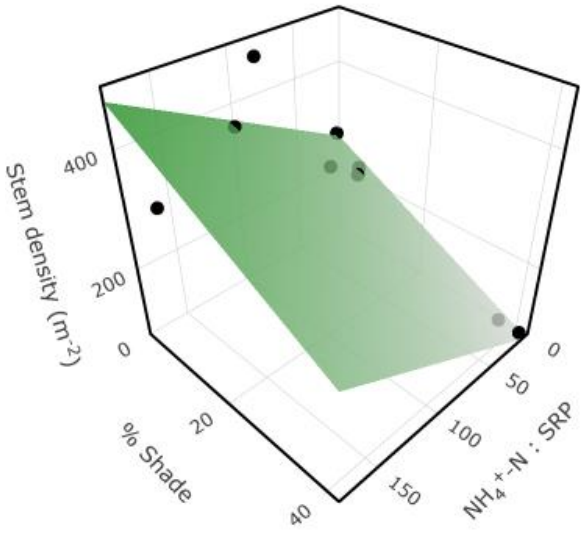

Figure 4.

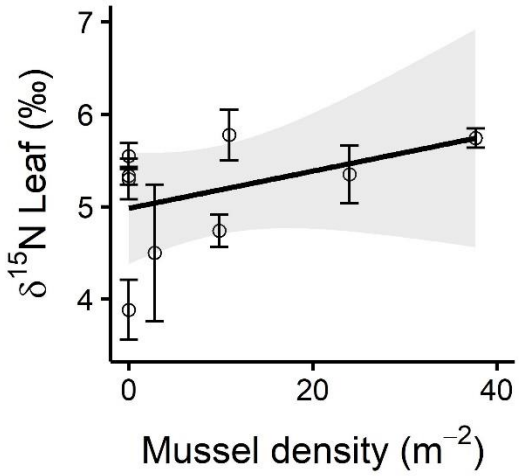

Figure 5.

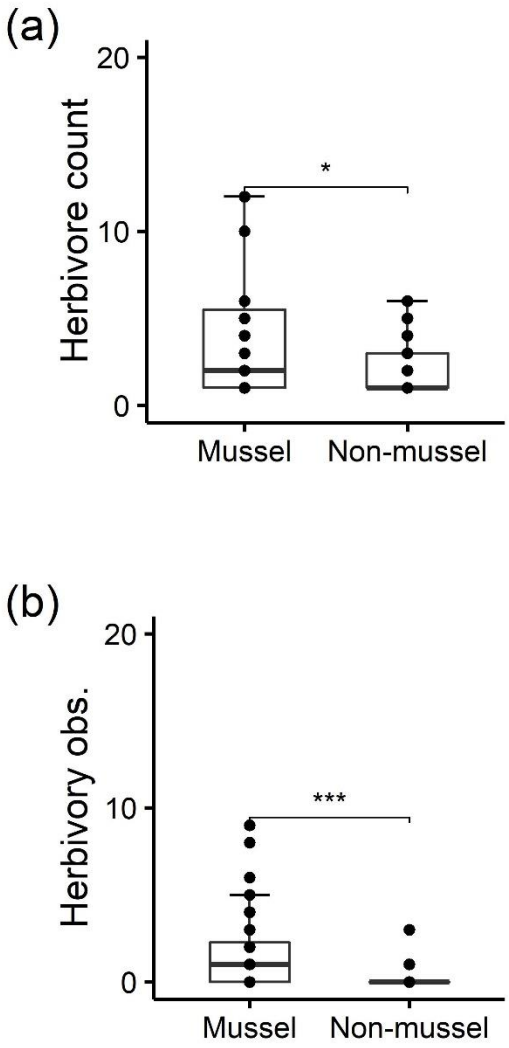
(a)
Herbivore count
20
10
0
*
Mussel
Non-mussel
(b)
Herbivory obs.
20
10
0
***
Mussel
Non-mussel

Figure 6.

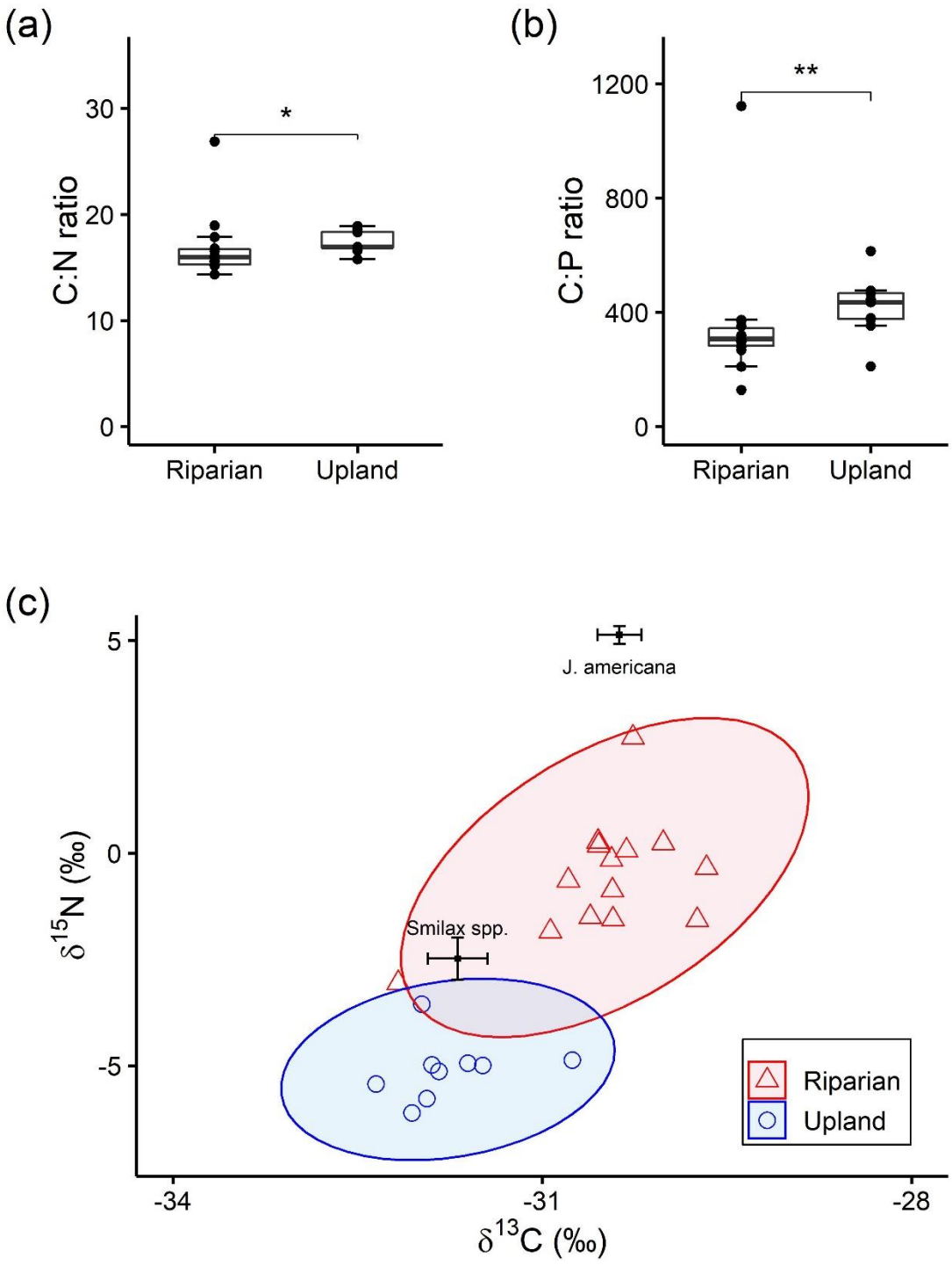
(a)
C:N ratio
30
20
10
0
*
Riparian
Upland
(b)
C:P ratio
1200
800
400
0
**
Riparian
Upland
(c)
J. americana
Smilax spp.
δ15N (‰)
5
0
-5
-34
-31
-28
δ13C (‰)
Riparian
Upland

Supplements

Appendix S1. Supplemental tables and figures.

Table S1. Means (SE) of all response, predictor, and environmental variables for each site. Stoichiometry variables are presented as molar ratios. Median sediment grain size and percent shade have no associated SE because they were collected at the site level.

	Site								
Variable	BD	JF	K2M	K2N	KS7M	KS7N	KTM	KTN	MU
Mussel density (m^{-2})	10.91	2.80	9.8	0	24	0	37.7	0	0
	(5.67)	(1.20)	(1.61)	(n/a)	(3.01)	(n/a)	(1.71)	(n/a)	(n/a)
Porewater SRP (µg P L^{-1})	4.14	5.79	4.55	3.58	5.38	4.55	5.79	4.14	4.55
	(0)	(0.96)	(0.41)	(0.55)	(0.41)	(0.41)	(0)	(0)	(0.41)
Porewater NH_4^+-N (µg N L^{-1})	192.12	59.22	366.51	42.30	31.02	204.61	27.20	48.21	25.38
	(96.19)	(23.05)	(154.15)	(8.86)	(5.36)	(15.85)	(3.61)	(12.25)	(2.21)
Porewater NH_4^+-N:SRP	102.69	17.57	172.40	29.82	12.99	102.67	11.22	25.77	12.41
	(51.41)	(9.66)	(72.53)	(n/a)	(2.30)	(13.67)	(1.54)	(6.55)	(0.86)
Shade (%)	1.3	42.12	9.1	1.82	0	5.98	4.94	8.32	36.92
Median sediment grain size	0	22.3	22.95	0	26.7	16.75	48.5	48.45	41.55
Stem density	369.60	94.00	352.00	223.20	269.33	490.00	218.40	234.40	70.00
	(45.86)	(18.00)	(21.50)	(55.99)	(61.92)	(90.24)	(46.11)	(68.96)	(11.72)
Stems clipped (%)	0.15	50.47	45.62	3.50	24.88	10.94	22.23	56.96	44.45
	(0.10)	(3.10)	(4.95)	(1.02)	(5.53)	(5.24)	(9.19)	(8.82)	(4.78)
$C:N_{leaf}$	16.91	14.68	17.65	13.21	15.77	18.59	20.14	20.58	12.86
	(1.16)	(0.66)	(0.71)	(0.52)	(1.39)	(0.91)	(1.40)	(0.46)	(0.80)
$C:N_{stem}$	45.08	43.98	50.28	39.39	41.08	41.80	56.02	54.42	48.93
	(2.09)	(1.52)	(2.09)	(2.15)	(4.85)	(1.71)	(2.55)	(1.71)	(2.61)
$C:N_{root}$	45.69	49.47	52.53	41.91	47.57	50.41	56.21	56.42	46.18
	(1.58)	(2.72)	(1.56)	(2.66)	(5.46)	(1.30)	(2.53)	(1.36)	(2.15)
$C:P_{leaf}$	416.52	344.56	424.93	355.55	429.44	441.64	568.31	466.47	346.15

	(31.49)	(71.78)	(16.88)	(21.10)	(43.32)	(20.71)	(30.46)	(29.69)	(17.50)
$C:P_{stem}$	405.69	579.87	467.19	448.82	445.45	302.44	689.13	485.08	516.67
	(30.55)	(11.73)	(20.67)	(34.47)	(82.32)	(38.38)	(76.76)	(28.35)	(16.34)
$C:P_{root}$	645.30	670.70	919.50	493.69	851.70	795.05	801.05	824.17	587.27
	(36.32)	(56.84)	(31.60)	(19.07)	(119.22)	(33.71)	(94.94)	(91.30)	(42.18)
$N:P_{leaf}$	12.99	12.29	12.75	14.27	14.34	12.61	15.00	11.95	14.30
	(0.37)	(2.03)	(0.56)	(0.95)	(0.53)	(0.80)	(0.60)	(0.68)	(0.54)
$N:P_{stem}$	4.78	6.97	4.93	6.14	5.78	3.83	6.55	4.70	5.63
	(0.37)	(0.38)	(0.28)	(0.74)	(0.92)	(0.51)	(0.81)	(0.24)	(0.26)
$N:P_{root}$	7.48	7.21	9.26	6.28	9.89	8.33	7.63	7.66	6.71
	(0.40)	(1.00)	(0.42)	(0.31)	(1.29)	(0.38)	(0.98)	(0.73)	(0.40)
$\delta^{13}C_{leaf}$ (‰)	-29.66	-31.05	-30.37	-29.80	-31.01	-30.80	-29.91	-30.15	-30.73
	(0.11)	(0.53)	(0.18)	(0.16)	(0.20)	(0.22)	(0.22)	(0.24)	(0.18)
$\delta\ ^{13}C_{stem}$ (‰)	-29.81	-31.07	-29.37	-29.59	-28.46	-29.47	-33.32	-37.54	-29.82
	(0.25)	(0.39)	(0.44)	(0.39)	(0.56)	(0.08)	(2.83)	(3.04)	(0.25)
$\delta\ ^{13}C_{root}$ (‰)	-28.96	-30.84	-29.28	-31.28	-30.07	-30.68	-32.41	-30.49	-30.58
	(0.63)	(0.65)	(0.38)	(1.83)	(0.22)	(0.18)	(2.35)	(0.35)	(0.26)
$\delta^{15}N_{leaf}$ (‰)	5.78	4.50	4.74	5.33	5.35	5.30	5.74	5.55	3.88
	(0.27)	(0.74)	(0.17)	(0.10)	(0.31)	(0.22)	(0.10)	(0.14)	(0.32)
$\delta^{15}N_{stem}$ (‰)	4.15	3.20	3.15	3.96	3.84	4.03	3.90	3.74	1.86
	(0.30)	(0.75)	(0.17)	(0.11)	(0.58)	(0.14)	(0.09)	(0.20)	(0.21)
$\delta^{15}N_{root}$ (‰)	3.56	2.98	2.84	3.39	3.33	3.31	4.40	4.08	2.26
	(0.20)	(0.77)	(0.22)	(0.10)	(0.38)	(0.12)	(0.11)	(0.13)	(0.27)

Table S2. Regression models and their coefficient and intercept estimates (± SE for *lm* models; ± MAD for *mblm* models). Bolded table rows describe statistically significant models (α = 0.05). *F* statistics describe full *lm* models, *V* statistics describe the slope of *mblm* models. R^2 values are not applicable to *mblm* models.

Model: response ~ terms	Model coefficients (β_i) & intercepts (β_0)	Test statistic	*P*	R^2_{adj}
lm: porewater_NH_4^+-N ~ $\beta_1$sed_size + β0	B_1 = -2.41 (2.27) β_0 = 171.82 (69.55)	$F_{1,7}$ = 1.13	0.323	0.02
lm: porewater_SRP ~ $\beta_1$mussel_density + β0	B_1 = 0.04 (0.02) β_0 = 4.38 (0.27)	$F_{1,7}$ = 4.44	0.073	0.30
lm: porewater_ NH_4^+-N: SRP ~ $\beta_1$sed_size + β0	B_1 = -1.31 (1.10) β_0 = 87.70 (33.92)	$F_{1,7}$ = 1.41	0.274	0.27
lm: **stem_density ~ $\beta_1$pore_N:P + β_2%_shade + β_0**	**β_1 = 1.24 (0.44)** **β_2 = -4.75 (1.65)** β_0 = 248.98 (42.62)	**$F_{2,6}$ = 10.86**	**0.010**	**0.71**
lm: leaf_C:N ~ β_1%_ shade + β0	β_1 = -0.08 (0.06) β_0 = 17.72 (1.15)	$F_{1,7}$ = 1.92	0.208	0.10
***lm*: leaf_C:P ~ + $\beta_1$sed_size + β_2%_ shade + β0**	**β_1 = 2.67 (0.83)** **β_2 = -3.34 (0.97)** β_0 = 394.76 (25.14)	**$F_{2,6}$ = 8.68**	**0.017**	**0.66**
lm: leaf_N:P ~ $\beta_1$pore_N:P + β0	β_1 = -0.01 (0.01) β_0 = 13.84 (0.49)	$F_{1,7}$ = 1.77	0.223	0.09
***lm*: stem_C:N ~ $\beta_1$sed_size + β0**	**β_1 = 0.26 (0.08)** **β_0 = 40.32 (2.32)**	**$F_{1,7}$ = 11.34**	**0.012**	**0.56**
lm: stem_C:P ~ $\beta_1$sed_size + β0	β_1 = 3.53 (1.80) β_0 = 392.83 (55.05)	$F_{1,7}$ = 3.87	0.090	0.26
lm: stem_N:P ~ $\beta_1$porewater_N:P + β0	β_1 = -0.01 (0.01) β_0 = 6.04 (0.40)	$F_{1,7}$ = 2.32	0.084	0.28
***lm*: root_C:N ~ $\beta_1$sed_size + β0**	**β_1 = 0.20 (0.07)** **β_0 = 44.60 (2.05)**	**$F_{1,7}$ = 8.68**	**0.022**	**0.49**
lm: root_C:P ~ $\beta_1$sed_size + $\beta_2$porewater_N:P + β0	β_1 = 5.44 (2.19) β_2 = 1.63 (0.68)	$F_{2,6}$ = 4.20	0.07	0.44

lm: root_N:P ~ $\beta_1$porewater_N:P + β0	β_0 = 505.36 (85.90) β_1 = 0.01 (0.01)	$F_{1,7}$ = 1.37	0.28	0.04
***mblm*: leaf_δ^{15}N ~ βmussel_density + β0**	β_0 = 7.39 (0.53) **β = 0.02 (0.03)**	**V_7 = 42**	**0.020**	-
mblm: stem_δ^{15}N ~ βmussel_density + β0	β_0 = 4.98 (0.52) β = 0.00 (0.02)	V_7 = 35	0.164	-
mblm: root_δ^{15}N ~ βmussel_density + β0	β_0 = 3.73 (0.31) β = 0.01 (0.01)	V_7 = 32	0.301	-
	β_0 = 3.12 0.28			

Table S3. Means (SE) stoichiometric and isotopic composition of leaf tissue from *Smilax spp.* (*n* = 10) and *J. americana* across sites (*n* = 9), and of *O. virginianus* riparian (*n* = 14) and upland (*n* = 9) fecal pellets.

Sample type	C:N	C:P	N:P	$\delta^{13}C$ (‰)	$\delta^{15}N$ (‰)
Smilax spp. leaves	26.88 (0.68)	1212.57 (69.34)	1212.57 (2.54)	-31.69 (0.24)	-2.48 (0.50)
J. americana leaves	16.71 (0.94)	421.51 (23.58)	421.51 (0.36)	-30.37 (0.18)	5.13 (0.21)
Riparian	16.86 (0.83)	353.33 (61.52)	353.33 (2.03)	-31.29 (0.16)	2.42 (0.36)
Upland	17.36 (0.34)	443.91 (41.90)	443.91 (2.62)	-32.59 (0.14)	-2.15 (0.22)

Figure S1. A map of the 9 sites sampled within the Kiamichi River watershed and the entrance to the Pashubbe Trailhead. Inset shows the location of the Kiamichi watershed within the US state of Oklahoma.